THE PHARMACEUTICAL CHEMICAL TENDENCY TOWARDS CONTINUOUS-FLOW PROCESSING: NOVEL CHEMICAL REACTIVITIES AND ENTITIES

PhD Thesis

By

Imane Nekkaa

Supervisors:

Prof. Dr. Ferenc Fülöp
Dr. István Mándity

University of Szeged
Institute of Pharmaceutical Chemistry

Szeged

2018

TABLE OF CONTENTS

LIST OF PUBLICATIONS AND LECTURES

Papers related to the thesis:

I. István M. Mándity, **Imane Nekkaa**, Gábor Paragi, Ferenc Fülöp: Homochirality of β-Peptides: A Significant Biomimetic Property of Unnatural Systems. *ChemistryOpen*. **2017**, *6*, 492–496.

II. **Imane Nekkaa**, Márta Palkó, István M. Mándity, Ferenc Fülöp: Continuous-flow retro-Diels–Alder Reaction: An Efficient Method for the Preparation of Pyrimidinone Derivatives. *Beilstein J. Org. Chem*. **2018**, *14*, 318–324.

III. **Imane Nekkaa**, Márta Palkó, István M. Mándity, Ferenc Miklós, Ferenc Fülöp: Continuous-flow retro-Diels–Alder Reaction: A Novel Process Window for Designing New Heterocyclic Scaffolds. *Eur. J. Org. Chem*. **2018**, 4456–4464.

IV. **Imane Nekkaa**, Dóra Bogdán, Tamás Gáti, Szabolcs Béni, Tünde Juhász, Márta Palkó, Gábor Paragi, Gábor K. Tóth, Ferenc Fülöp, István M. Mándity: Flow-chemistry Enabled Efficient Patterning of β-Peptides: Backbone Topology *vs*. Helix Formation. Submitted for publication

Scientific lectures related to the thesis:

V. **Imane Nekkaa**, István M. Mándity, Ferenc Fülöp:
Stereochemical Discrimination in the Synthesis of β-Peptide Oligomers: Origin of Homochirality.
XXXVII. Kémiai Előadói Napok, Szeged, 2015. Október 26–28.

VI. **Imane Nekkaa**, István M. Mándity, Ferenc Fülöp:
Stereochemical Discrimination in the Synthesis of β-Peptide Oligomers: Origin of Homochirality.
8th International Conference Chemistry towards Biology. 28th August–1st September 2016. Brno, Czech Republic.

VII. **Imane Nekkaa**, István M. Mándity, Ferenc Fülöp:
Homochirality in the Unnatural Peptide World: A Significant Biomimetic Property.
A Szegedi Ifjú Szerves Kémikusok Támogatásáért Alapítvány, Szeged 2017, May 26.

VIII. **Imane Nekkaa**, István M. Mándity, Ferenc Fülöp:
Homochirality of β-Peptides: A Significant Biomimetic Property of Unnatural Systems.
7th BBBB International Conference on Pharmaceutical Sciences. New Trends and Achievements in Pharmaceutical Sciences and Pharmacy Practice, 5–7 October 2017, Balatonfüred, Hungary.

IX. **Imane Nekkaa**, Márta Palkó, István M. Mándity, Ferenc Fülöp:
Continuous-flow retro-Diels–Alder Reaction: An Efficient Method for the Preparation of Pyrimidinone Derivatives.
Flow Chemistry Europe 2018, 6–7 February 2018, Cripps Court, Magdalene College, Cambridge, UK.

X. **Imane Nekkaa**, Márta Palkó, István M. Mándity, Ferenc Miklós, Ferenc Fülöp:
Continuous-flow retro-Diels–Alder Reaction: A Novel Process Window for Designing New Heterocyclic Scaffolds.
Heterociklusos és Elemorganikus Kémiai Munkabizottság ülése. Balatonszemes, 2018, June 6–8.

ABBREVIATIONS

ABHEC	3-aminobicyclo[2.2.1]hept-5-ene-2-carboxylic acid
ACHC	2-aminocyclohexanecarboxylic acid
ACPC	2-aminocyclopentanecarboxylic acid
Ala	Alanine
AOBHEC	3-amino-7-oxabicyclo[2.2.1]hept-5-ene-2-carboxylic acid
Boc	*tert*-butoxycarbonyl
CF	continuous-flow
DA	Diels-Alder
Dmab	dimethylamine borane
DBU	1,8-diazabicyclo[5.4.0]undec-7-ene
DIPEA	*N*,*N*-diisopropylethylamine
de	diastereomeric excess
ee	enantiomeric excess
EOF	electroosmotic flow
Fmoc	9*H*-fluoren-9-ylmethoxycarbonyl
FVP	flash vacuum pyrolysis
HATU	1-[*bis*-(dimethylamino)methyliumyl]-1*H*-1,2,3-triazolo[4,5-*b*]pyridine-3-oxide
HPLC	high-performance liquid chromatography
ihDA/rDA	inverse-electron-demand hetero-/retro-Diels–Alder reaction
Leu	leucine
MACOS	microwave-assisted continuous-flow organic synthesis
MS	mass spectrometry
NCE	new chemical entities
NMM	*N*-methylmorpholine
PFP	pentafluorphenyl
*p*TSA	*para*-toluenesulfonic acid
rDA	retro-Diels-Alder
RP	reversed-phase
SPPS	solid-phase peptide synthesis
TentaGel	polyethylene glycol–polystyrene copolymer resin without any linker
TMS	trimethylsilyl

1. INTRODUCTION AND AIMS

The pharmaceutical industry is still under tremendous pressure to deliver new and successful drugs to the market. To meet this demand requires continuous change by providing new strategies and innovative solutions to improve and speed the journey from early discovery to production. Synthetic chemistry plays a key part in the drug discovery process. New reactivity patterns are discovered every day, along with new reactions and applications of established reactions. In terms of laboratory-based techniques to support these efforts, continuous-flow (CF) processing is emerging as one of the techniques that can significantly impact the synthetic process.[1,2]

This interest can be explained, at least in part, by the number of potential advantages that CF processes have over traditional batch chemistry.[3-5] Namely, the well-regulated flow reactor concept provides an increased parameter space for chemical synthesis and enables reactions to be performed with an unprecedented level of control. It is due to the greatly enhanced heat and mass transfer and improved mixing properties,[6,7] which can translate into higher product quality. A further advantage is that reactions can be carried out at high temperature and pressure accredited to superheating of organic solvents in an inherently greater safety resulting from the small reactor volumes. The accurate tuning of flow reactor parameters, *e.g.* residence time, can further govern the outcome of chemical reactions by determining the reaction rate and the conversion as well as influencing product selectivities.[8-10] Thus, flow chemistry has long been selected to provide a simple means to use more rigorous reaction conditions and revisit difficult reactions that have been neglected in the past.

Focusing on the latter understanding, our major aim was to probe the versatility of the CF technology by developing novel sustainable synthetic methodologies with possible usefulness for the pharmaceutical industry. For this purpose, a study was conducted where the following areas were reinvestigated comparing classical batch methods to CF-based techniques: *i*) retro-Diels–Alder (rDA) reaction [II], *ii*) cyclisation reactions, *i.e.* a three-step domino ring-closure reaction and spirocyclisation (cyclocondensation) [III], *iii*) synthesis of β-peptide foldamers *via* CF solid-phase peptide synthesis (SPPS) followed by rDA reaction [I, IV].

Cyclic β-amino acids have embraced significant interest in organic and medicinal chemistry since they can be widely applied as key moieties in peptide chemistry, in drug

design, and in heterocyclic and combinatorial chemistry. Moreover, enantiomerically pure β-amino acids and their derivatives are used as chiral auxiliaries or chiral building blocks in asymmetric synthesis.[11-17] Herein, the CF benefits have been harnessed to improve our synthetic pathway by searching a time-efficient access to pharmaceutically relevant intermediates and potentially bioactive compounds in a safe, simple and efficient manner, starting from β-aminonorbornene carboxylic acid derivatives [I-IV].

The rDA reaction is an important tool for synthetic chemists in their search towards the synthesis and design of novel heterocyclic scaffolds. However, it has been less explored compared to its parent reaction (Diels–Alder) due to the harsh reaction conditions involved. The endothermic requirements of rDA have led to the use of high temperature conditions, which make it an ideal reaction to be performed under CF processes, where high heat and mass transfer are operative. rDA reaction represents a straightforward and an efficient approach to various racemic and enantiomeric fused pyrimidinones [II,III] as valuable new chemical entities (NCE), with diverse pharmacological potentials.[18,19]

In pharmaceutical applications, foldamers play the role as a novel class of drug scaffolds with tailored molecular shape and surface. These unnatural oligomers have strong tendency to adopt specific and predictable conformations in solution.[20,21] Some of the most thoroughly investigated foldamers are the β-peptides, which possess additional biomimetic properties akin to natural α-peptides including hierarchical self-organisation,[22] conformational polymorphism and real folding reactions.[23-25] By application of the CF rDA reaction on homooligomer peptides containing [1*R*,2*R*]-2-aminocyclohexanecarboxylic acid ([1*R*,2*R*]-ACHC) units possessing an enantiomeric bicyclic residue in the middle of the chain, the effect of new structural elements on conformation was studied too [IV]. It is known that in the case of β-peptides the formation of the homochiral peptide from a racemic starting mixture is still ambiguous compared to natural α-peptides. Through the investigation of the stereochemical discrimination in the synthesis of β-peptides towards the homochiral oligomers, we wanted to gain an insight into the origin of biological homochirality [I].

Publications on which the thesis is based are referred to in square brackets, while other references are given as superscripts.

2. THEORETICAL BACKGROUND

2.1. Principles behind the use of flow reactors

CF reactors have been increasingly used in synthetic organic chemistry to facilitate chemistries, which are otherwise difficult to carry out. It has affected many fields over the last 20 years. A broad range of research in which CF reactors have been propagated includes catalysis,[26-28] nanoparticle synthesis,[29] sensors,[30] electrochemistry[31] and polymerisation.[32] On the basis on channel diameter, CF reactors can be broadly divided into microscale, mesoscale, and large scale.[33] Compared with the conventional batch method, reactors whose flow channels have hydraulic diameters of below 1 mm offer several advantages, such as improved heat and mass transfer as a consequence of the increased surface area to volume ratio.[34-37] Precise temperature control enables suppression of by-product formation.[38,39] Other benefits include efficient mixing,[40] higher conversion and selectivity,[41,42] reduction of the environmental burden and increased process safety through the minimisation of reagent and solvent quantities.[43]

Various basic variances between classical batch experiments and the CF methods can be deduced (Figure 1).[44,45] For instance, in standard reaction vessels the conversion depends on the reaction time, whereas in a CF apparatus a continuous stream of reactant flows through the reactor channels where the transformations take place, and the conversion becomes a function of the distance covered in the reactor.[46] As a consequence, the chemical process becomes space-resolved.

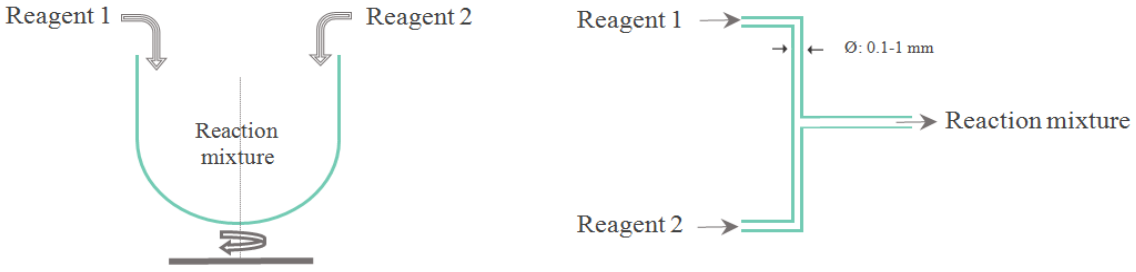

Traditional chemical reactor

Key factors:

- Concentration
- Temperature
- Mixing
- Reaction time

Continuous-flow reactor

Key factors:

- Residence Time
- Heat and mass transfer
- Mixing
- Pressure

Figure 1. Principle of traditional batch reactor *vs*. CF microreactor.

While the flow rate is controlled by means of conventional HPLC pumps (hydrodynamic flow), other means, such as electroosmotic or centrifugal flow are also possible.[47] In a continuous process, the reaction time is assigned as the interval spent by

a given molecule in the active reactor zone and is referred to as the residence time.[6] The conversion correlates with the residence time and can easily be fine-tuned through adjustment of the flow rate or varying the channel length. By screening different types of reactions allows the selection of those, which may be suitable for turning from batch to continuous processes. A few classes of reactions that may take advantage of microreactors and flow conditions are as follows: *i*) extremely fast reactions may be exploited by improving mixing and general transport phenomena; in addition, improved heat transfer should effectively prevent hot spot formation (*e.g.* organometallic reactions), *ii*) kinetically controlled rapid reactions, where a strict control over temperature and residence time may improve selectivity (*e.g.* coupling reactions), *iii*) hazardous reactions that may be carried under more controlled conditions by using flow systems, which also limit hazards due to decreased volumes.[48-51]

Mixing efficiency. Mixing is highly influential in the conversion and selectivity of reactions. In batch reaction vessels, the mixing is mainly achieved by classical mechanical stirring through turbulence at high Reynolds numbers (*Re*) that is the fluid elements exhibit a random motion, which facilitates convective mass transport (Figure 2a).[7] In contrast, the laminar flow of the fluids distinguishes microreactors from classical CF reactors.[7,47] Hereby, the fluid elements flow in parallel lamellae and mixing is governed by molecular diffusion only (Figure 2b).[52] Laminar flow has the advantages of restraining gradient formation in concentration, temperature, pressure, volume and time. Furthermore, the complex channel structure in microreactors generates secondary flow structures at high flow velocities, which lead to very efficient and fast mixing. Transport limitations are therefore reduced with respect to conventional reactor configurations. This leads to important applications in process intensification.[53] According to Fick's law, the velocity of diffusion depends on the channel diameter, which clearly suggests that miniaturisation of the axial dimensions can dramatically enhance the mass transfer in flow reactors.[54] Moreover, the mixing properties in capillary channels can be further improved by using concentric or parallel streams rather than straight lines, and many flow setups include an initial mixing zone prior to the inlet of the actual reactor.[5]

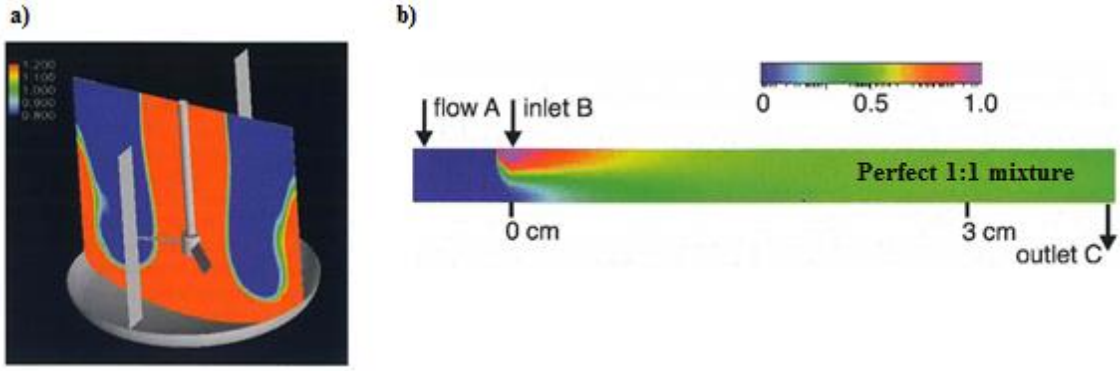

Figure 2. Concentration profiles for mixing (a) in batch, (b) in the CF reactor simulated for a neutralisation reaction between HCl (A) and NaOH (B).[55]

Mass transfer/Heat exchange. One of the most claimed advantages of the modern compact-scale CF reactors is the enhanced heat and mass transfer, compared with conventional batch processes.[5] Mass transfer is a key element of many chemical transformations; the increased surface area-to-volume ratio of microreactors effectively increases mass transfer.[4,55] Efficient and rapid mass transfer can dramatically reduce the reaction time and improve the reaction rate relative to conventional batch experiments. The temperature in flow reactors depends on the kinetics of a chemical reaction.[56] In a complex reaction network with several parallel and sequential reactions, the product distribution is strongly influenced by the temperature of the system. In the course of a chemical reaction, heat is exchanged *via* the reactor surface and, therefore, the surface area-to-volume ratio is a critical factor in efficient reactor design. Heat exchange in microreactors is sufficiently efficient that even highly exothermic reactions can be conducted under nearly isothermal conditions[47] with improved production safety.[5,57] Even explosive reactants[58] or highly unstable intermediates can be handled easily.[59] On the other hand, the superior heat absorption abilities in flow channels can greatly reduce the reaction times of endothermic transformations. This is in contrast to large-scale reactors where significant axial and radial temperature gradients exist. By quickly responding to temperature changes, the formation of undesired by-products can be successfully suppressed.[55,60] As a result of the effective heat and mass transfer, an additional advantage is the much better reproducibility of CF reactions as compared with those in a conventional apparatus.[46] High temperatures in the CF technology are most commonly attained through the use of external ovens, and built-in Peltier elements can be used to achieve better control over temperature. Microwave dielectric heating

has also been integrated into flow devices, and indirect inductive heating techniques have recently been introduced.

Pressure control. When the dimensions are small, even very high pressures result in only modest forces on the reactor walls. Moreover, high pressures can be attained easily in capillary microreactors, and reactions have been carried out safely at pressures above 400 bar.[56] Consequently, microreactors are ideal for studying reactions at high temperature and pressure.[61] Examples of chemical reactions under high pressure conditions of CF processes are cycloadditions, Diels–Alder (DA) reaction, condensation reactions, etc. Pressure increases the miscibility of liquids and the solubility of solids or gases enhances synthetic efficiency. High-pressure conditions are widely employed in CF reaction technology, as modular backpressure valves ensure simpler access to harsh conditions than conventional high-pressure autoclaves.[62] The contained environment and the ease of pressurizing in modern CF reactors remove the boiling point barrier and allow the superheating of solvents in a safe and simple manner, thereby providing novel process windows in an increased parameter space for chemical synthesis.[63,64] Under very high temperature/pressure (T/P) conditions, an unprecedented amount of energy can be supplied to chemical reactions, which leads to improved kinetics and, consequently, the dramatic shortening of reaction times, even in transformations with very high activation barriers.[64,66] With suitable apparatus, even supercritical conditions can be achieved for many organic solvents.

2.2. Application of CF in the synthesis and transformation of heterocycles

2.2.1. Cycloaddiditon and cyclcondensation reactions

Cycloaddition and cyclocondensation reactions are important in the synthesis of heterocycles. They have been prepared in flow to afford a range of valuable *N*-heterocycles with high biological activities and offer synthetic diversity when generating compound libraries.[67-75] In traditional batch-based methodologies such reactions present a challenge (particularly on a relatively large scale), because reaction conditions can be harsh in order to attain acceptable yields. Accordingly, in order to deliver these entities in a flexible, high-yielding fashion, avoiding time-consuming purification procedures as well as hazardous or obnoxious chemical inputs wherever

possible, the flow chemistry methodology has been adopted, at least in part, by the number of potential advantages that CF processes have over traditional batch chemistry.

There are several key demonstrations of these reactions under flow conditions. One of the first examples was introduced by Ley *et al*. using eight parallel microcapillary flow discs (MFDs).[76] The MFD reactor was constructed from a flexible, plastic microcapillary film (MCF) comprising parallel capillary channels with diameters in the range of 80–250 μm. MCFs were wound into spirals and heat treated to form solid discs, which were then used to carry out CF reactions at elevated temperatures and pressures with a controlled residence time. Employing this reactor, the authors demonstrated the scalable synthesis of tetrahydroisobenzofuran derivative **1** *via* DA reaction as illustrated in Scheme 1a. To perform the reaction, reactant solutions were brought together under a pressure-driven flow, where they were mixed prior to heating in a microcapillary flow reactor, using a flow rate of 6 mL min^{-1} within a residence time of 28 min. The authors obtained the target product **1** with almost full conversion and in an isolated yield of 98%, which equates to an impressive throughput of 3.9 kg day^{-1} of the final crystalline product.

More recently, Organ *et al.* reported a series of DA reactions conducted in Pd-coated capillaries through microwave-assisted continuous-flow organic synthesis (MACOS) processed in a single reactor (Scheme 1b).[77] The combination of microwave heating and CF reactor design has long been realised as an ideal marriage of technologies. The feasibility of this system was first demonstrated by Strauss[78] and since then a number of groups have offered their own solutions. They addressed scale-up issues of microwave-assisted reactions, with the limited penetration depth of microwave irradiation into absorbing media and the physical limitations on the dimensions of a standing wave cavity, by combining CF processing with microwave heating.[79-83] When Organ *et al*. performed the reaction in the absence of a Pd coating in an oil bath at 205 °C, only a moderate conversion to (1*R*,4*S*)-dimethyl-7-oxabicyclo[2.2.1]hepta-2,5-diene-2,3-dicarboxylate (**2**) was obtained. This was subsequently increased upon employing a Pd-coated capillary. Utilizing microwave irradiation as a means of heating the flow reactor, the authors found the best conversion to the DA product when the Pd coating was in contact with the reactant (catalytic effect). Much lower activities were obtained with the reactor coated outside (due to a thermal effect) or completely in the absence of Pd.

Based on these findings, a series of DA cycloadditions were performed, whereby conversions were consistently higher than those obtained in an oil bath.

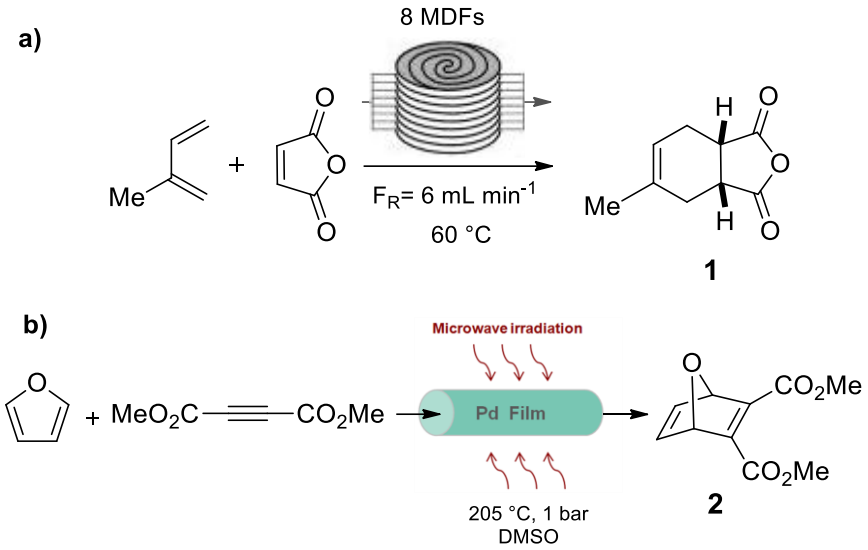

Scheme 1. Examples of DA cycloadditions conducted in flow.

Moreover, macroporous monolith reactors are also applied in a variety of organic transformations investigating several strategies to prepare monolithic microreactors in flow reactions.[84-86] For example, Galarneau *et al.* developed alumina-grafted macro- and meso-porous silica monoliths (Al-MonoSil, 6 mm diameter, 1–4 cm length) as CF reactors for the DA reaction between cyclopentadiene and crotonaldehyde.[87] Given the moderate Lewis acidity and the interconnected system of 5-μm macropores within the monolith, the Al-MonoSil behaved as a suitable heterogeneous catalyst for efficient CF DA reaction with only a low pressure drop (0.5 atm). This system delivered high conversion and productivity of 13 kg adduct per week and per liter of the monolith catalyst. Both Al-MonoSil and zeolites have Brønsted and Lewis acid sites with suitable porosity for organic reactions. Recently, Stevens *et al.* achieved the DA reactions of cyclopentadiene (**3**) and methyl acrylate (**4**) under CF conditions catalyzed by heterogeneous H-Beta type zeolite (Scheme 2a).[88] The use of H-Beta type zeolite with the largest pore diameter and surface area gave a high conversion (>95%) and end-selectivity (89:11) using a 1:1 stoichiometry of diene and dienophile. The catalytic activity and the productivity of the adduct under the flow process were 3.5 and 14 times higher, respectively, compared with the lab-scale batch process. Moreover, the zeolite catalyst could be used multiple times by including a 5-h calcination step to regenerate the used zeolite.

Asymmetric DA reactions using chiral heterogeneous catalysts under CF conditions have also been achieved. As an illustrative example, the Luis group developed chiral Ti-TADDOLate immobilised on cross-linked polystyrene monolith and carried out the flow reaction of cyclopentadiene with 3-crotonoyl-1,3-oxazolidin-2-one.[89] In this study, however, the flow process using the obtained chiral heterogeneous catalyst afforded low yield and enantioselectivity that is it had no significant advantage compared with the batch process. On the other hand, the heterogeneous organocatalyst worked efficiently in the addition of Et_2Zn to benzaldehyde under CF conditions. Benaglia *et al.* developed an immobilised MacMillan-type imidazolidinone catalyst on silica and a cross-linked polystyrene monolith and examined their catalytic activity. The CF reaction between cyclopentadiene and cinnamylaldehyde (**5**) with the packed-bed reactor of the heterogeneous MacMillan-type catalyst maintained stable conversion with good enantioselectivity over several days (Scheme 2b).[90] The polystyrene monolith was then studied in the 1,3-dipole addition of *N*-benzyl-*C*-phenyl nitrone with cinnamylaldehyde (**5**).[91] However, because of the extremely low turnover frequency of this catalyst, this process required long contact times of 12.4 h for full conversion of substrates, and achieved low productivity.

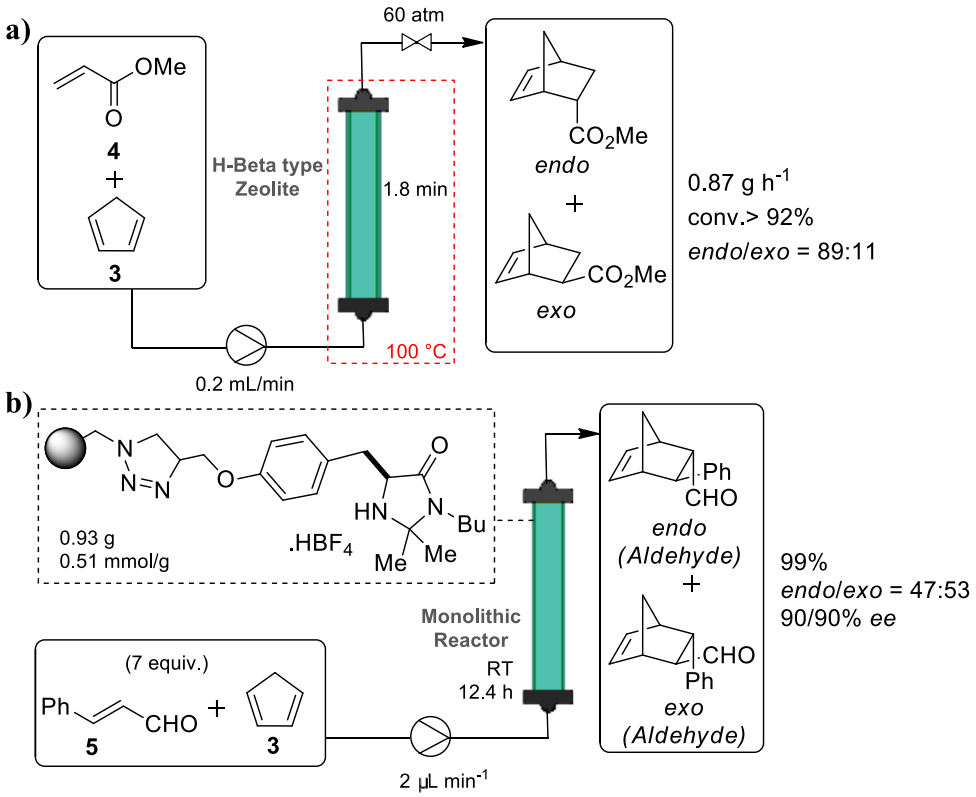

Scheme 2. Examples of catalyzed DA reactions performed in CF mode: (a) H-Beta type zeolite catalyst, (b) monolithic reactor for CF stereoselective cycloaddition.

Another example of the DA cyclisation was reported by Djuric *et al*. for the synthesis of benzoisoindolines and benzoisoquinolines through inter- and intra-molecular DA cycloaddition of *ortho*-quinodimethanes (*o*-QDMs) as shown in Scheme 3a.[92] These highly reactive dienes are accessed through the thermal electrocyclic ring-opening of benzocyclobutenes. Due to the aromaticity of these systems, this reaction occurs typically with flash vacuum pyrolysis (FVP) or with prolonged heating in high-boiling solvents, thus greatly limiting its application in drug discovery programs. Djuric *et al.* adapted a new methodology by applying a modified and automated high T/P Phoenix™ flow reactor. The instrument is capable of achieving up to 450 °C and 200 bar of pressure and allows the use of superheated conventional solvents and, therefore, reaction times can be dramatically shortened.[92] By employing the same reactor, the research group also synthesized several libraries of fused pyrimidinone and quinolone derivatives *via* the Gould–Jacobs reaction (Scheme 3b).[93] The condensation of an aryl amine with an alkoxymethylene compound followed by thermal ring-closure reaction under high T/P flow conditions allowed the synthesis of fused pyrimidinone and quinolone derivatives in good to high yields within 0.5–8 min.

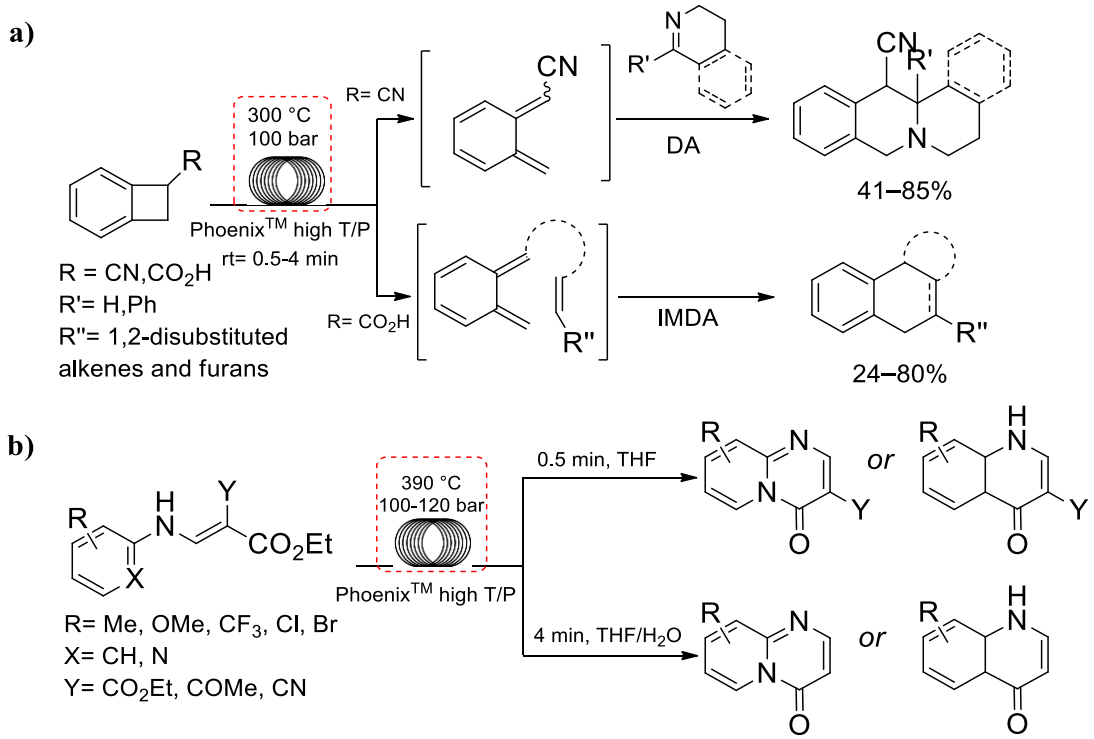

Scheme 3. (a) Inter- and intra-molecular DA cycloadditions of *o*-QDMs. (b) Reaction sequence leading to Gould–Jacobs-type products.

Ley *et al*. reported the cyclisation *via* 1,3-dipolar cycloaddition of non-stabilised *N*-(methoxymethyl)-*N*-(trimethylsilyl)benzylamine (**6**) with nitroalkenes **7** using flow

reactors.[94] A solution of the alkene and trifluoroacetic acid (TFA) required to generate the dipole was flowed through a T-piece, where it was combined with a stream of the azomethine ylide precursor (Scheme 4a).[94] The combined stream was then passed through a heated reactor coil and subsequent scavenger columns in order to remove any unreacted alkene. By using this method, 10 different examples of 3-nitropyrrolidine scaffolds were synthesized in good yields (74–93%). A similar cycloaddition reaction has also been reported in flow by the Fray group.[95] The same azomethine ylide precursor (**6**) was used to synthesize the pyrrolidine ring. Using different alkene substrates, they were able to perform the reaction at 70 °C in 10 min (Scheme 4b).

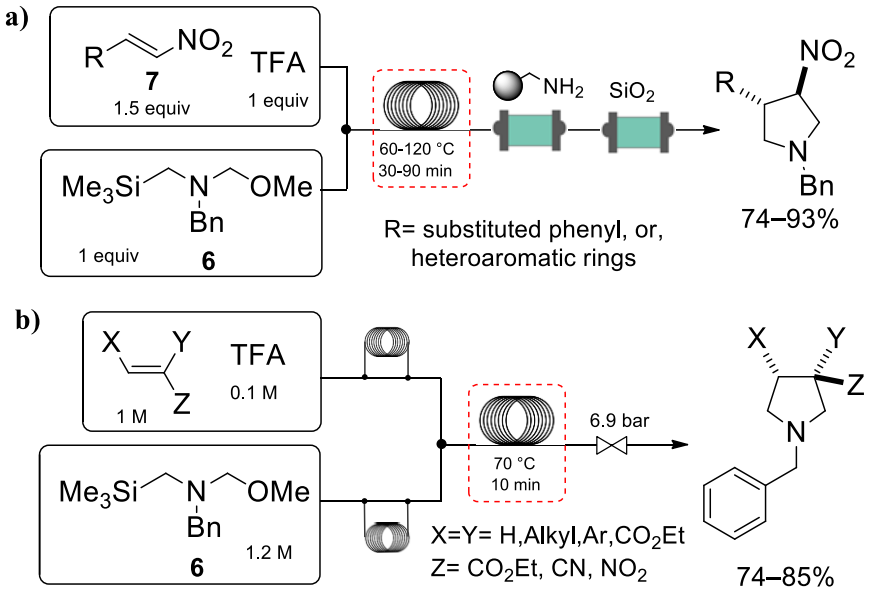

Scheme 4. Examples of 1,3-dipolar cycloaddition for the synthesis of pyrrolidine.

In their work synthesizing pyrazoles under high T/P flow conditions, Kappe *et al.* prepared varied inhibitors of canonical transient receptor potential channels (TRPC).[96] The use of high temperatures allowed the condensation of hydrazines with enones enabling the fast synthesis of several pyrazoles. Subsequent palladium-catalyzed Buchwald–Hartwig amidation under microwave conditions afforded a range of bioactive TRPC inhibitors in good yields. Another application of high temperature flow conditions for heterocycle formation was reported by Herath and Cosford.[97] Microreactors were used to perform a Hantzsch pyrrole synthesis using HBr generated during the reaction to directly hydrolyze *tert*-butyl acetoacetate ester **8** to afford pyrrole-3-carboxylic acids **9a-h** (Scheme 5a). [97] Product acids could also be further reacted with amines to the corresponding amides. A further report by Cosford *et al.* demonstrates the synthesis of thiazoles making use of high temperature microreactors in a two-step

synthesis (Scheme 5b).[98] Initially, the condensation of α-bromoketones with thioamide gives β-ketothiazoles by the Hantzsch thiazole synthesis. A stream of aldehyde with urea was then combined with the main stream and heated for 10 min yielding dihydropyrimidinones **10** *via* the Biginelli reaction. The same research group reported the two-step synthesis of imidazo[1,2-*a*] heterocycles using microreactors.[99]

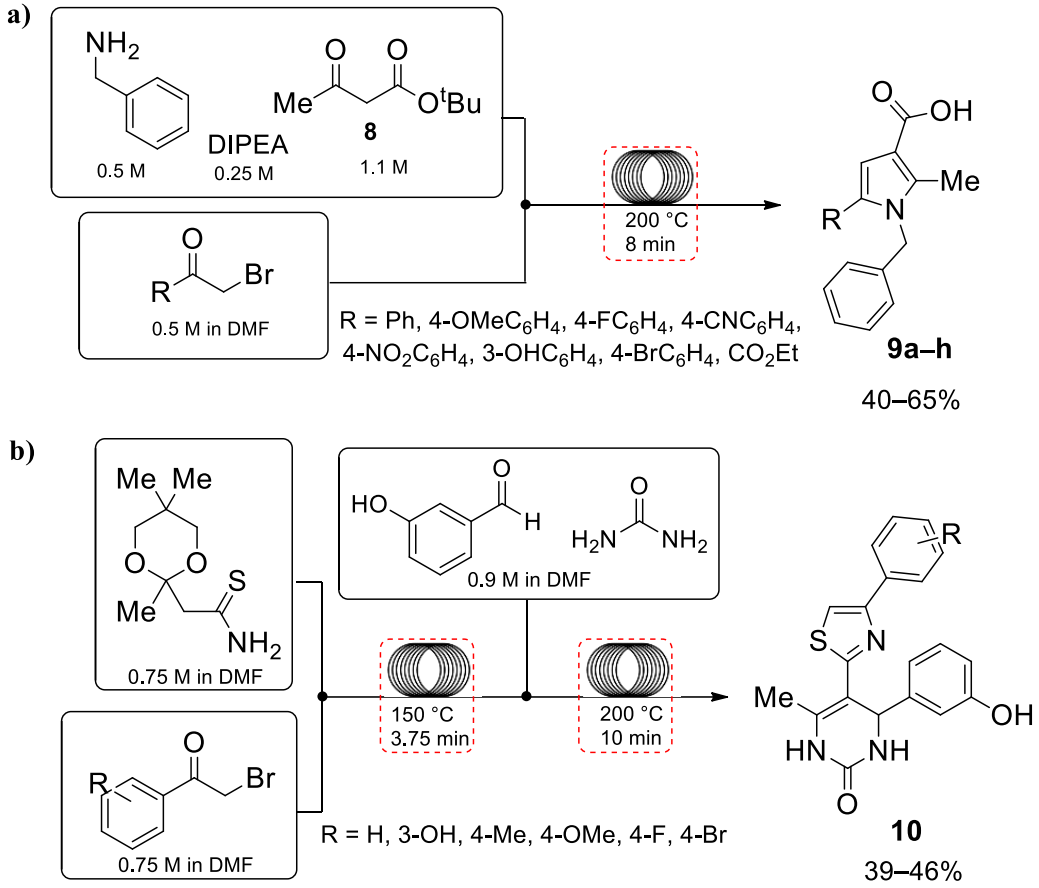

Scheme 5. Examples of cyclocondensation reactions in flow.

Furthermore, Mason *et al.*[100] presented a series of cyclodehydrations of a number of Bohlmann–Rahtz aminodienones illustrating the use of CF processing to transfer operations from commercial microreactors and microwave batch reactors to mesoscale production using different technology platforms, including a microwave flow reactor. It is noteworthy that CF processing offers ready automation, improved reproducibility, enhanced safety and considerable process reliability, whereas microwave heating promises improved kinetics and even selective coupling, thus providing opportunities for the rapid processing of materials. As a last example, the end-to-end multistep CF setup reported by Ley *et al*. is briefly discussed here.[101] It is a four-step conversion of anilines into *N*-arylated pyrazoles *via* amine-redox cycle followed by hydrolysis of the

hydrazine surrogate ensuing cyclocondensation. The telescoped flow process offers a distinct advantage over the corresponding batch procedures due to the *in situ* formation and use of several reactive intermediates. Critically, this end-to-end style of synthesis avoids the stock-piling and storage of hazardous drug intermediates (diazonium salts and hydrazines) by directly advancing them to the next step as they are produced.

2.2.2. Retro-Diels–Alder reaction

Heterocyclic skeletal transformations are among the most powerful synthetic strategies for the construction of complex molecular frameworks from simple feedstocks.[102-104] In this context, the DA and rDA reactions are the prevailing approaches, since they lead to valuable *N*-heterocycles of high biological activity, such as isoindolo-, pyrrolo- and 2-spiro-quinazolinones. The DA reaction comprises a reversible [4+2] cycloaddition between a conjugated diene and a substituted alkene (dienophile). The reverse process of the DA reaction is the rDA reaction as illustrated in Scheme 6.[105]

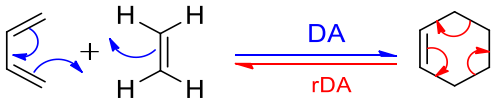

Scheme 6. DA/rDA reaction of cyclohexene

The thermal [$_{\pi}4+_{\pi}2_{s}$] cycloreversion of an organic compound containing a double bond in a six-membered ring leads to the formation of a diene and a dienophile (DA adducts). This pyrolytic dissociation arises when one or both fragments are notably stable.[106] The unsaturation present in the original starting material is protected in the DA adduct, and the same atoms are involved both in the bond formation and bond cleavage steps.[107-109] The rDA process is an efficient technique for the introduction of a double bond into a heterocyclic skeleton[110] as well as for the enantiodivergent[111] and the enantiocontrolled[112] syntheses of heterocyclic compounds. A particular characteristic of the DA/rDA approach makes use of the rigidity and chirality of the DA adducts, which are attainable in reactions between cyclic dienes and cyclic dienophiles. Because of the endothermic nature of rDA fragmentation, high temperatures are usually needed in order to overcome the high activation barrier of the cycloreversion. In some cases, extreme conditions such as FVP (at 600–900 °C), shock tube, photochemical (laser) activation or the use of gamma-radiation are required. Although these methods have

several advantages, the end products often undergo rearrangements or decomposition. Application of the rDA under traditional batch conditions for the laboratory-scale preparation of heteromonocycles or condensed-ring heterocycles has been widely examined and discussed.[113-117] rDA products can be gained by distillation under reduced pressure,[118] boiling in a solvent,[119,120] and applying microwave irradiation[121-124] or FVP.[124,125]

The harsh reaction conditions required for rDA coupled with the problems associated with instability of the products under these conditions have prompted chemists to look for alternate mild conditions for effecting rDA reactions. Various efforts were undertaken in this direction; for instance, the inclusion of trimethylsilyl (TMS) group or by creating a strain in the molecule.[126,127] The trimethoxysilyl group imparts a positive effect on rDA reactions by lowering the activation energy.[128] It is possible to perform an rDA reaction under mild conditions by judiciously incorporating a heteroatom in the DA adduct. The Kotha group reported a novel observation performing the rDA reaction by introducing a cyclopropane ring at C-7 of the norbornene system.[129] This result clearly indicated that an increased delocalisation in the transition state involving the cyclopropane orbitals is responsible for the bond-breaking process and thus increasing the rate of the rDA reaction. Noteworthy, the thermal rDA reaction of anthracene cycloadducts can speed up by electron-donating groups. In a similar manner, the incorporation of an oxide anion substituent strongly accelerates the rDA process too.[130,131]

Flow chemical approaches have been found to ensure better control of chemical processes due to improved heat and mass transfer. Unconventional and harsh reaction conditions such as greatly elevated temperatures and pressures can be generated easily allowing the superheating of organic solvents far beyond their boiling point in a controlled and safe manner. The rDA reaction, for its characteristics such as being a thermally-driven process, is an ideal reaction to be performed in CF. In spite of this, precedents are scarce. In fact, the CF rDA method was utilised only once by the Myers group performing the preparation of a precursor intermediate for the construction of diverse tetracycline antibiotics.[132] As an illustration, a solution of reactants (0.02 M) were dissolved in diphenyl ether and pumped continuously using a peristaltic pump through a stainless-steel tube submerged in an oil bath heated to 250 °C at a flow rate of 12 mL min^{-1} (Scheme 7).

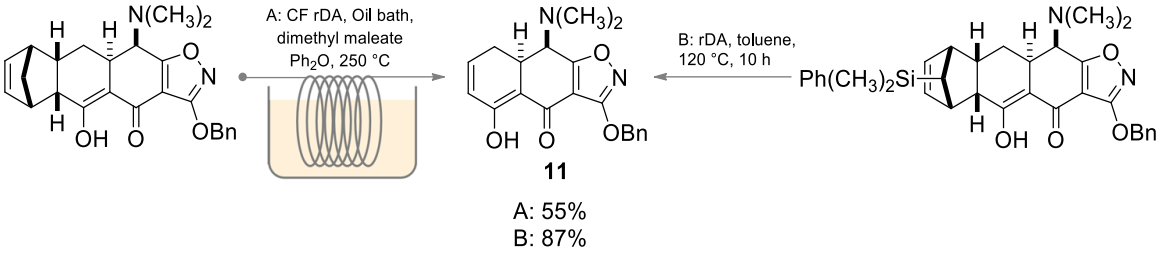

Scheme 7. rDA reaction for the preparation of an intermediate of tetracycline antibiotics.

By applying these conditions, the authors obtained rDA product **11** in a moderate yield (55%). Due to the difficulties of handling the CF reactor and the use of a large volume of high-boiling solvent, the authors headed towards the development of an alternative protocol to perform the rDA reaction. The use of dimethylsilylcyclopentadiene was particularly appealing because of its simplicity and the possibility that 5-silylcyclopentadiene might be recycled. Thus, by using this method, the authors could get retrodiene product **11** in an improved yield (87%) compared to those achieved by the CF method.

Moreover, there are a few other examples, which might be related to the application of rDA reaction under CF conditions. For example, Martin *et al*. introduced the synthesis of annulated pyridines from 2-substituted acetylene pyrimidines under superheated CF conditions by an intramolecular inverse-electron-demand hetero-/retro-Diels–Alder reaction (ihDA/rDA).[133] The flow system was equipped with a high-temperature 316 stainless steel tube flow reactor placed into a GC oven and a 250 psi back-pressure regulator (BPR). Using this stable and scalable flow process, a series of annulated pyridines were produced in good to excellent yields and in significantly reduced reaction times when compared to the corresponding batch process. In the same context, Blanchard and coworkers reported the synthesis of various polycyclic fused- and spiro-4-aminopyridines from pyrimidines through a [4+2]/retro-[4+2] cycloaddition between a pyrimidine and an ynamide, which constitutes the first examples of ynamides behaving as electron-rich dienophiles in [4+2] cycloaddition reactions.[134] In addition, running the ihDA/*r*DA reaction in the continuous mode in superheated toluene to overcome the limited scalability of MW reactions, results in a notable production increase compared to batch mode.

2.3. Application of CF in the synthesis of β-peptide foldamers

Foldamers are artificial self-organizing biomimetic polymers,[135-142] similar to natural peptides, proteins, RNA and DNA. These systems have a strong tendency to form highly stable and versatile secondary structures, such as helices, strands and turns (Figure 3).[142-145] Foldamers have numerous biomedical activities.[146,147] There are antibacterial amphiphills,[148] cell and membrane penetrating peptides,[149] anti-Alzheimer compounds,[150] and compounds effectively modulating protein–protein interactions.[151] Based on this fact, they are nowadays considered as proteomimetics.[146] Some of the most thoroughly investigated foldamers are the β-peptides,[152] which possess additional biomimetic properties akin to natural β-peptides including hierarchical self-organisation, conformational polymorphism, and real folding reactions.[23]

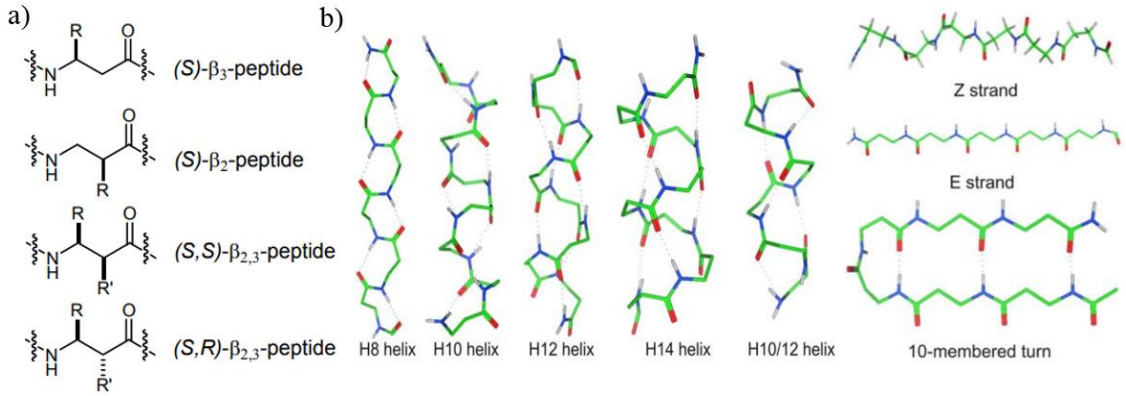

Figure 3. β-Peptide foldamers: (a) general substitution pattern of β-peptides and (b) examples of β-peptide secondary structures.

Foldamer synthesis is generally achieved by two methods: *i*) solution-phase synthesis and *ii*) solid-phase peptide synthesis (SPPS) either with a *tert*-butoxycarbonyl/benzyl (Boc/Bzl)[153] or with a 9-fluorenylmethoxycarbonyl/*tert*-butyl (Fmoc/^{t}Bu)[154] technique.

2.3.1. Continuous-flow solution-phase peptide synthesis

In solution-phase peptide synthesis, two protected amino acids are mixed in the presence of a suitable activator/base in the liquid phase. This method was used for the first synthesis of [1*R*,2*R*]-ACHC homooligomers by applying Boc for amino protection and the benzyl ester for carboxyl protection with the activation performed with 1-ethyl-3-(3-dimethylaminopropyl)carbodiimide (EDCI) and 4-(*N*,*N*-dimethylamino)pyridine (DMAP).[135] However, this method suffers from various drawbacks: the reaction time is very long and carbodiimide activation can lead to racemisation. Furthermore, decreased

solubility caused by the protected oligomer can give truncated sequences resulting in difficulties in product purification. To avoid the mentioned difficulties and the need for more complex peptides, SPPS has been applied. In addition, significant effort has been devoted to developing CF solution-phase peptide assembly protocols. For instance, Haswell *et al*. demonstrated the synthesis of di- and tri-β-alanine (Ala) peptides using a borosilicate glass microreactor in which reagents were mobilised by electroosmotic flow (EOF).[155-158] The method involves the use of a photolithographic technique and wet etching for fabricating microchannel in the reactor with materials comprised of negatively charged functional groups (Scheme 8). The bulk solvent flow was induced by EOF and the direction and magnitude of the flow may be readily altered by varying the applied voltage. Within this miniaturised systems, a solution of reagents (0.1 M), Fmoc-β-alanine, EDCI and dimethylamine borane (Dmab) ester of β-alanine, used in the reaction were placed, respectively, in the reservoirs A, B and C, whereas reservoir D was used to collect the products (Scheme 8). Platinum electrodes were placed in each of the reservoirs and an external voltage was applied to the channels inducing EOF of the reagents. For 20 min, at room temperature, only a moderate conversion to the final di-β-Ala peptide **12** was observed. By using dicyclohexylcarbodiimide (DCC, 0.5 M) as an alternative carbodiimide coupling reagent, the dipeptide was afforded in a good yield of 93% (Scheme 8a). Furthermore, this protocol was successfully employed in the synthesis of tripeptide **13** involving a preactivated pentafluorphenyl (PFP) ester, albeit with a low yield of 30% (Scheme 8b).

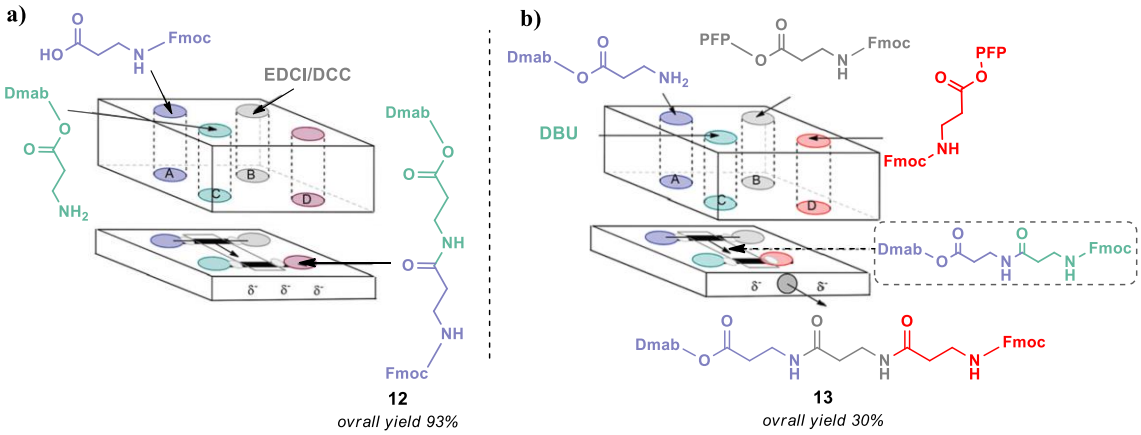

Scheme 8. Schematic representation of flow-based microreactor used for the preparation of (a**)** β-alanine di-peptide and (b) β-alanine tri-peptide.[157]

When utilizing mechanical pumping, Flogel *et al*. introduced the synthesis of a series of tetra-β-peptides using a silicon-based CF microreactor.[159] They have also claimed

that this synthesis was the first (*i*) to achieve Boc and Fmoc amino acid coupling in only 1–5 min at high temperature (120 °C); (*ii*) to use β_2- and β_3-homoamino acids containing a fluorous benzyl group, with the aim to facilitate the purification *via* fluorous solid-phase extraction (FSPE) for β-peptide synthesis; and (*iii*) to show the relevance of a $C_{10}H_4F_{17}$-substituted benzylic ester protecting group in solution-phase coupling. The flow reactor was designed to be compatible with a wide range of organic solvents and can be operated over a broad temperature range (–80 °C to +150 °C) with a total prequench volume of 78.3 mL. The system was utilised to furnish tetrapeptide **14** (Scheme 9). Assembly of tetrapeptide **14** was first conducted by forming the β_3–β_3 peptidic bond, which was synthesised at 90 °C in 3 min with 2 equiv. of the acid fluoride [Boc-β_3h(*R*)Ala-F] and 4 equiv. of *N*-methylmorpholine (NMM). The formation of the sterically more demanding β_3–β_2 peptide bond required higher temperatures and extended residence time with a maximum conversion obtained at 120 °C in 5 min [2 equiv. of acid fluoride Boc-β_3h(*R*)Val-F, 4 equiv. of NMM]. The final β_2–β_3 coupling was also established at 120 °C in 1.5 min and the tetramer was obtained in an overall yield of 81%.

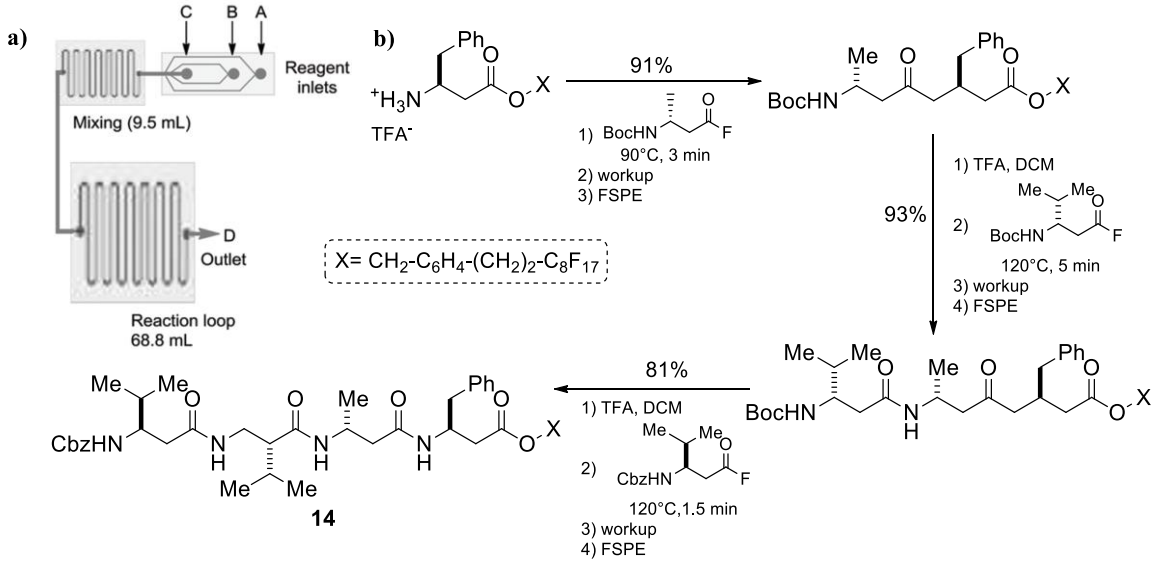

Scheme 9. (a) Schematic representation of the microreactor showing the three inlets: A = acid fluoride; B = amino acid benzyl ester; C = NMM, D = the outlet and quench port (TFA and the internal standard); (b) β-peptide synthesis *via* CF in the solution phase.[159]

2.3.2. *Continuous flow solid-phase peptide synthesis (CF-SPPS)*

This technique is based on the reaction of an *N*-protected amino acid immobilised on an insoluble support usually a polymer, in most cases, through the carboxylic function. The reaction is extended by the removal of *N*-protection and the addition of the second protected amino acid. The excess reagents used are removed by simple washing and filtration. Although SPPS has advantages features, it has several drawbacks, including the requirement of an expensive resin, and additional steps like attachment of the first amino acid to the resin and its final removal. In this regard, microreactors could overcome some of these shortcomings. Moreover, the long coupling times may be reduced by the application of microwave-assisted SPPS.[160] Thus, a CF-SPPS mesoscale reactor consisting of HPLC-based modules, which allowed the construction of peptides and foldamers with only 1.5 equiv. amino acids, has been developed by our research group.[161] The reactor consists of an HPLC pump for liquid delivery, an autosampler injecting the reagents necessary for peptide synthesis, mainly the deprotection solution and the coupling mixture. The coupling mixture can be prepared directly by the autosampler or can be premixed manually before the synthesis. The resin is filled into the HPLC column and heated by a column thermostat. Finally, a pressure regulator is an important part of the system. Through a complete reaction parameter optimisation, all 20 proteinogenic amino acids can be coupled with only a 1.5-fold excess of amino acids. The technology was tested by the synthesis of two difficult sequences. In both cases, the CF-SPPS technology showed superior performance compared to microwave-assisted SPPS technology when only a 1.5-fold excess was utilised. Such a low excess is tremendously important in the coupling of artificial, exotic and expensive amino acids, which are used for the construction of foldameric systems. By the utilisation of the CF-SPPS technology, various foldameric systems were assembled (The schematic representation of the reactor is shown in the Materials and Methods section; page 21, Figure 5).

3. MATERIALS AND METHODS

3.1. Continuous-flow protocols

Continuous-flow retro-Diels–Alder (CF rDA) reactor: CF rDA reactions were performed on a modular flow system equipped with heated 304 stainless steel tubing coil with 14 mL internal volume [Supelco premium grade 304 empty stainless steel tubing; dimensions: length (L) × outer diameter (OD) × inner diameter (ID) = 100 ft×1/16 in×0.03 in; product number 20553] and an adjustable back-pressure regulator (ThalesNano, BPR, 0–300 bar). The tube reactor was heated in a Heraeus oven to the desired temperatures (Figure 4). Solutions of the starting materials were loaded into the reactor *via* an HPLC pump. The most important reaction parameters such as temperature, pressure, flow rate and substrate concentration were systematically fine-tuned to determine optimal conditions. The residence time was set by the use of coils with different lengths. The crude products were analysed by thin-layer chromatography and, if necessary, column chromatographic purification was carried out. The products of the CF reactions were characterised by means of NMR (^{1}H, ^{13}C), HPLC–MS and FT-IR spectroscopy. In the cases of chiral compounds, *ee* was assigned with a Phenomenex IA column.

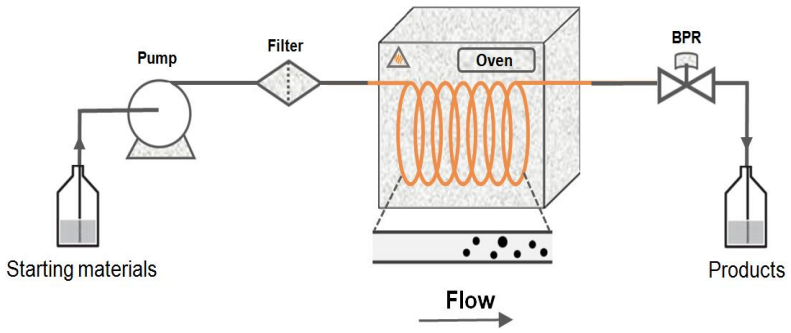

Figure 4. Setup of the continuous-flow retro-Diels–Alder reactor.

Continuous-flow solid-phase peptide synthesizer (CF-SPPS): Peptides were synthesized by using a standard solid-phase technique utilizing the CF-SPPS reactor constructed previously.[161] The CF reactor consists of an HPLC pump, an HPLC injector or autosampler, a cylindrical fillable HPLC PEEK column, and an HPLC BPR as shown in Figure 5.

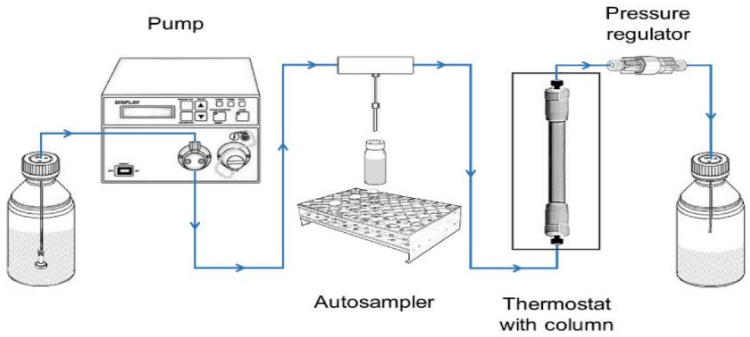

Figure 5. Schematic representation of the CF-SPPS reactor.[162]

CF hydrogenation reactor: Reactions were performed in an H-Cube® flow reactor apparatus equipped with a gas-generation unit consisting of a reservoir for deionised water and a built-in electrolysis cell for the generation of H_2. The gas generated *in situ* is combined *via* a gas–liquid mixer with the solution of the substrate, and then the mixture is transported to the catalyst (10% Pd/C) bed, where the triphasic reaction takes place.

3.2. Synthesis

Pyrimidinone-fused moieties prepared by flow synthesis:

Domino ring-closure and spirocyclisation reactions: Racemic or enantiomeric β-aminonorbornene carboxamide (1 mmol) and γ-keto acids or cycloalkanones (1.2 mmol) were dissolved in toluene or ethanol (EtOH) (50 mL). The system temperature in the flow rector illustrated in Figure 4 was set to 100 °C, the pressure to 10 bars and the flow rate to 0.2 mL min^{-1}. When the pressure and the temperature of the flow system were stable, the solutions were loaded into the reactor passing through the heated reactor coil. Within a reaction time of 6 h, the flow output was collected. The solvent was removed by evaporation and the solid residue was, if necessary, dissolved in a mixture of ethyl acetate and methanol (EtOAc/MeOH) (9:1 v/v) and transferred to a neutral SiO_2 column, or simply crystallised in Et_2O and the crystals were filtered and washed with Et_2O. The analytical and spectroscopic data of the intermediate pyrimidinone derivatives were identical to those found in the previous batch methods.

Retro-Diels–Alder reaction. The racemic or enantiomeric intermediate pyrimidinone derivatives (100 mg) were introduced into the flow reactor (Figure 4) in a solution of acetonitrile (MeCN) or toluene or toluene/MeOH (4:1, 25 mL). The pressure was kept

at a constant value of 10 bars and the flow rate was varied in the range 0.5–0.2 mL min^{-1}. The solutions were pumped into the reactor and passed through the heated reactor coil at 150–250 °C, within a residence time of 10–60 min and collecting the flow output. The solvent was removed by evaporation, the residues were either crystallised in Et_2O (5 mL) or transferred to a SiO_2 column, dissolved and eluted in EtOAc/MeOH (9:1). The analytical and spectroscopic data of the retrodiene products were identical to those found in the previous batch and in microwave processes. Details of syntheses, physical and analytical data on new compounds described in the thesis and descriptions of NMR spectroscopic analyses can be found in the experimental parts of the enclosed publications.[II, III]

Peptide synthesis: Peptides were synthesized on a solid support by means of CF-SPPS (Figure 5) involving Fmoc chemistry with chain lengths of the oligomers varying between 3–6 units. The peptide chains were elongated on TentaGel R RAM resin (0.19 mmol g^{-1}) carried out manually on a 0.1-mmol scale. Couplings were performed with HATU/DIPEA {HATU = [2-(7-aza-1H-benzotriazol-1-yl]-1,1,3,3-tetramethyluronium hexafluorophosphate, DIPEA = N,Ndiisopropylethylamine} without difficulties. The formed peptide sequences were cleaved from the resin with TFA/H_2O (95:5) at room temperature in 3 h. TFA was then removed and the resulting free peptides were solubilised in aqueous AcOH (10%), filtered and lyophilised. The crude peptides were purified by using reversed-phase HPLC (RP-HPLC).

CF hydrogenation: Reactions were performed in an H-Cube® flow reactor apparatus. The unsaturated precursor purified previously was dissolved in MeOH and hydrogenation was carried out on 10% Pd/charcoal catalyst (50 atm, 1 mL min^{-1} flow rate). Characterisations were performed by using HPLC–MS.

Diastereodiscriminative peptide coupling: Peptide solutions (0.01 mmol) were prepared separately with HOBt (0.12 mmol) and DIC {HOBt = hydroxybenzotriazole; DIC = *N*,*N*′-diisopropylcarbodiimide} (0.12 mmol) in CH_2Cl_2/DMF (2:1) in the absence or in the presence of water (2:1:1) followed by adding Boc-protected racemic amino acids (0.1 mmol). The mixtures were stirred for 48 h, CH_2Cl_2 was removed by evaporation, and water was added to the residue followed by lyophilisation. The products were treated with TFA/H_2O (95:5) to remove the Boc protecting group. The solutions were

then stirred for 30 min, TFA was removed in vacuo, the residue was diluted with water and then lyophilised. Samples were analysed by HPLC–MS.

3.3. Analytical investigations

HPLC measurements: Crude peptides were purified by using RP-HPLC over a Nucleosil C18 (7 μm) 100 Å column (16 mm×250 mm). All structures were analysed by HPLC–MS with a Phenomenex 5 μm C18(2) 100 Å column (250×4.60 mm). Solvent systems consisted of AcOH (0.1%) in water (A) and AcOH (0.1%) in MeCN (B); gradient: 5%–100% B over 35 min, at a flow rate of 1 mL min^{-1}. Chromatograms and spectra were recorded in positive ionisation mode with electrospray ionisation (ESI) on a Thermo LCQ Fleet mass spectrometer.

Nuclear magnetic resonance (NMR): Fused pyrimidinone moieties were measured at ambient temperature, with a Bruker AM 400 or Bruker Ascend^{TM} 500 spectrometer using tetramethylsilane as internal standard. ^{1}H-NMR spectra were recorded at 400.13 MHz or 500.20 MHz and ^{13}C-NMR spectra were recorded at 100.62 MHz or 125.77 MHz in $CHCl_3$ or d_6-DMSO.

4. RESULTS AND DISCUSSION

4.1. Continuous-flow retro-Diels-Alder decomposition of pyrimidinone-fused moieties

Fused pyrimidinone derivatives are well known for their pharmacological properties. These compounds have several therapeutic applications as anticancer,[163] interferon inducer,[164] antiviral,[165] anti-hypertensive,[166] hypoglycaemic,[167] anticonvulsive,[168] anti-histaminic[169] and anti-inflammatory drugs.[170] The pyrrolo- and pyrido[2,1-*b*]quinazolinones include well-known alkaloids isolated from a number of plant families. Because of these therapeutic interests, their syntheses have been studied very thoroughly.[171] Herein, we have designed a novel synthetic process for the preparation and transformation of distinct pyrimidinone-fused moieties, such as pyrrolopyrimidinones, pyrimidoisoindoles, and spiropyrimidinones, by means of the highly-controlled CF rDA reaction.[II, III]

4.1.1. Preparation of the intermediate functionalised pyrimidinone derivatives

To test the viability of our CF rDA protocol, the intermediate quinazolinone derivatives (starting materials) were selected to comprise; *i*) molecules where good, medium and no conversion was observed under batch rDA conditions, *ii*) more complex racemic or enantiomeric fused pyrimidinone moieties, *iii*) molecules which have never been subjected to rDA reactions under batch conditions. The intermediate pyrimidinones **16**–**38** have been previously prepared by literature methods. Cyclisation of the corresponding amino acids or esters **15a–c** with ethyl *p*-chlorobenzimidate resulted in tricyclic *diexo* or *diendo* pyrimidinones **16**, **17b** and **17c** (Scheme 10).[110,116,172-175]

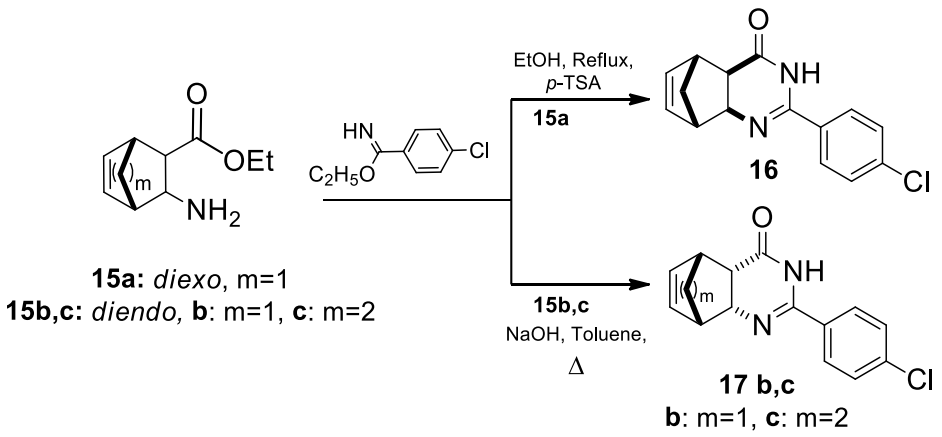

Scheme 10. Synthesis of the tricyclic pyrimidinone derivatives **16**, **17 b**,**c**.

Furthermore, the preparation of methanopyrrolo-, methanopyrido- and methanoazepino[2,1-*b*]quinazolinones **18–21** was processed by ring enlargement of *diexo*-norbornene-fused azetidinone **5d** with lactim ethers (Scheme 11).[176]

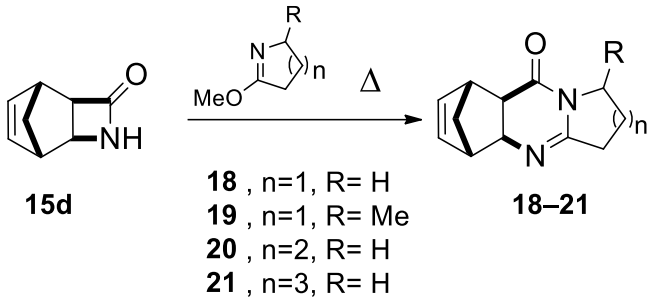

Scheme 11. Synthesis of quinazolinone derivatives **18–21**.

For the preparation of methylene- and ethylene-bridged 2-thioxopyrimidinones **22**, **23b** and **23c**, the most common method is the reaction of the appropriate amino esters **15a–c** with phenyl isothiocyanate, followed by cyclisation of the resulting thiourea with hydrogen chloride under reflux (Scheme 12).[172,175]

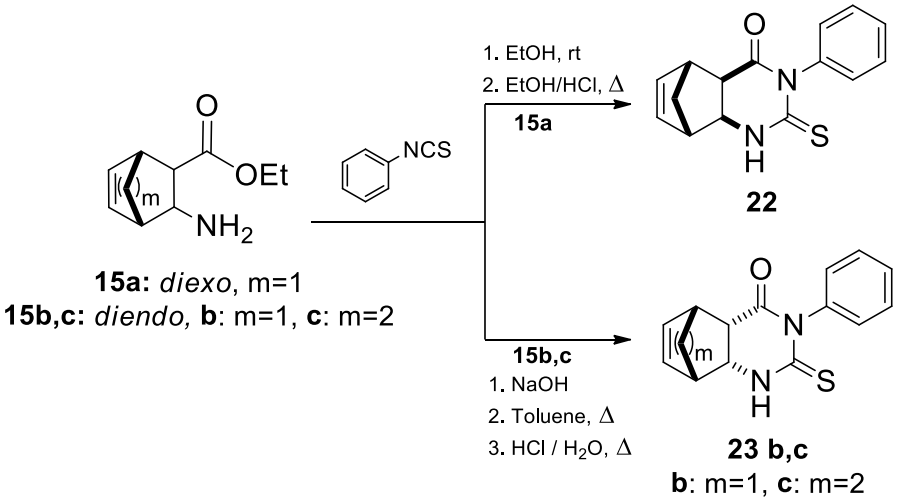

Scheme 12. Synthesis of thioxopyrimidinone derivatives **22**, **23 b**,**c**.

Moreover, the cyclisation of racemic *diexo*-3-aminobicyclo[2.2.1]hept-5-ene-2-carboxamide **15e** or *diexo*-3-*N*-methylbicyclo[2.2.1]hept-5-ene-2-carboxamide **15f** with γ-oxocarboxylic acids in toluene under reflux in the presence of *para*-toluenesulfonic acid (*p*TsA), through three-step domino reactions, resulted in single diasteroisomers of pyrrolo[1,2-*a*]quinazolines **24–26** or isoindolo[2,1-*a*]quinazolines **27–29** (Scheme 13).[177,178]

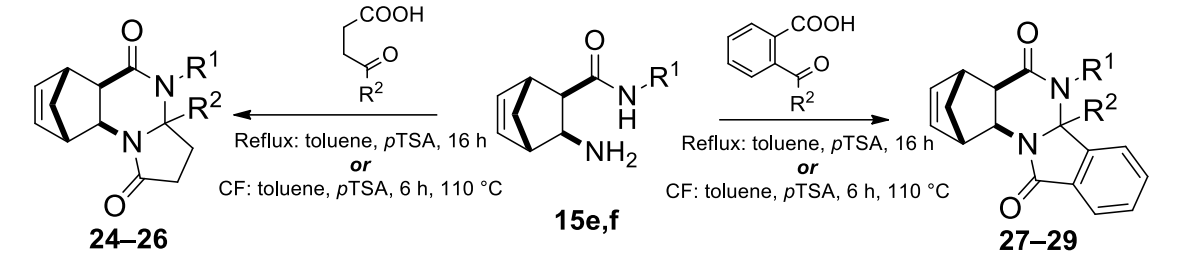

24: R^1= H, R^2= Me
25: R^1= R^2= Me
26: R^1= Me, R^2= 4-MeC_6H_4

15e: R^1= H; **15f**: R^1= Me

27: R^1= Me, R^2= H
28: R^1= R^2= Me
29: R^1= Me, R^2= 4-MeC_6H_4

Scheme 13. Synthesis of pyrrolo- and isoindolo[2,1-*a*]quinazoline derivatives **24–29**.

Upon heating with cyclohexanone under reflux in EtOH, β-aminonorbornene carboxamides **15e**, **15g** and **15h** were cyclised to give methylene- and epoxy-bridged 2-spiroquinazolinones **30–32**.[179] These compounds could alternatively be prepared under dry (solvent-free) conditions by stirring for 2 days.[180] Spiropiperidine derivatives **33–35** were formed by the condensation of carboxamides **15e**, **15g** and **15h** with 1-benzylpiperidin-4-one in water at room temperature,[180] or under reflux in EtOH (Scheme 14). For the preparation of spiro[quinazoline-2,2′-adamantane] derivatives **36–38**, we developed an alternative synthetic pathway involving the use of microwave irradiation on **15e**, **15g**, **15h** with adamantanone in EtOH (Scheme 14). This reaction has previously also been carried out in a vibrational ball mill with iodine (I_2) as a catalyst.[181]

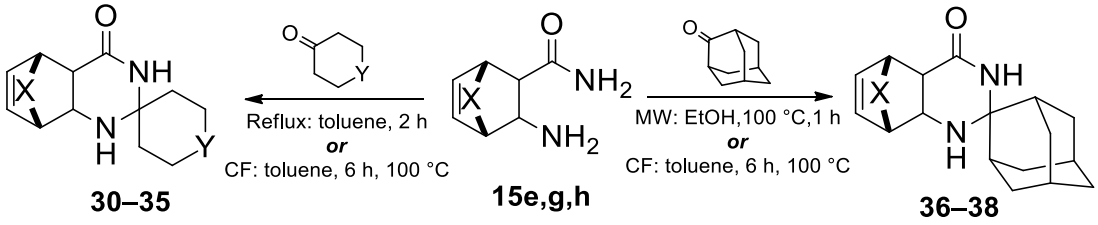

30: *diexo*, X= CH_2 , Y= CH_2
31: *diendo*, X= CH_2 , Y= CH_2
32: *diexo*, X= O , Y= CH_2
33: *diexo*, X= CH_2 , Y= NBn
34: *diendo*, X= CH_2 , Y= NBn
35: *diexo*, X= O , Y= NBn

15e: *diexo*, X= CH_2
15g: *diendo*, X= CH_2
15h: *diexo*, X= O

36: *diexo*, X= CH_2
37: *diendo*, X= CH_2
38: *diexo*, X= O

Scheme 14. Synthesis of spiroquinazolinone derivatives **30–38**.

In addition, we wanted to develop further this cyclisation reaction by searching for a time-efficient method for the synthesis of functionalised intermediates **24–38**. To this end, a CF-based strategy seemed highly appropriate, since this approach has emerged as

an intensely studied area of current research, being used for the synthesis of many different heterocyclic scaffolds.[93] β-Amino amides **15e–15h** were mixed with γ-keto acids or cyclic ketones and loaded into the CF reactor constructed previously (Figure 4), using the same operating conditions and solvents used before in batch syntheses. Mixtures of **15e** or **15f** and γ-keto acids were dissolved in toluene and introduced into the flow reactor at 110 °C, with 6 h as the reaction time. Tetra- and pentacyclic derivatives **24–29** were obtained in slightly higher yields (79–93%) than found previously in batch method. Heating the solutions of **15e**, **15g**, or **15h** with cycloalkanones in EtOH at 100 °C gave spiroquinazolinones **30–38** with reaction times of 6 h in similar yields (79–95%). Note, however, that shorter reactions were needed for cyclisation in CF reactor.

4.1.2. CF rDA method development and validation

Our next step was to investigate the transformation of quinazolinone derivatives **16–38** into the retrodiene products **39–53** through thermal [4+2] cycloreversion involving the elimination of cyclopentadiene, cyclohexadiene or furan from DA adducts. To this end, a modular flow system was designed as illustrated in Figure 4. The reactor coil was heated in an oven to the desired temperature and solutions of starting materials **16**–**38** were loaded into the reactor *via* an HPLC pump. Solvents were selected on the basis of the solubility of the starting materials. The rDA reaction is basically a thermally-driven process. Consequently, by careful reaction parameter optimisation, a balance should be found between the desired rDA cycloreversion reaction and the unwanted thermal degradation of the rDA product. The conversion and yield of a reaction under CF conditions are influenced directly by the residence time and reaction temperature, which are crucial determining factors in flow chemistry.[8-10] Thus, these two parameters were fine-tuned and the full reaction parameter optimisation is shown only for compound **16** in Table 1.

Table 1. Reaction parameter optimisation by increasing the conversion and minimising the degradation of the product by the example of compound **16**.

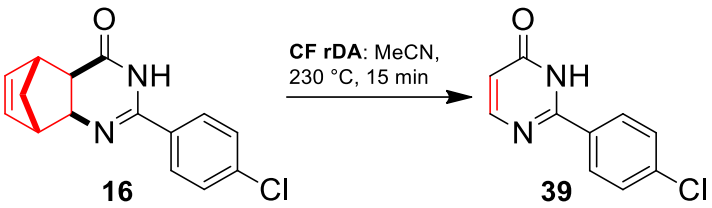

Entry	Temperature [°C]	Residence time [min]	Conversion [%]	Degradation product [%]
1	200	10	64	-
2	210	10	82	-
3	220	10	83	-
4	230	10	86	0
5	240	10	100	7
6	250	10	100	18
7	**230**	**15**	**100**	**0**
8	230	30	100	13

In order to validate our protocol, we initiated the CF rDA investigation of tri- and tetracyclic derivatives **16–23**, since these molecules gave good (>80%), medium (70–80%) and no conversion under batch rDA conditions. The tricyclic *diexo*-2-(4-chlorophenyl)tetrahydro-5,8-methano-4(3*H*)-quinazoline (**16**) was dissolved in MeCN and first the effect of the temperature was studied. The results showed that with 10 min residence time the best conversion value (86%) was obtained at 230 °C (Table 1, entry 4). It should be noted that at higher temperature, a significant amount of degradation product was observed and brown oil was isolated (Table 1, entries 5 and 6). To further improve the conversion, the residence time was increased by utilizing longer coils (Table 1, entries 7 and 8). Complete conversion could be obtained at 15 min residence time and the desired rDA product **39** was isolated with 92% yield (Table 1, entry 7, Table 2, entry 1). With longer residence times, again, degradation of the product was observed (Table 1, entry 8). Importantly, the complete reaction parameter optimisation was carried out only in 105 min. The parameters of the optimised reaction conditions for all starting materials and related results are summarised in Table 2.

Table 2. Results with the use of the CF rDA process for the synthesis of pyrimidinone **39–44** under the optimised reaction conditions.

Entry	Starting material	CF rDA Product	CF optimised reaction conditions			
			Solvent	Temp [°C]	Residence time [min]	Yield[a] [%]
1	**16**	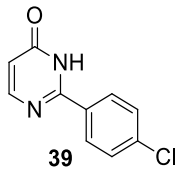 **39**	MeCN	230	15	**92**
2	**17b**			250	10	**95**
3	**17c**		Toluene	230	30	**93**
4	**18**	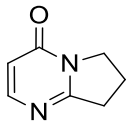 **40**	MeOH	130	10	**95**
5	**19**	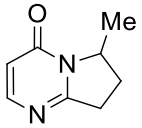 **41**		150	10	**97**
6	**20**	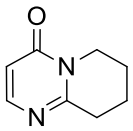 **42**		120	10	**95**
7	**21**	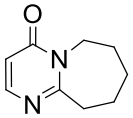 **43**		130	10	**94**
8	**22**	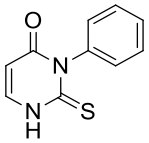 **44**	MeCN	210	15	**96**
9	**23b**			220	10	**96**
10	**23c**			250	30	**30**

[a] Isolated yield.

In the case of *diendo*-isomer **17b**, higher temperature (250 °C) but a shorter residence time was satisfactory to isolate **39** in a yield of 95% (Table 2, entry 2). Furthermore, we proceeded to investigate the elimination of cyclohexadiene from compound **17c**. Because of solubility reasons, the solvent was changed to toluene, which is known to be compatible with high-temperature conditions.[133] Retrodiene product **39** was afforded with full conversion and in a good yield of 93% (Table 2, entry 3), which is higher than the maximum yield (85%) reached in our previous batch work.[115] Importantly, this result was achieved with a residence time of 30 min.

Subsequently, tetracyclic methanopyrrolo-, methanopyrido- and methanoazepino[2,1-*b*]quinazolinones **18–21** were examined. Because of their excellent solubility, reactions were carried out in MeOH (Table 2, entries 4–7). Importantly, much milder reaction conditions gave satisfactory results. With the utilisation of 120–150 °C and only 10 min residence time, full conversions to the retrodiene products **40–43** were obtained in high yields (94–97%). Lower yields were previously found (70–80%) using a batch process, even upon melting compounds **18–21** for 20 min.[176]

The effect of the thioxo group on the rDA reaction was investigated too with compounds **22**, **23b** and **23c**. In the case of **22**, a yield of 96% was reached at full conversion at 210 °C in 15 min residence time (Table 2, entry 8). In the reaction of **23b** (the *diendo* isomer of **22**), a slightly higher temperature with an appropriate residence time of only 10 min was satisfactory to have **44** with an isolated yield of 96% (Table 2, entry 9).

On the basis of these encouraging results, we decided to further examine the scope and limitation of the CF rDA reaction. For this purpose, *diendo*-3-phenyl-2-thioxohexahydro-5,8-ethanoquinazolin-4(1*H*)-one (**23c**) was selected, since this compound did not lose cyclohexadiene to form monocyclic **44** under batch and microwave conditions.[175] A solution of **23c** in MeCN was treated in the heated coil reactor at 250 °C, with a residence time of 30 min. Importantly, according to HPLC–MS analysis, compound **23c** underwent thermal decomposition but only a moderate conversion (36%) was detected and **44** was isolated by means of column chromatography with a yield of 30% (Table 2, entry 10). This result is due to the lack of the quasi-aromatic character of the leaving cyclohexadiene, and possibly also due to the temperature limitation of our system. Surprisingly, however, we could detect traces of *diendo*-3-phenyl-4a,5,8,8a-tetrahydro-5,8-ethanoquinazolin-4(3*H*)-one (**45**), resulting from desulfurisation of **23c** (Scheme 15). This observation prompted us to investigate whether desulfurisation can occur under flow conditions. In the literature, a similar desulfurisation batch reaction was performed with nickel catalysis, in EtOH/water (2:1) solution.[182] Thus, thioxo derivative **23c** was dissolved in this mixture, and the CF method was repeated. Desulfurisation of **23c**, at 250 °C without adding any catalytic metal, provided tricyclic **45** in good yield (90%). Most probably, the reaction was catalyzed by nickel, a component of the 304 stainless steel reactor coil.[183] These results also underline the importance to select appropriate solvents and tubing[184] for thermally-

driven reactions. In support of our results, tricyclic **45** was also prepared in another way: the mixture of 3-aminobicyclo[2.2.2]oct-5-ene-carboxylic acid, triethyl orthoformate, aniline and acetic acid was subjected to microwave irradiation at 120 W at 80 °C for 20 min. After completion of the reaction, as monitored by TLC, 20% methanolic solution in water was added to get precipitation. The solid was filtered off and washed with water to get *diendo*-3-phenyl-4a,5,8,8a-tetrahydro-5,8-ethanoquinazolin-4(3*H*)-one **45** (65% yield).

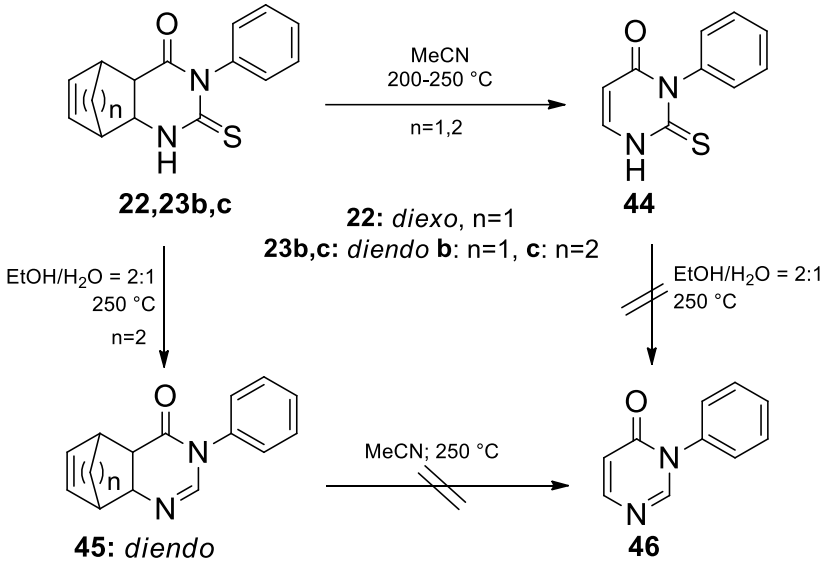

Scheme 15. Synthesis of tricyclic ethanoquinazolin-4(3*H*)-one **45**.

A further attempt was made to perform the rDA reaction with **45** at 250 °C with a residence time of 15 min in MeCN. However, the formation of **46** was not observed, that is the starting tetrahydroquinazolinone derivative **45** did not undergo a thermally-driven rDA reaction (Scheme 15). Furthermore, by applying the same conditions on **44**, no desulfurisation occurred and the formation of **46** was not detected either.

There are previous literature results with respect to the preparation of pyrimidinones **39**–**44** under batch conditions.[115,172-176] These were performed by: *i*) heating under neat conditions or *ii*) heating under reflux in solvents having a high boiling point [chlorobenzene (CB) or 1,2-dichlorobenzene (DCB)], and *iii*) under microwave conditions in DCB. A comparison between the literature findings and our CF rDA results is presented in Figure 6. These findings validate that the proposed CF rDA protocol is superior to the existing conventional batch technologies. As shown, pyrimidinone derivatives **39**–**44** were gained in excellent yields and shorter reaction

times when compared to the corresponding batch processes, especially in case of compound **23c**, which did not undergo decomposition under batch conditions.

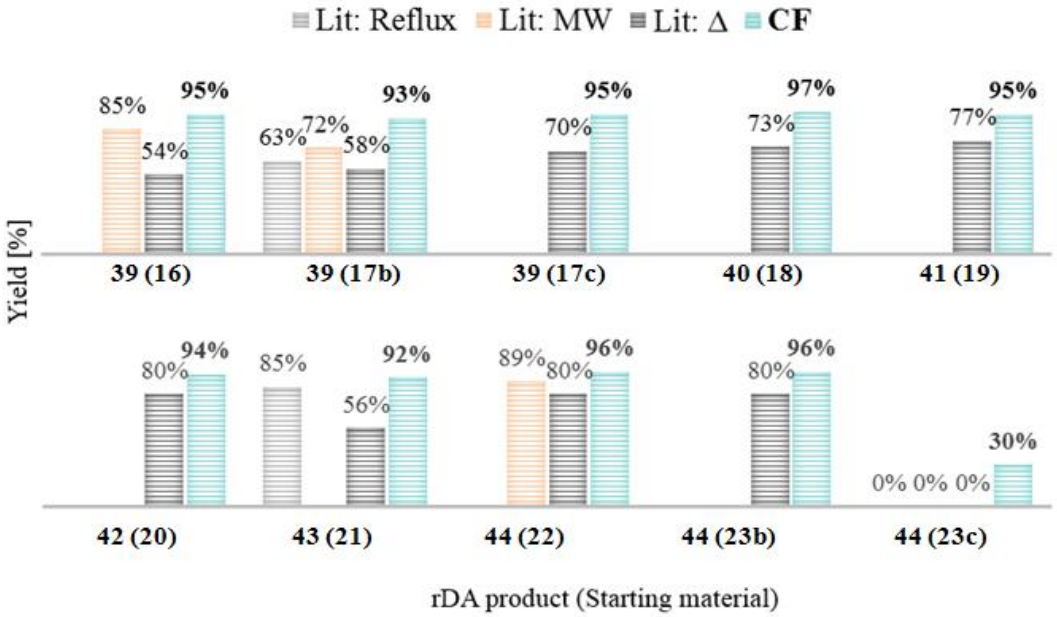

Figure 6. Comparison in terms of isolated yields between CF rDA and different batch methods for the synthesis of pyrimidinone derivatives **39–44**. (Lit: literature data[115,172-176])

Our next effort was to test the viability of the CF rDA protocol with more complex fused pyrimidinone moieties **24–29**, which appeared to be a challenge to the CF rDA method to provide retrodiene products **47–52**. Therefore, by screening different polar and aprotic solvents, MeCN or MeOH was preferred over nonpolar solvents, especially, when high concentrations were employed. Therefore, we opted for MeCN as a suitable and benign solvent and used it subsequently to study the effect of temperatures. It was quickly established that temperatures of 220–250 °C gave full conversions without the unwanted thermal degradation of the rDA products within 15 min residence time, whereas lower temperatures significantly slowed down the reactions. With these conditions in hand, tetracyclic pyrrolo[1,2-*a*]quinazolinones **24–26** and pentacyclic isoindolo[1,2-*a*]quinazolinones **27–29** were dissolved in MeCN and after 5 min of stirring at ambient temperature, the homogeneous mixtures were introduced into the reactor through an HPLC pump (Figure 4). Heating the mixtures at 220 °C or 250 °C led to the expected pyrrolopyrimidinones **47–49** (Table 3, entries 1–3) and pyrimidoisoindoles **50–52** (Table 3, entries 4–6) with a residence time of 15 min in isolated yields over 90% after purification *via* column chromatography. These results match the parent batch experiments in terms of isolated yields.[177,178]

Table 3. Results with the use of the CF rDA process for the synthesis of pyrimidinone **47–52** under the optimised reaction conditions.

Entry	Starting material	CF rDA Product	CF optimised reaction conditions			
			Solvent	Temp [°C]	Residence time [min]	Yield[a] [%]
1	**24**	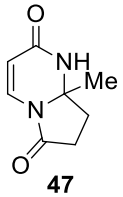 **47**	MeCN	250	15	**98**
2	**25**	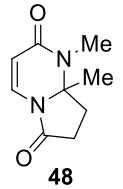 **48**		220	15	**97**
3	**26**	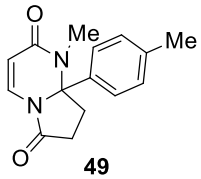 **49**		220	15	**95**
4	**27**	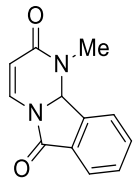 **50**		220	15	**98**
5	**28**	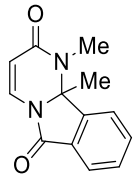 **51**		220	15	**96**
6	**29**	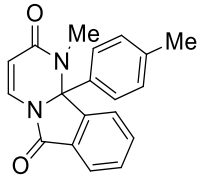 **52**		250	15	**97**

[a] Isolated yield.

4.1.3. Testing the capacity of the CF rDA protocol for providing NCE

Herein, we turned our attention to investigate chemical skeletons, which have not been subjected to rDA reactions previously through conventional batch approaches. Hence, spiroquinazolinone derivatives **30–38** were selected to be tested under CF rDA

conditions. We started our study by optimizing the operating parameters. Namely, spiroquinazolinone **30–38** were first dissolved in MeCN and loaded into the CF reactor at different temperatures based on their melting points with respect to their stereochemistry (*diendo* versus *diexo* condensation). The initial assessment of the obtained results revealed that compounds **30–38** underwent thermal decomposition affording only moderate conversions to retrodiene products **53–55** with significant amounts of rDA degradation products. Following these disappointing results, we decided to optimize further our operating parameters. After screening different solvents we found that a mixture of toluene and MeOH (4:1 v/v) worked best to give new 2-spiropyrimidin-4-ones **53–55**. In an illustrative procedure, a solution of *diexo*-methylene-bridged 2-spiroquinazolinone **30** in toluene/MeOH (4:1) was introduced into the heated 304 stainless steel coil reactor at 240 °C with a residence time of 60 min (Table 4, entry 1). The residence time was increased by utilizing longer coil in order to further improve the conversion. Under these conditions, 1,5-diazaspiro[5.5]undec-3-en-2-one (**53**) was isolated in an increased yield of 73%. Furthermore, we wanted to investigate the CF rDA effect on *diendo*-isomer **31** in the hope that we could further increase the yield of **53**. Since *diendo*-stereoisomers are thermally unstable compared to their *diexo*-analogues, they more easily underwent the rDA reaction. Thus, **31** was treated under the same conditions (Table 4, entry 2). With a residence time of 60 min **53** was obtained in almost the same yield (75%) as demonstrated previously in the case of its *diexo*-isomer **30**. This result shows that a change in stereochemistry does not have any significant effect on the reaction yield. Subsequently, we headed towards the epoxy-bridged 2-spiroquinazolinone **32** with the expectation that removal of the furan ring as a diene at lower temperatures would be much easier than that of cyclopentadiene. This may improve the yield by increasing the conversion and minimizing the quantity of degradation products because of the lower temperatures used. Therefore, we utilised a temperature of 150 °C. Accordingly, complete conversion could be obtained at 60 min residence time and the desired spiro-compound **53** was isolated with a yield of 95% (Table 4, entry 3).

Encouraged by these promising results, a series of experiments were then undertaken to gain a better understanding of the thermally-driven CF rDA effect on the transformation of other spiroquinazolinone scaffolds. Accordingly, we treated compounds **33–38** under the CF reaction conditions described above. Benzylpiperidine

derivative **54** and adamantane **55** were obtained in good yields of 92% and 86%, respectively (Table 4, entries 6, 9). Importantly, the yields obtained from the epoxy-bridged spiro-compounds were always higher than those for the methylene-bridged analogues.

Table 4. Results with the use of the CF rDA process for the synthesis of spiropyrimidinones **53–55** as NCE.

Entry	Starting material	CF rDA Product	CF optimised reaction conditions			
			Solvent	Temp [°C]	Residence time [min]	Yield[a] [%]
1	**30**	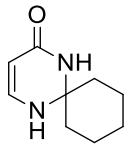 **53**	Toluene /MeOH (4:1)	240	60	**73**
2	**31**			240	60	**75**
3	**32**			150	60	**95**
4	**33**	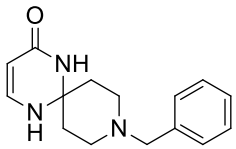 **54**		240	60	**53**
5	**34**			240	60	**70**
6	**35**			150	60	**92**
7	**36**	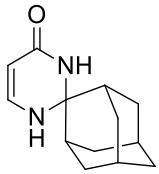 **55**		240	60	**51**
8	**37**			240	60	**57**
9	**38**			150	60	**86**

[a] Isolated yield.

In line with our previous findings, we wanted to explore whether spirocompounds **30–38** undergo thermal decomposition under conventional batch conditions. For this purpose, we envisaged to adopt two different batch methods. The parent method included a simple heating of spiroquinazolinone derivatives **30–38** at their melting points, whilst in the second method the rDA reactions were performed under microwave conditions. To this end, in solvent-free experiments, compounds **30–38** were heated at around 10 °C above their melting points. Although HPLC–MS analysis showed the full degradation of starting materials **30–38**, rDA products **53–55** were not detected in any case. In contrast, when microwave irradiation was applied on compounds **30–38**, slightly higher than medium or no conversions to retrodiene products **53–55** were found.

The best MW-promoted cycloreversion for the synthesis of compounds **53–55** was achieved with epoxy-spiroquinazolinone **32**, **35** and **38** irradiated in DCB at 180 °C for 30 min. These conditions afforded isolated yields of 78%, 89%, and 78%, respectively (Figure 7). The obtained values are lower than those found in the CF rDA process (Table 4, entries 3, 6, 9). A thorough comparison for spiropyrimidinones **53–55** prepared by the batch and the CF process is shown in Figure 7. These data clearly demonstrate the superiority of the CF technology compared to the existing conventional batch methods.

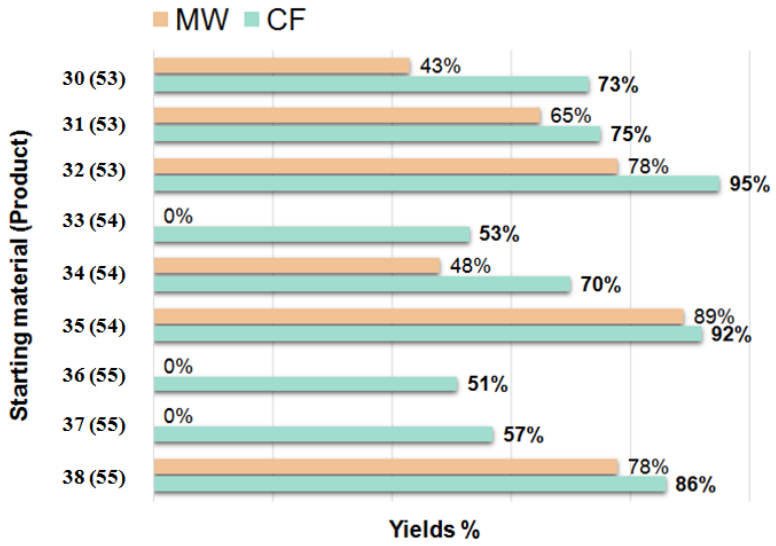

Figure 7. Comparison in terms of isolated yields between CF rDA and microwave processes for the synthesis of new spiropyrimidinone chemical scaffolds **53–55**. MW-induced rDA (orange); CF rDA (blue).

4.1.4. Investigation of the scope and applicability extent of the CF rDA method

To establish the range of applicability of our CF rDA process, the syntheses of enantiomerically pure pyrrolo[1,2-*a*]pyrimidine **49** and pyrimido[2,1-*a*]isoindole **50** through rDA reaction under CF conditions were undertaken (Scheme 16). The source of chirality, (1*R*,2*R*,3*S*,4*S*)-3-amino-*N*-methylbicyclo[2.2.1]hept-5-ene-2-carboxamide [(–)-**15f**] was prepared by known literature protocols.[185] In a stereocontrolled ring-closing reaction, (–)-**15f** was reacted with 3-oxo-3-(*p*-tolyl)propanoic acid to afford single diastereoisomer (+)-**26** in good yield (82%). The ready loss of cyclopentadiene through the CF rDA protocol at 220 °C resulted in (*S*)-1-methyl-8a-(*p*-tolyl)-1,7,8,8a-tetrahydropyrrolo[1,2-*a*]pyrimidine-2,6-dione enantiomer (+)-**49** in high yield (97%) with an *ee* value of 97%. When carboxamide (–)-**15f** was treated with 2-formylbenzoic acid, pentacyclic isoindolo[1,2-*a*]quinazolinone (+)-**27** was formed and then isolated in

yield of 83%. The CF-induced thermolysis of (+)-**27**, at 250 °C, gave the expected (*S*)-1-methyl-1,10b-dihydropyrimido[2,1-*a*]isoindole-2,6-dione [(–)-**50**] within a residence time of 15 min at full conversion, in yield of 97% and with an *ee* value of 98%.

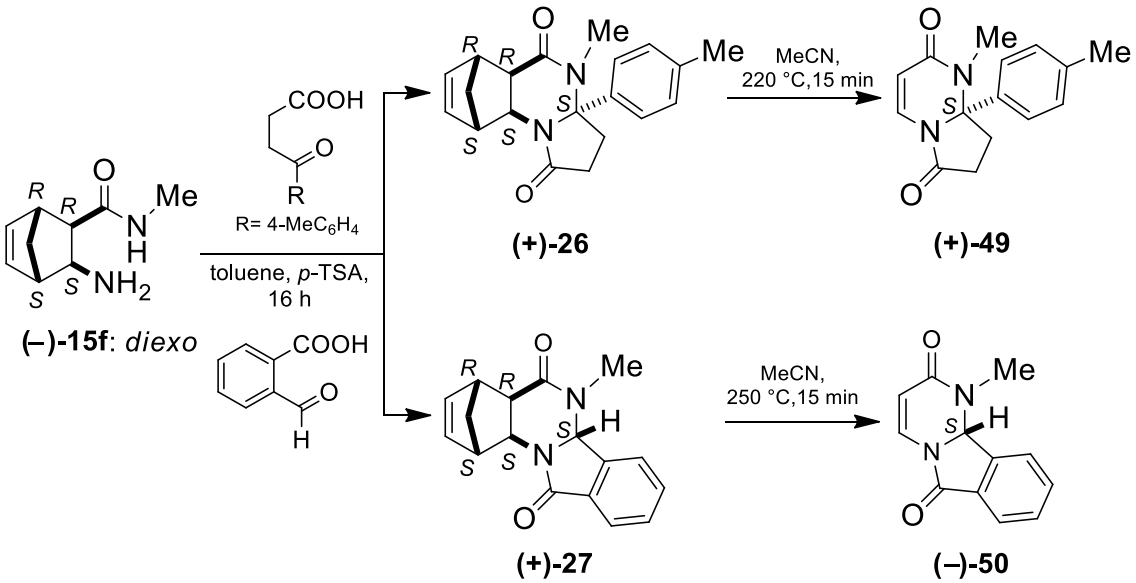

Scheme 16. The syntheses of enantiomerically pure pyrrolo[1,2-*a*]pyrimidine **49** and pyrimido[2,1-*a*]isoindole **50** through CF rDA reaction.

4.2. Continuous-flow enabled efficient patterning of β-peptide foldamers

Efficient design of the secondary structures of the peptidic foldamers is a great challenge. For assessment of the effect of the new structural elements on β-peptide conformation, we examined the helix-forming property of oligomers containing enantiomeric bicyclic β-amino acid residues and their chemical derivatives.[IV] To this end, pentamers made of [1*R*,2*R*]-ACHC building blocks possessing an enantiomer of bicyclic residue in the middle of the peptide chain were assembled by revolutionary CF-SPPS (Figure 5) synthetic methods and illustrated in Scheme 17. As bridged residues, enantiomers of *diexo*-3-aminobicyclo[2.2.1]hept-5-ene-2-carboxylic acid (*diexo*-ABHEC) and *diexo*-3-amino-7-oxabicyclo[2.2.1]hept-5-ene-2-carboxylic acid (*diexo*-AOBHEC) were used to compare the ability of folding regarding the configuration and study the effect of an oxygen-bridged residue on self-organisation. The reference secondary structures formed by the homochiral sequences are known. For example, the homochiral homooligomers of [1*R*,2*R*]-ACHC facilitate an H14 helix,[135] while *diexo*-ABHEC enantiomer residues promote a chain dependent right and left handed consecutive 6-strands.[186] In contrast, with alternating backbone configuration of oligomers containing [2*S*,3*R*]/[2*R*,3*S*]-ABHEC enantiomer units, with protected or free

at both ends, they are not capable of helix formation; their secondary structures are a bend-strand[187] or a circle-like fold.[188] Note that *diexo*-AOBHEC units adopt an 8-membered hydrogen-bonded ring conformation.[189]

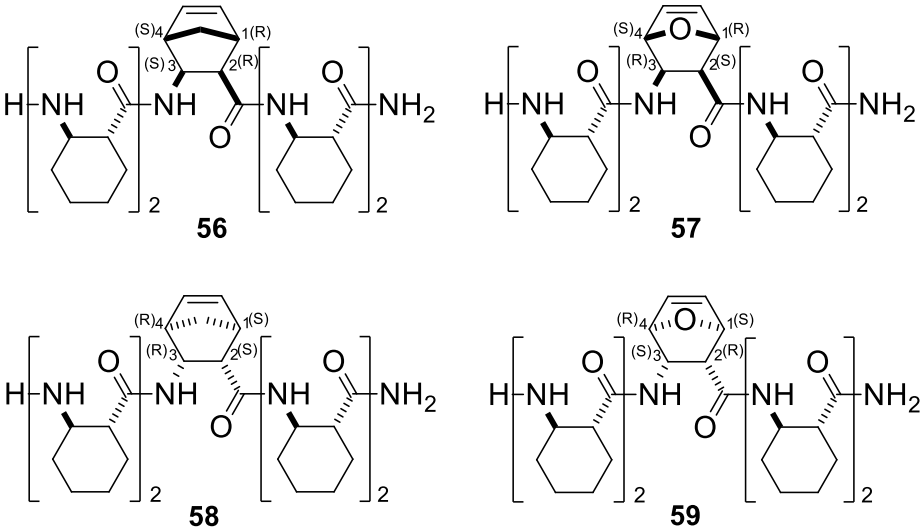

Scheme 17. The investigated structures possessing an enantiomeric bicyclic residue in the middle of the peptide chain.

To investigate the effect of *Z*-dehydro-β-alanine on self-organisation, compounds **56–59** containing *diexo*-ABHEC and *diexo*-AOBHEC units were subjected to the CF rDA protocol. As an illustration, solutions of β-peptide homooligomers **56–59** dissolved in MeOH were introduced into the CF rDA reactor (Figure 4). Heating the mixtures of **57** and **59** at 150 °C or **56** and **58** at 230 °C led to the expected oligomer **60** within a residence time of 14 min, with full conversion (Scheme 18) and in yields over 90% after purification by RP-HPLC techniques. These results probe the versatility of the CF rDA protocol by providing distinct peptidic structures.

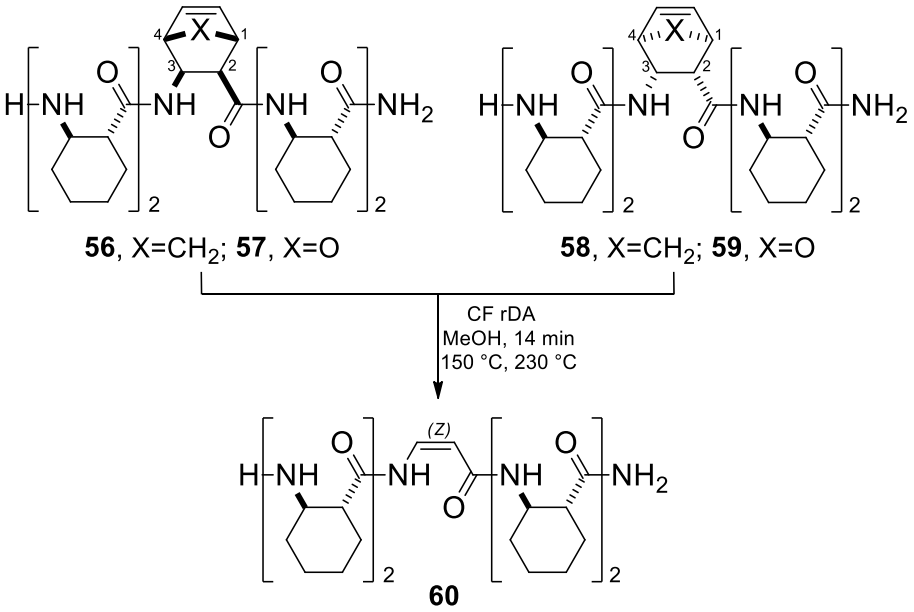

Scheme 18. The synthesis of oligomer **60** through CF rDA reaction.

As a next step, we studied the folding behaviour of peptide **61** containing saturated β-alanine by changing the third unit from *Z*-dehydro-β-alanine to β-alanine unit. Thus, we intended to further capitalize on the CF methodology benefits for the preparation of peptide **61** (Scheme 19). Accordingly, CF rDA product **60** was saturated in an H-Cube® CF hydrogenation reactor on a 10% Pd/charcoal catalyst to afford oligomer **61** in good yield (95%).

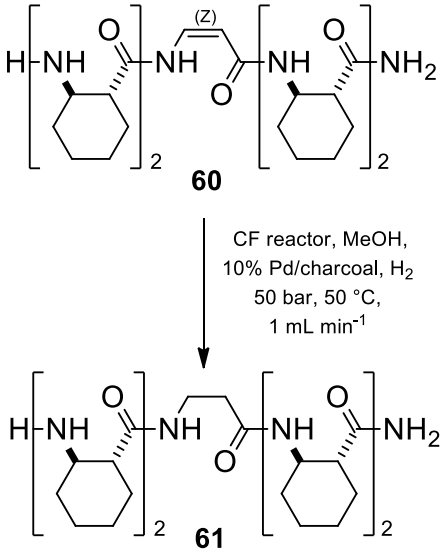

Scheme 19. The synthesis of oligomer **61** through CF hydrogenation reaction.

Peptides **56–61** were analysed by HPLC–MS and characterised through the use of different NMR methods. The analytical HPLC chromatograms of foldamers in diastereomeric relation, *e.g.* **56** vs. **58** and **57** vs. **59** showed drastic differences. Foldamers **56** and **57** possess substantially higher retention time than those observed for **58** and **59**. This finding suggests that **56** and **57** are more hydrophobic than **58** and **59**. According to previous results,[144] the ordered helical structure is more hydrophobic since the amide bonds are in the centre of the structure and only the hydrophobic side-chains interact with the chromatographic system. Helix formation, consequently, might be anticipated for compounds **56** and **57**.

4.3. Stereochemical discrimination in the synthesis of β-peptide oligomers: origin of homochirality

Homochirality is an inherent property of vital polymers, *i.e.*, peptides, proteins, RNA, DNA, as well as oligo- and polysaccharides.[190-192] It is still not clear whether homochirality is a result of an autocatalytic procedure or if it originates from extraterrestrial optically active non-racemic mixtures. For the natural α-peptides, numerous assays have been carried out to clarify the origin of this phenomenon, mainly by studying the stereochemical discrimination in their synthesis.[193-195] In the case of β-peptide foldamers, however, the formation of the homochiral peptide from a racemic starting mixture is still ambiguous compared to the natural α-peptides. Herein we proved, that the stereochemical discrimination towards the homochiral oligomers manifests for β-peptides too, akin to the biological homochirality of natural polymers.[I]

The effect of secondary structures and the side-chain size and length on the stereochemical course of the homochiral oligomer formation was investigated. Thus, β-peptide foldamers containing various cyclic side-chains and possessing different secondary structures were selected for the examination of diastereo-discriminative peptide coupling with chain lengths varying from trimer to hexamer. As a reference, the natural α-L-leucine (L-Leu) oligopeptides were selected. The investigated peptide structures were assembled by CF-SPPS (Figure 5) and are shown in Scheme 20.

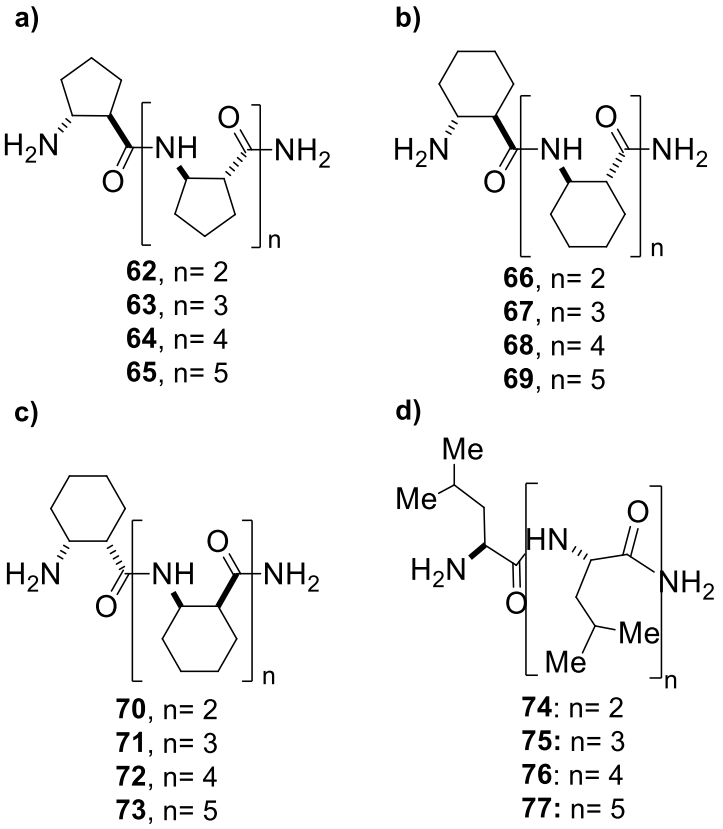

Scheme 20. The investigated structures possessing five- and six-membered side-chains and *cis* or *trans* relative configuration.

Oligomers **62–65** are composed of [1*R*,2*R*]-2-aminocyclopentanecarboxylic acid ([1*R*,2*R*]-ACPC) building blocks and are known to form H12 helix.[136] As a next step, the five-membered cyclic side-chains were changed for six-membered cyclohexane rings (compounds **66–69**), while retaining the same stereochemistry. That is the oligomers were constructed from [1*R*,2*R*]-ACHC residues and they form an H14 helix.[135] To investigate the effect of a strand structure, oligomers **70–73** created from [1*S*,2*R*]-ACHC were assembled too. Homochiral homooligomers made from *cis*-β-amino acids are known to form strand structure.[22,196] As a control structure, homooligomeric α-peptides **74–77** composed of L-Leu were synthesized too. The isobutyl side-chain was selected in accordance with the β-amino acids described above, since only aliphatic side chains were tested.

Having the desired peptide structures in hand, the stereochemical discrimination property of these peptides was tested by means of the solution-phase peptide coupling technique as demonstrated in Scheme 21 with the example of oligomers built from [1*R*,2*R*]-ACHC. The purified peptides (**66–69**) were dissolved in the mixture of CH_2Cl_2/DMF (2:1) and 10 equiv. of Boc-protected racemic amino-acid **(±)-78** was

coupled by the utilisation of DIC and HOBt coupling agents and the mixture was stirred for 48 h. Importantly, the effect of water on the stereochemical discrimination was investigated too, since it is known to be a crucial factor.[193,194] Thus, the reactions described previously were performed in the solvent system CH_2Cl_2/DMF/water (2:1:1) in 48 h. The solvents were removed *in vacuo*, Boc deprotection was carried out by TFA treatment and the two diastereomeric products were first lyophilised and then analysed by means HPLC–MS technique. The homochiral chain elongated reference compounds were always synthesized independently and the heterochiral diastereomers were identified by the HPLC–MS chromatogram.

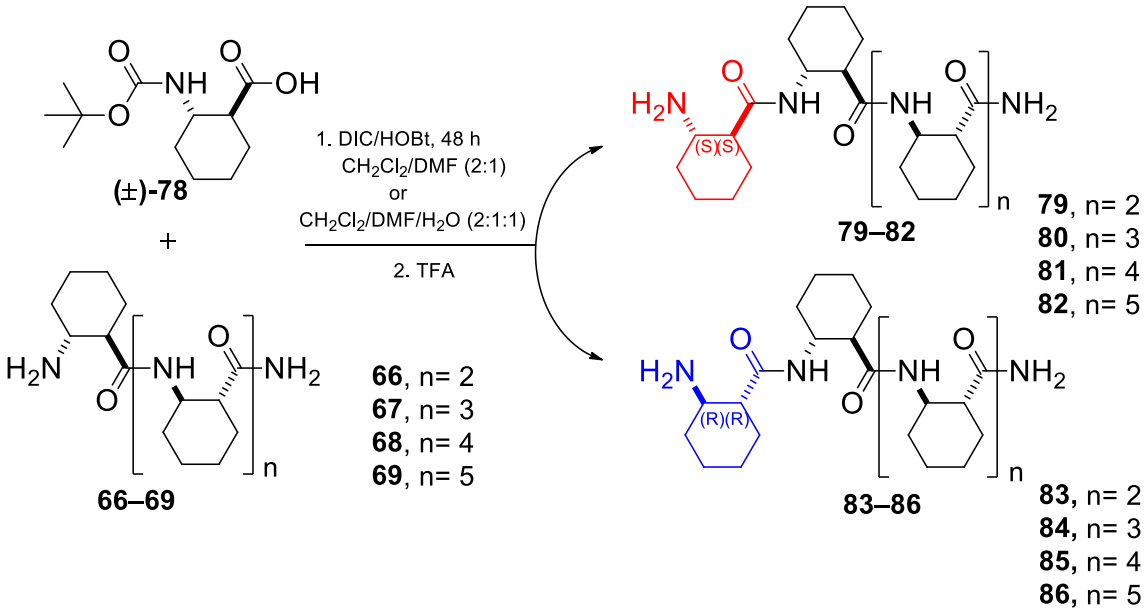

Scheme 21. Chain elongation of β-peptides **66**–**69** with racemic **(±)-78** yielding diastereomers **79**–**82** (heterochiral) and **83**–**86** (homochiral) shown by the example of [1*R*,2*R*]-ACHC residue.

Herein two HPLC–MS chromatograms are presented for the coupling of Boc-protected racemic amino-acid **(±)-78** with trimer **66** in the absence (Figure 8a) and presence (Figure 8b) of water. These results revealed that the formation of the homochiral homooligomer **83** was predominant when water was used as a co-solvent in the diastereo-discriminative coupling.

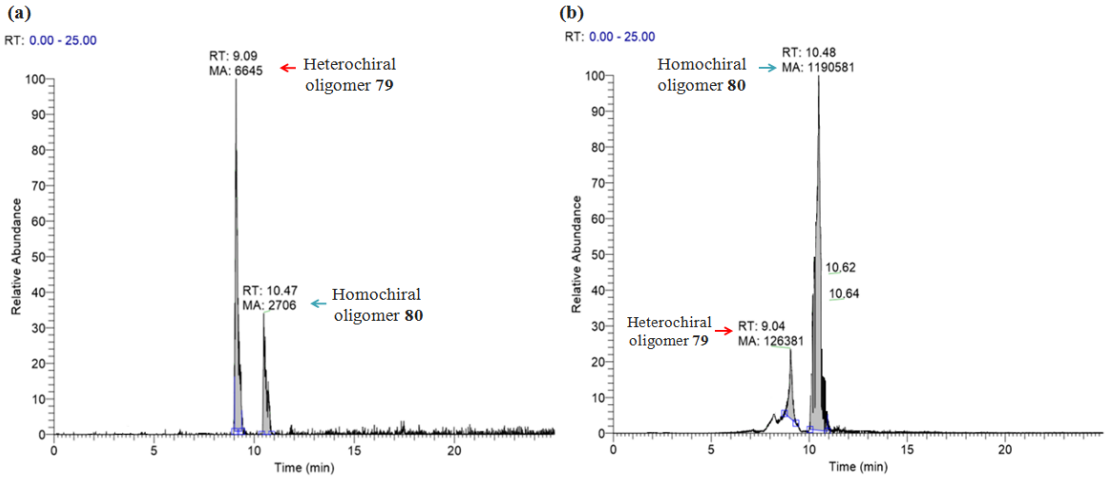

Figure 8. HPLC–MS chromatograms of the coupling of racemic **(±)-78** with trimer **66** (a) in the absence and (b) in the presence of water.

Based on the area integrals of the homochiral and heterochiral peptides, the diastereomeric excess (*de*) of the reaction was calculated for all peptides both in the presence and in the absence of water. The *de* values are shown in Figure 9 in a chain-length-dependent manner.

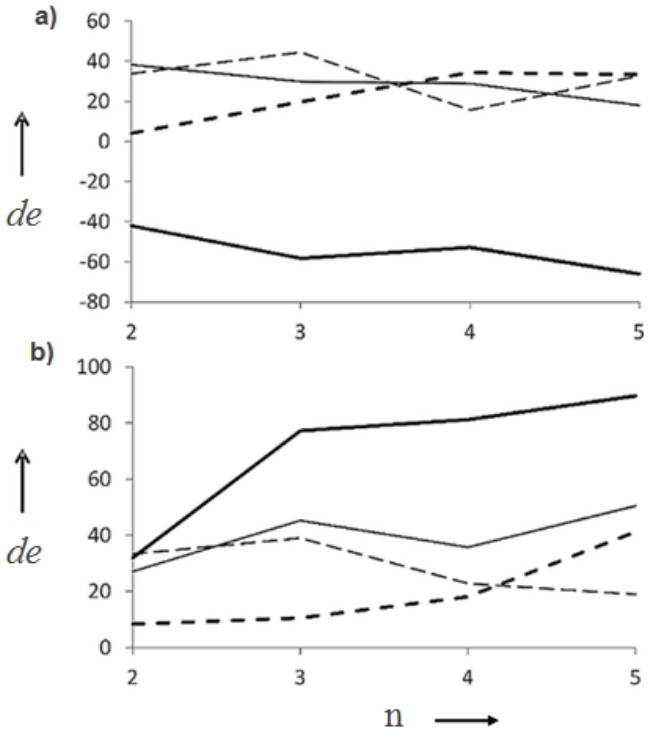

Figure 9. Diastereomeric excess (*de*) values obtained for **62–65** (thin solid line), **66–69** (thick solid line), **70–73** (thin dashed line), **74–77** (thick dashed line) in absence (a) and in presence of water (b) as a function of chain-length (n).

In the absence of water, a strong tendency towards the homochiral structures was observable for peptides containing the [1*R*,2*R*]-ACPC unit (**62–65**). A slight decrease in

selectivity was found as a function of chain length. The situation is completely different for the oligomers composed of [1*R*,2*R*]-ACHC (**66–69**), which contain a more bulky side-chain. The selectivity changed, the formation of the heterochiral product became favoured (Figure 8a), and a nice chain-length-dependent correlation was found. It is important to note that a simple change in the side-chain caused a drastic difference in the stereochemical discrimination properties of β-peptides. To investigate the effect of *cis* relative configuration, compounds containing [1*S*,2*R*]-ACHC (**70–73**) were also studied. Again, a definite tendency was observed towards the homochiral oligomers. The chain length did not significantly alter the *de* value. As a reference, α-peptides composed of L-Leu were investigated. The diastereoselectivity showed a clear chain-length-dependent manner and the homochiral product was favoured. Importantly, the chain elongation of the trimer L-Leu showed only very minor diastereo-differentiation.

In general, the presence of water enhanced the selectivity toward the formation of homochiral homooligomers. In the case of peptides built of [1*R*,2*R*]-ACPC, *de* values increased compared to those formed in non-aqueous experiments and a clear chain-length-dependent increase could also be observed. The most dramatic difference compared to the experiment performed without water can be observed for oligomers comprising [1*R*,2*R*]-ACHC. The selectivity changed to the opposite direction and homochiral compounds were profoundly formed during the coupling of the Boc-protected racemic [1*R*,2*R*]-ACHC (Figure 8b). In this case, a more dominant chain-length-dependent fashion can be observed and, importantly, the diastereoselective chain elongation of the hexamer reached a *de* of almost 90%. The effect of *cis* relative configuration was also investigated in the presence of water. The results indicate again the profound formation of the homochiral oligomer. Interestingly, *de* values decreased to some extent as a function of chain length. The reference L-Leu oligomers preferred the incorporation of the homochiral amino acids in a chain-length-dependent manner. Nonetheless, water, in general, increased the *de* values compared to the results of the water-free experiments.

To understand the effect of water on the diastereoselective chain-elongation reaction, the effect of water on the foldameric systems itself should be considered. Foldameric systems are known to show secondary structure-dependent self-association with water as the solvent.[22,23] Helical structures self-associate into vesicles, whereas strand structures form nano-sized fibrils as shown in Figure 10, reported by transmission

electron microscopy (TEM) measurements. It has been reported that the self-association of peptides is a crucial factor behind biological homochirality.[193,194]

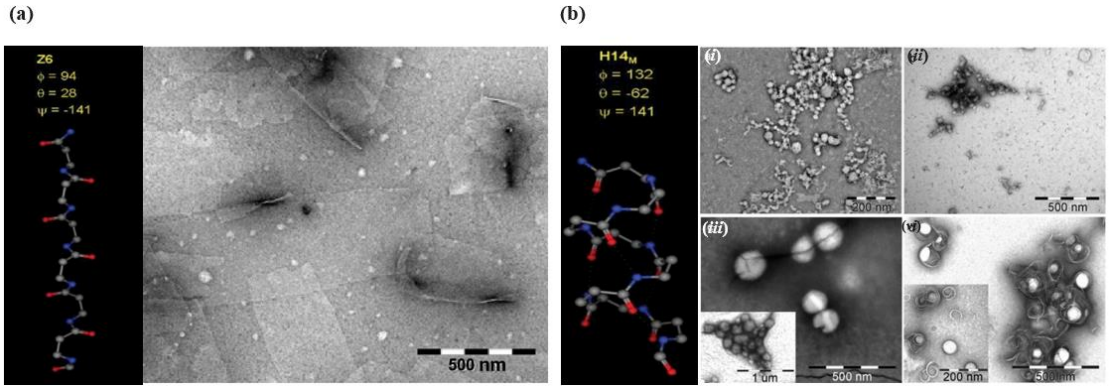

Figure 10. TEM images of (a) the amyloid-like fibrils formed by the heptamer [1*R*,2*S*]-ACPC (strand structure); (b) the vesicles obtained for [1*R*,2*R*]-ACHCn for *i*) **67**, *ii*) **68**, and *iii*) **69**, *vi*) the multilamellar vesicles after sonication of **68**.[22,23]

Consequently, theoretical calculations were performed to investigate the effect of self-association of β-peptides on stereochemical discrimination. Oligomer **68** containing [1*R*,2*R*]-ACHC selected as an example showed the most dramatic water-dependent diastereo-discrimination. DFT calculations were carried out at the OLYP/tz2p level of theory and the transition states were calculated for the systems composed of Boc-protected [1*R*,2*R*]- and [1*S*,2*S*]-ACHC hydroxybenzotriazole esters and oligomer **67**. The structure of the latter was previously optimised in the form of an H14 helix. The reason for selecting β-peptide **67** is that it forms a helical structure with the shortest chain length, which is the optimum structure for quantum-chemical calculations with acceptable calculation times. Solvent effects were taken into account by means of the COSMO solvent model utilizing the permittivity of chloroform and water. The calculated relative barrier energies are shown in Table 5.

Table 5. Relative barrier energies (in kcal mol^{-1}) for the transition state of the chain elongation **67** in water and chloroform.

Solvent	Homochiral chain elongation	Heterochiral chain elongation
Chloroform	2.4	1.0
Water	4.8	0.0

The reaction barrier of the heterochiral construct was found to be lower than those for the homochiral one in both solvents. Consequently, the simplified model system cannot reproduce the changes in the trends caused by the absence or presence of water.

However, investigating the 3D structure of the homo- and heterochirally elongated compounds, self-association might increase geometrical strain.

Molecular modelling was carried out to further examine the effect of self-association on the stereochemical discrimination in the chain elongation of β-peptides. First a membrane segment was constructed and optimised by utilizing the MMFF94 force field. The assembly is shown in Figure 11a. For this purpose, oligomer **68** was selected, as it has been reported to form solely an H14 helix.

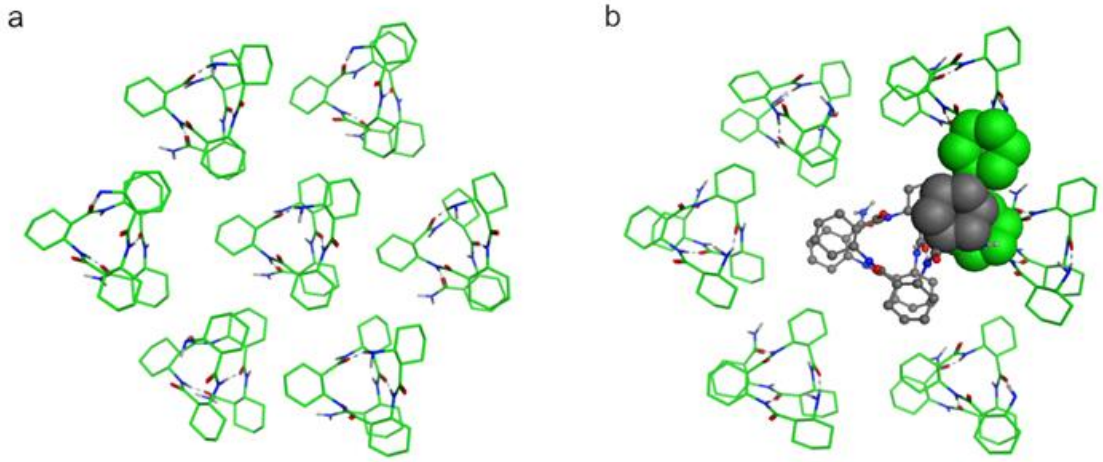

Figure 11. a) Molecular model for the vesicular membrane segment formed of **68**; b) The incorporation of the heterochirally chain-elongated construct (grey-coloured ball and stick representation) into the membrane. The clashes of the side-chains are depicted by the overlapping of the space-filling model of the involved residues.[I]

Our effort to perform similar density functional investigations and calculate the height of the barrier was not successful, because of the size of the systems. However, hetero- and homo-chirally elongated oligomers were merged into the membrane. For the heterochiral constructs, a clear collision was found between the helices of oligomer **68** building the membrane segment and the investigated compound shown in Figure 11b. This interaction hinders and blocks the heterochiral chain elongation and, consequently, the formation of homochiral oligomers is favoured.

SUMMARY

Novel, sustainable flow-based synthetic methodology was implemented for the synthesis of racemic and enantiomerically enriched tricyclic and tetracyclic fused pyrimidinones as valuable NCE and precursors of a series of pharmacologically active materials through the rDA reaction. The design of the reactor enabled accurate control of both residence time and reaction temperature.

In the first attempt for testing the capacity of the proposed CF rDA protocol, HPLC–MS measurements revealed full conversions of **16**–**23** to the desired pyrimidinones **39–44**, whereas only a moderate conversion of **23c** to **44** was observed. In the case of compounds **16–23** mainly retrodiene decomposition occurred through the splitting-off of cyclopentadiene or cyclohexadiene, since these compounds possess rings with a quasi-aromatic character. The stereochemistry (*diendo* versus *diexo* condensation) of the starting pyrimidinones (**16**, **17**, **22** and **23**) has no significant effect on reaction yields. By using this safe, stable and scalable flow process, pyrimidinones **39**–**44** were synthesized in high purities.

As a further investigation on the ability of the CF rDA approach, the synthesis of more complex enantiomeric and racemic fused pyrimidinone derivatives pyrrolopyrimidinones (**47**–**49**), pyrimidoisoindoles (**50**–**52**), and spiropyrimidinones (**53**–**55**) were tested. The preparation of intermediates **24**–**38** through domino ring closure or spirocyclisation under CF conditions was achieved in high yields. This protocol represents an alternative time-efficient route. In the case of pyrrolo[1,2-*a*]quinazoline and isoindolo[2,1-*a*]quinazoline derivatives **24**–**29**, HPLC–MS measurements revealed full conversions to the desired pyrrolopyrimidinones and isoindolopyrimidinones **47**–**52**. In contrast, only moderate conversions to new spiropyrimidinones **53**–**55** were observed for methylene-bridged spiroquinazolinones **30**, **31**, **33**, **34**, **36**, and **37**. It is interesting that epoxy-bridged spiroquinazolinones **32**, **35** and **38**, in which an oxygen atom has been introduced at position C-7 of the β-aminonorbornene carboxamide skeleton, gave retrodiene products **53**–**55** in almost quantitative yields.

It is important to note, that the CF reactor set-up ensured enhanced safety and afforded higher yields than those found with batch and microwave processes. These results could be achieved through careful reaction parameter optimisation. It is

particularly true for **23c**, **33**, **36** and **37**, which were unreactive (0% yield) under batch conditions, in contrast to yields of 30–57% obtained when employing the CF rDA protocol. Thus, this method proved its ability to provide new, otherwise inaccessible, chemical entities (**44**, **45** and **53–55**) in good yields with short processing times. Moreover, the method allowed the replacement of high-boiling and toxic solvents, *e.g.*, CB or DCB, which are commonly employed in batch process by less harmful, environmentally benign solvents such as toluene, MeCN, MeOH, and EtOH.

Furthermore, the CF methods allowed the efficient construction of six new β-peptide systems (**56–59**) built from [1*R*,2*R*]-ACHC residues containing enantiomeric bicyclic residue as the third building block. Upon investigating their helical folding ability, we proved the versatility of the CF rDA protocol, which provided distinct peptidic structures. Namely, oligomer **60** was obtained in high yields, when **56–59** were treated under CF rDA conditions. β-Alanine-containing peptide **61** was afforded upon subjecting **60** to the CF hydrogenation reactor.

We further proved that biological homochirality as an inherent property is also occurring with unnatural compounds like β-peptide foldamers. The phenomenon was investigated by means of diastereoselective amino acid coupling. β-Peptide oligomers composed of either *cis* or *trans* alicyclic β-amino acids showed a tendency towards the homochiral constructs. Theoretical calculations indicated that water plays a crucial role in this phenomenon through the induction of self-association. In all cases, water enhanced the diasetereoselectivity towards the homochiral oligomers by promoting biological homochirality.

The results collected and discussed in this PhD thesis might be readily extended to the preparation of other synthetically important building blocks requiring harsh conditions in batch methods. The simple, efficient and scalable production implemented with a short processing time might open up new horizons for a potential CF industrial synthesis of heterocycles and β-peptides.

ACKNOWLEDGMENTS

I would like to express my deepest appreciation to my supervisor, **Prof. Ferenc Fülöp**, for his inspiring ideas, his valuable discussions and his constructive criticism. I would like to thank him for encouraging my research and for allowing me to grow as a research scientist.

I would also like to extend my deepest gratitude to my co-supervisor **Dr. István M. Mándity** for wisely helping me and paving my way in a foreign field, for his immense patience, his encouragements, and guidance and, in particular, for believing in me in times of doubts. His work methodology shaped my research.

I would like to express my grateful thanks to **Dr. Márta Palkó** for her valuable help, availability, guidance and useful advice during my PhD work.

I am deeply indebted to all **my colleagues** in the NMR laboratory, for all the help they gave. I am thankful to all their contributions of time, joy and enthusiasm, which were contagious and motivational for me.

I thank all members of the Institute of Pharmaceutical Chemistry for their help and providing a friendly atmosphere.

I wish to address special thanks to **Dr. Rachida Bouallouche** and **Dr. Ouafia Balamane**, my teachers during my master studies, for their valuable help, moral support and useful advice.

My heartfelt thanks to **my parents**, **my sister**, **my brothers** and **my friends** for their unconditional love, support, understanding and patience.

REFERENCE

1. L. Proctor, P. J. Dunn, J. M. Hawkins, A. S. Wells, M. T. Williams, Continuous Processing in the Pharmaceutical Industry. Green Chemistry in the Pharmaceutical Industry; Wiley-VCH: Weinheim, Germany, **2010**.
2. K. Geyer, T. Gustafsson, P. H. Seeberger, *Synlett*. **2009**, *15*, 2382-2391.
3. M. B. Plutschack, B. Pieber, K. Gilmore, P. H. Seeberger, *Chem. Rev*. **2017**, *117*, 11796-11893.
4. B. P. Mason, K. E. Price, J. L. Steinbacher, A. R. Bogdan, D. T. McQuade, *Chem. Rev.* **2007**, 107, 2300-2318.
5. R. L. Hartman, J. P. McMullen, K. F. Jensen, *Angew. Chem. Int. Ed.* **2011**, 50, 7502-7519.
6. J. Wegner, S. Ceylan, A. Kirschning, *Chem. Commun.* **2011**, 47, 4583-4592.
7. A. J. deMello, *Nature* **2006**, 442, 394-402.
8. I. M. Mándity, S. B. Ötvös, G. Szöllősi, F. Fülöp, *Chem. Rec.* **2016**, *16*, 1018-1033.
9. C. T. Hsieh, S. B. Ötvös, Y. C. Wu, I. M. Mándity, F. R. Chang, F. Fülöp, *ChemPlusChem* **2015**, *80*, 859-864.
10. I. M. Mándity, S. B. Ötvös, F. Fülöp, *ChemistryOpen* **2015**, *4*, 212-223.
11. L. Kiss, F. Fülöp, *Chem. Rev.* **2014**, *114*, 1116-1169.
12. E. Juaristi, V. Soloshonok, Enantioselective Synthesis of β-Amino Acids, Second Edition, Wiley: Hoboken, NJ. **2005**.
13. T. A. Martinek, F. Fülöp, *Chem. Soc. Rev*. **2012**, *41*, 687-702.
14. E. Mayans, A. Gargallo, A. Álvarez-Larena, O. Illa, R. M. Ortuño, *Eur. J. Org. Chem*. **2013**, 1425-1433.
15. S. H. Choi, M. Ivancic, I. A. Guzei, S. H. Gellman, *Eur. J. Org. Chem*. **2013**, 3464-3469.
16. M. Risseeuw, M. Overhand, G. W. J. Fleet, M. I. Simone, *Amino Acids* **2013**, *45*, 613-689.
17. F. Fülöp, *Chem. Rev*. **2001**, *101*, 2181-2204.
18. M. A. Ivanov, L. A. Aleksandrova, *Russ. J. Bioorg. Chem.* **2013**, *39*, 22-39
19. Q. Zhao, M. Vargas, Y. Dong, L. Zhou, X. Wang, K. Sriraghavan, J. Keiser, J. L. Vennestrom, *J. Med. Chem.* **2010**, *53*, 4223-4233.
20. S. H. Gellman, S. H. *Accounts of Chemical Research* **1998**, *31*, 173-180.
21. D. J. Hill, M. J. Mio, R. B. Prince, T. S. Hughes, J. S. Moore, *Chemical Reviews* **2001**, *101*, 3893-4012.
22. T. A. Martinek, A. Hetényi, L. Fülöp, I. M. Mándity, G. K. Tóth, I. Dékány, F. Fülöp, *Angew. Chem. Int. Ed*. **2006**, *45*, 2396-2400.
23. A. Hetényi, I. M. Mándity, T. A. Martinek, G. K. Tóth, F. Fülöp, *J. Am. Chem. Soc.* **2005**, *127*, 547-553.
24. D. Seebach, A. K. Beck, D. J. Bierbaum, *Chemistry & Biodiversity.* **2004**, *1*, 1111-1239.
25. D. Seebach, D. F. Hook, A. Glättli, *Peptide Science.* **2006**, *84*, 23-37.
26. E.V. Rebrov, A. Berenguer-Murcia, H.E. Skelton, B.F.G. Johnson, A.E.H. Wheatley, J.C. Schouten, *Lab Chip*. **2009**, *9*, 503-506.
27. S. Kobayashi, *Chem. Asian J*. **2016**, *11*, 425-436.
28. J. Kobayashi, Y. Mori, K. Okamoto, R. Akiyama, M. Ueno, T. Kitamori, S. Kobayashi, *Science*. **2004**, 304, 1305-1308.
29. T. Maki, J.-i. Kitada, K. Mae, *Chem. Eng. Technol*. **2013**, *36*, 1027-1032.
30. G. Wirnsberger, B.J. Scott, G.D. Stucky, *Chem. Commun*. **2011**, 119-120.
31. K. Watts, A. Baker Thomas Wirth, *J. Flow Chem*. **2014**, *4*, 2-11.
32. E. Kumacheva, H. Zhang, Z. Nie, Polymerization in Microfluidic Reactors, in: T. R. Dietrich (Ed.), Microchemical Engineering in Practice, Wiley-VCh, Weinheim, **2009**, pp. 361-383.
33. L. Malet-Sanz, F. Susanne, *Med. Chem*. **2012**, *55*, 4062-4098.

34. K. Jähnisch, V. Hessel, H. Löwe, M. Baerns, *Angew. Chem. Int. Ed*. **2004,** *43*, 406-446.
35. N. Kockmann, *ChemBioEng Rev*. **2016**, *3*, 5-15.
36. O. Wörz, K. Jäckel, T. Richter, A. Wolf, *Chem. Eng. Technol*. **2001**, *24*, 138-142.
37. P. Watts, C. Wiles, S. Haswell, E. Pombo-Villar, *Lab Chip*. **2002**, *2*, 141-144.
38. X. Zhang, S. Stefanick, F.J. Villani, *Org. Process Res. Dev*. **2004**, *8*, 455-460.
39. S. Laue, V. Haverkamp, L. Mleczko, *Org. Process Res. Dev*. **2016**, 20, 480-486.
40. T. Schwalbe, V. Thomas, G. Autze Wille, *Chimia*. **2002**, *56*, 636-646.
41. F. Liguori, P. Barbaro, *J. Catal*. **2014**, *311*, 212-220.
42. J. Bravo, A. Karim, T. Conant, G.P. Lopez, A. Datye, *Chem. Eng. J*. **2004**, *101*, 113-121.
43. P. Watts, S.J. Haswell, *Chem. Soc. Rev*. **2005**, *34*, 235-246.
44. S. V. Luis, E. Garcia-Verdugo, *Chemical Reactions and Processes under Flow Conditions*, The Royal Society of Chemistry: **2009**.
45. T. Wirth, *Microreactors in Organic Synthesis and Catalysis*, Wiley-VCH: **2008**.
46. J. Wegner, S. Ceylan, A. Kirschning, *Adv. Synth. Catal.* **2012**, 354, 17-57.
47. P. Watts, C. Wiles, *Chem. Commun.* **2007**, 443-467.
48. N. Kockmann, M. Gottsponer, D.M. Roberge, *Chem. Eng. J*. **2011**, *167*, 718-726.
49. H. G. Jolliffe, D. I. Gerogiorgis, *Chem. Eng. Res. Des*. **2015**, *97*, 175-191.
50. N. Roberge, D. M. Gottsponer, M. Eyholzer, M. Kockmann, *Chem. Today*. **2009**, *27*, 8-11.
51. M. Movsisyan, E. I. P. Delbeke, J. K. E. T. Berton, C. Battilocchio, S. V. Ley, C. V. Stevens, *Chem. Soc. Rev.* **2016,** *45*, 4892-4928.
52. T. J. Ober, D. Foresti, J. A. Lewis, *Proc. Natl. Acad. Sci*. **2015**, *112*, 12293-12298.
53. V. Hessel, D. Kralisch, N. Kockmann, T. Noël, Q. Wang, *ChemSusChem*. **2013**, *6*, 746-789.
54. K. D. Nagy, B. Shen, T. F. Jamison, K. F. Jensen, *Org. Proc. Res. Dev.* **2012**, 16, 976-981.
55. T. Schwalbe, V. Autze, G. Wille, *Chimia* **2002**, *56*, 636–646.
56. A. Tanimu, S. Jaenicke, K. Alhooshani, *Chem. Eng. J*. **2017**, *327*, 792-821.
57. N. Kockmann, D. M. Roberge, *Chem. Eng. Technol.* **2009**, 32, 1682-1694.
58. J. C. Brandt, T. Wirth, *Beilstein J. Org. Chem.* **2009**, 5.
59. H. Usutani, Y. Tomida, A. Nagaki, H. Okamoto, T. Nokami, J.-i. Yoshida, *J. Am. Chem. Soc.* **2007**, 129, 3046-3047.
60. J.-i. Yoshida, A. Nagaki, T. Iwasaki, S. Suga, *Chem. Eng. Technol.* **2005**, 28, 259-266.
61. V. Hessel, D. Kralisch, N. Kockmann, Novel Process Windows: Innovative Gates to Intensified and Sustainable Chemical Processes, Wiley VCh, Weinheim, **2014**.
62. T. Razzaq, C. O. Kappe, *Chem Asian J.* **2010**, 5, 1274–1289.
63. V. Hessel, B. Cortese, M. H. J. M. de Croon, *Chem. Eng. Sci.* **2011**, 66, 1426-1448.
64. V. Hessel, *Chem. Eng. Technol.* **2009**, 32, 1655-1681.
65. E. R. Murphy, J. R. Martinelli, N. Zaborenko, S. L. Buchwald, K. F. Jensen, *Angew. Chem. Int. Ed.* **2007**, 46, 1734-1737.
66. M. Damm, T. N. Glasnov, C. O. Kappe, *Org. Process Res. Dev.* **2009**, 14, 215-224.
67. S. Kobayashi, K. A. Jorgensen, Cycloaddition Reactions in Organic Synthesis, Wiley-VCH Verlag GmbH & Co. KGaA, **2002**, pp. 5-327.
68. Methods and Applications of Cycloaddition Reactions in Organic Syntheses, ed. N. Nishiwaki, John Wiley & Sons, New York, **2014**.
69. B. Alcaide, P. Almendros, C. Aragoncillo, *Chem. Soc. Rev.* **2010**, *39*, 783-816.
70. J. Adrio, J. C. Carretero, *Chem. Commun*. **2014**, *50*, 12434-12446.
71. G. Masson, C. Lalli, M. Benohoud, G. Dagousset, *Chem. Soc. Rev.* **2013**, *42*, 902-923.
72. W. S. Hamama, M. E. Ibrahim, A. E. Metwalli, H. H. Zoorob. *Res Chem Intermed.* **2017**, *43*, 5943-5983.
73. R. Buchtík, J. Hlaváč, J. Slouka, P. Fryčák. *J. Heterocyclic Chem*. **2006**, *43*, 613-621.

74. Y. I. Sakhno, S. M. Desenko, S. V. Shishkina, O. V. Shishkin, D. O. Sysoyev, U. Groth C. O. Kappe, V. A. Chebanov. *Tetrahedron.* **2008**, *64*, 11041-11049.
75. J. -t. Cheng, X. -y. Chena, S. Ye, *Org. Biomol. Chem*. **2015**, *13*, 1313-1316.
76. C. H. Hornung, M. R. Mackley, I. R. Baxendale, S. V. Ley, *Org. Proc. Res. Dev*. **2007**, *11*, 399-405.
77. G. Shore, M. G. Organ, *Chem. Commun.* **2008**, 838-840.
78. T. Cablewski, A. F. Faux, C. R. Strauss, *J. Org. Chem*. **1994**, *59*, 3408-3412.
79. T. N. Glasnov and C. O. Kappe, Macromol. *Rapid Commun*. **2007**, *28*, 395-410.
80. I. R. Baxendale, J. J. Hayward, S. V. Ley, *Comb. Chem*. *High Throughput Screen*. **2007**, *10*, 802-836.
81. M. D. Bowman, J. L. Holcomb, C. M. Kormos, N. E. Leadbeater, V. A. Williams, *Org. Process Res. Dev.* **2008**, 12, 41-57.
82. K. Mennecke, R. Cecilia, T. N. Glasnov, S. Gruhl, C. Vogt, A. Feldhoff, M. A. L. Vargas, C. O. Kappe, U. Kunz, A. Kirschning, *Adv. Synth. Catal.* **2008**, *350*, 717-730.
83. R. J. J. Jachuck, D. K. Selvaraj, R. S. Varma, *Green Chem*. **2006**, *8*, 29-33.
84. J. A. Tripp, F. Svec, J. M. J. Fréchet, *J. Comb. Chem*. **2001**, *3*, 216-223.
85. A. Sachse, A. Galarneau, F. Di Renzo, F. Fajula, F. Fajula, B. Coq, *Chem. Mater*. **2010**, *22*, 4123-4125.
86. A. El Kadib, R. Chimenton, A. Sachse, F. Fajula, A. Galarneau, B. Coq, *Angew. Chem. Int. Ed*. **2009**, *48*, 4969-4972.
87. A. Sachse, V. Hulea, A. Finiels, B. Coq, F. Fajula, A. Galarneau, *J Catal*. **2012,** *287*, 62-67.
88. S. Seghers, L. Protasova, S. Mullens, J. W. Thybaut, C. V. Stevens. *Green Chem*. **2017**, *19*, 237-248.
89. B. Altava, M. I. Burguete, E. García-Verdugo, S.V. Luis, M. J. Vicent. *Green Chem*. **2006**, *8*, 717-726.
90. V. Chiroli, M. Benaglia, F. Cozzi, A. Puglisi, R. Annunziata, G. Celentano. *Org Lett*. **2013**, *15*, 3590-3593.
91. V. Chiroli, M. Benaglia, A. Puglisi, R. Porta, R. P. Jumde, A. Mandoli. *Green Chem*. **2014**, *16*, 2798-2806.
92. J. Tsoung, Y. Wang, S. W. Djuric, *React. Chem. Eng*. **2017**, *2*, 458-461.
93. J. Tsoung, A. R. Bogdan, S. Kantor, Y. Wang, M. Charaschanya, S. W. Djuric, *J. Org. Chem.* **2017**, *82*, 1073-1084.
94. M. Baumann, I. R. Baxendale, S. V. Ley, *Synlett*. **2010**, *5*, 749-752.
95. M. Grafton, A. C. Mansfield, M. J. Fray, *Tetrahedron Lett.* **2010**, *51*, 1026-1029.
96. D. Obermayer, T. N. Glasnov, C. O. Kappe, *J. Org. Chem*. **2011**, *76*, 6657-6669.
97. A. Herath, N. D. Cosford, *Org. Lett*. **2010**, *12*, 5182-5185.
98. N. Pagano, A. Herath, N. D. Cosford, *J. Flow Chem*. **2012**, *1*, 28-31.
99. A. Herath, R. Dahl, N. D. Cosford, *Org. Lett*. **2009**, *12*, 412-415.
100. M. C. Bagley, V. Fusillo, R. L. Jenkins, M. C. Lubinua, C. Mason, *Org. Biomol. Chem*. **2010**, *8*, 2245-2251.
101. J. S. Poh, D. L. Browne, S. V. Ley, *React. Chem. Eng.* **2016**, *1*, 101-105.
102. C. A. Carson, M. A. Kerr, *Chem. Soc. Rev*. **2009**, *38*, 3051-3060.
103. R. A. Yoder, J. N. Johnston, *Chem. Rev*. **2005**, *105*, 4730-4756.
104. Y. Cheng, Z. T. Huang, M.-X. Wang, *Curr. Org. Chem*. **2004**, *8*, 325-351.
105. O. Diels, W. E. Thiele, *Chem. Ber*. **1938**, *71*, 1173-1178.
106. H. Wollweber, *Diels–Alder-Reaction;* Georg Thieme Verlag: Stuttgart, **1972**, pp 152-270.
107. A. Ichihara, *Synthesis* **1987**, 207-222.
108. B. Rickborn, "The Retro–Diels–Alder Reaction Part I: C–C Dienophiles" in *Organic Reactions;* John Wiley & Sons, Inc., **2004.**

109. A. J. H. Klunder, J. Zhu, B. Zwanenburg, *Chem. Rev.* **1999**, *99*, 1163-1190.
110. G. Stájer, F. Csende, F. Fülöp, *Curr. Org. Chem.* **2003**, *7*, 1423-1432.
111. I. González-Temprano, I. Osante, E. Lete, N. Sotomayor, *J. Org. Chem.* **2004**, *69*, 3875-3885.
112. K. Suzuki, K. Inomata, Y. Endo, *Org. Lett.* **2004**, *6*, 409-411.
113. F. Csende, G. Stájer, F. Fülöp in Comprehensive Organic Synthesis, 2nd ed. (Eds.: P. Knochel, G. A. Molander), Elsevier, Amsterdam, **2014**, vol. 5, pp. 518-594.
114. G. Stájer, F. Miklós, I. Kanizsai, F. Csende, R. Sillanpää, P. Sohár, *Eur. J. Org. Chem*. **2004**, 3701-3706.
115. F. Miklós, G. Stájer, F. Fülöp, *Lett. Org. Chem*. **2006**, 3, 915-916.
116. F. Csende, F. Fülöp, G. Stájer, *Curr. Org. Synth*. **2008**, 5, 173-185.
117. G. Bernáth, G. Stájer, F. Fülöp, P. Sohár, *J. Heterocycl. Chem*. **2000**, *37*, 439-449.
118. C. F. Nising, U. K. Ohnemuller, S. Bräse, *Synthesis* **2006**, 2643-2645.
119. C. A. Citron, S. M. Wickel, B. Schulz, S. Draeger, J. S. Dickschat, *Eur. J. Org. Chem.* **2012**, 6636-6646.
120. D. R. Clay, A. G. Rosenberg, M. C. McIntosh, *Tetrahedron: Asymmetry* **2011**, *22*, 713-716.
121. T. Gallagher, S. Sanchez, J. H. Bateson, P. J. O'Hanlon, *Pure Appl. Chem.* **2009**, *77*, 2033-2040.
122. J. P. Eddolls, M. Iqbal, S. M. Robert, M. G. Santoro, *Tetrahedron* **2004**, *60*, 2539-2550.
123. M. Iqbal, Y. Li, P. Evans, *Tetrahedron* **2004**, *60*, 2531-2538.
124. Y. Arai, T. Kontani, T. Koizumi, *Chem. Lett.* **1991**, 2135-2138.
125. S. A. Hasbullah, S. Jones, *Tetrahedron: Asymmetry* **2010**, *21*, 2719-2725.
126. P. Roach, R. Warmuth, *Angew. Chem., Int. Ed*. **2003**, *42*, 3039-3042.
127. R. A. Aitken, J. I. G. Cadogan, I. Gosney, *J. Chem. Soc*. *Perkin Trans. 1*, **1994**, 927-931.
128. M. Fernández-Zertuche, S. López-Cortina, M. E. Meza-Aviña, M. Ordóñez, A. Ramírez-Solís, *Arkivoc*, **2003**, 89-99.
129. S. Kotha, S. Banerjee, M. P. Patil and R. B. Sunoj, *Org. Biomol. Chem*. **2006**, *4*, 1854-1856.
130. M. E. Bunnage, K. C. Nicolaou, *Chem. Eur.J*. **1997**, *3*, 187-192.
131. O. Papies, W. Grimme, *Tetrahedron Lett*. **1980**, *21*, 2799-2802.
132. D. A. Kummer, D. Li, A. Dion, A. G. Myers. *Chem. Sci.* **2011**, *2*, 1710-1718.
133. R. E. Martin, M. Lenz, T. Alzieu, J. D. Aebi, L. Forzy, *Tetrahedron Lett.* **2013**, *54*, 6703-6707.
134. G. Duret, R. Quilan, B. Yin, R. E. Martin, P. Bisseret, M. Neuburger, V. Gandon, N. Blanchard, *J. Org. Chem.*, **2017**, *82*, 1726-1742.
135. D. H. Appella, L. A. Christianson, I. L. Karle, D. R. Powell, S. H. Gellman, *J. Am. Chem. Soc.* **1996**, *118*, 13071-13072;
136. D. H. Appella, L. A. Christianson, D. A. Klein, D. R. Powell, X. L. Huang, J. J. Barchi, S. H. Gellman, *Nature*, **1997**, *387*, 381-384;
137. D. Seebach, M. Overhand, F. N. M. Kuhnle, B. Martinoni, L. Oberer, U. Hommel, H. Widmer, *Helv. Chim. Acta*, **1996**, *79*, 913-941;
138. P. I. Arvidsson, M. Rueping, D. Seebach, *Chem. Commun*, **2001**, 649-650;
139. F. Fülöp, T. A. Martinek, G. K. Tóth, *Chem. Soc. Rev*, **2006**, *35*, 323-334;
140. A. Altmayer-Henzien, V. Declerck, J. Farjon, D. Merlet, R. Guillot, D. J. Aitken, *Angew. Chem. Int. Ed*. **2015,** *54*, 10807-10810.
141. M. Alauddin, E. Gloaguen, V. Brenner, B. Tardivel, M. Mons, A. Zehnacker-Rentien, V. Declerck, D. J. Aitken, *Chem. Eur. J*. **2015**, *21*, 16479-16493.
142. T. A. Martinek, F. Fülöp, *Chem. Soc. Rev*. **2012**, *41*, 687-702.
143. T. A. Martinek, I. M. Mándity, L. Fülöp, G. K. Tóth, E. Vass, M. Hollósi, E. Forró, F. Fülöp, *J. Am. Chem. Soc*. **2006**, *128*, 13539-13544.

144. I. M. Mándity, E. Wéber, T. A. Martinek, G. Olajos, G. K. Tóth, E. Vass, F. Fülöp, *Angew. Chem. Int. Ed.* **2009**, *48*, 2171-2175.
145. A. Altmayer-Henzien, V. Declerck, D. Merlet, J.-P. Baltaze, J. Farjon, R. Guillot, D. J. Aitken, *J. Org. Chem*. **2013**, *78*, 6031-6039.
146. I. M. Mándity, F. Fülöp, *Expert Opin. Drug Discovery* **2015**, *10*, 1163-1177.
147. C. M. Goodman, S. Choi, S. Shandler, W. F. DeGrado, *Nat. Chem. Biol*. **2007**, *3*, 252-262.
148. C. Ghosh, G. B. Manjunath, P. Akkapeddi, V. Yarlagadda, J. Hoque, D. S. S. M. Uppu, M. M. Konai, J. Haldar, *J. Med. Chem*. **2014**, *57*, 1428-1436.
149. T. B. Potocky, J. Silvius, A. K. Menon, S. H. Gellman, *ChemBioChem.* **2007**, *8*, 917-926.
150. L. Fülöp, I. M. Mándity, G. Juhász, V. Szegedi, A. Hetényi, E. Wéber, Z. Bozsó, D. Simon, R. Benkő, Z. Király, T. A. Martinek, *Plos One* **2012**, *7*, e39485.
151. V. Azzarito, J. A. Miles, J. Fisher, T. A. Edwards, S. L. Warriner, A. J. Wilson, *Chem. Sci*. **2015,** *6*, 2434-2443.
152. R. P. Cheng, S. H. Gellman, W. F. DeGrado, *Chem. Rev*. **2001,** *101*, 3219-3232.
153. R. B. Merrifield, *J. Am. Chem. Soc*. **1963,** *85*, 2149.
154. L. A. Carpino, *Acc. Chem. Res*. **1987,** *20*, 401.
155. P. Watts, C. Wiles, S. J. Haswell, E. Pombo-Villar, P. Styring, *Chem. Commun.* **2001,** 990-991.
156. P. Watts, C. Wiles, S. J. Haswell, E. Pombo-Villar, *LabChip*, **2002**, 2, 141-144.
157. P. Watts, C. Wiles, S. J. Haswell, E. Pombo-Villar, *Tetrahedron*, **2002**, *58*, 5427-5439.
158. V. George, P. Watts, S. J. Haswell, E. Pombo-Villar, *Chem. Commun*, **2003**, 2886-2887.
159. O. Floegel, J. D. C. Codee, D. Seebach, P. H. Seeberger, *Angew. Chem., Int. Ed*., **2006**, *45*, 7000-7003.
160. J. K. Murray, S. H. Gellman, *Org. Lett*. **2005,** *7*, 1517-1520.
161. I. M. Mándity, B. Olasz, S. B. Ötvös, F. Fülöp, *ChemSusChem*, **2014**, *7*, 3172-3176.
162. A. Szloszár, F. Fülöp, I. M. Mándity, *ChemistrySelect*, **2017**, *2*, 6036-6039.
163. R. Dudhe, P. K. Sharma, P. Verma, A. Chaudhary, *J. Adv. Sci. Res.* **2011**, *2*, 10-17.
164. S. M. Vroegop, D. L. Chapman, D. E. Decker, L. A. Galinet, R. J. Brideau, K. A. Ready, C. J. Dunn, S. E. Buxser, *Int. J. Immunopharmacol*. **1999**, *21*, 647-662.
165. A. E. Rashad, A. H. Shamroukh, R. E. Abdel-Megeid, A. Mostafa, A. Kandil, R. Elshesheny, M. A. Ali, K. Banert, *Eur. J. Med. Chem*. **2010**, *45*, 5251-5257.
166. C. A. Bernhart, F. B. Haudricourt, J. L. Assens, J. Gougat, C. Lacour, A. Roccon, C. Cazaubon, J. C. Brelière, G. Le Fur, D. Nisato, *Bioorg. Med. Chem. Lett.* **1994**, *4*, 157-162.
167. M. Yamaguchi, K. Wakasugi, R. Saito, Y. Adachi, Y. Yoshikawa, H. Sakurai, A. Katoh, *J. Inorg. Biochem*. **2006**, *100*, 260-269.
168. D. C. White, T. D. Greenwood, A. L. Downey, J. R. Bloomquist, J. F. Wolfe, *Bioorg. Med. Chem*. **2004**, *12*, 5711-5717.
169. D. L. Temple, J. P. Yevich, R. R. Covington, C. A. Hanning, R. J. Seidehamel, H. K. Mackey, M. J. Bartek, *J. Med. Chem*. **1979**, *22*, 505-510.
170. J. V. dos Anjos, R. M. Srivastava, J. H. Costa-Silva, L. Scotti, M. T. Scotti, A. G. Wanderley, E. S. Leite, S. J. de Melo, F. J. Junior, *Molecules* **2012**, *17*, 809-819.
171. S. Johne, *The Quinazoline Alkaloids, in Progress in the Chemistry of Organic Natural Products*, Spinger-Verlag, Vienna, New York, **1984**, Vol. 46, p. 160.
172. G. Stájer, A. E. Szabó, J. Pintye, G. Bernáth, P. Sohár, *Chem. Soc., Perkin Trans. 1* **1985**, 2483-2487.
173. G. Stájer, A. E. Szabó, F. Fülöp, G. Bernáth, P. Sohár, *Chem. Ber.* **1987**, *120*, 259-264.
174. G. Stájer, A. E. Szabó, G. Bernáth, P. Sohár, *Synthesis* **1987**, 290-292.
175. M. Palkó, P. Sohár, F. Fülöp, *Molecules* **2011**, *16*, 7691-7705.
176. F. Fülöp, M. Palkó, G. Bernáth, P. Sohár, *Synth. Commun.* **1997**, *27*, 195-203.

177. F. Fülöp, F. Miklós, E. Forró, *Synlett*, **2008**, 1687-1689.
178. F. Miklós, Z. Tóth, M. M. Hänninen, R. Sillanpää, E. Forró, F. Fülöp, *Eur. J. Org. Chem.* **2013**, 4887-4894.
179. F. Miklós, T. Á. Bagi, F. Fülöp, *Arkivoc*. **2009**, 5-12.
180. F. Miklós, F. Fülöp, *Eur. J. Org. Chem.* **2010**, 959-965.
181. F. Miklós, A. Petrisor, F. Fülöp, *Arkivoc*. **2015**, 158-171.
182. M. Chakrabarty, S. Sarkar, Y. Harigaya, *Synthesis* **2003**, 2292-2294.
183. A. Kawano, S. Masuda, M. Saito, H.Tsuchiya, S. J. Fujimoto, *Electrochem. Soc*. **2016**, *163*, C506–C513.
184. A. R. Bogdan, K. James, *Chem. Eur. J*. **2010,** *16*, 14506-14512.
185. G. Stájer, A. E. Szabó, G. Bernáth, P. Sohár, *J. Chem. Soc. Perkin Trans. 1*, **1987**, 237-240.
186. S. Chandrasekhar, B. N. Babu, A. Prabhakar, A.; Sudhakar, M. S. Reddy, M. U. Kiran, B. Jagadeesh, *Chem. Commun*. **2006**, 1548-1550.
187. S. Chandrasekhar, A. Sudhakar, M. U. Kiran, B. N. Babu, B. Jagadeesh, *Tetrahedron Lett.* **2008**, *49*, 7368-7371.
188. I. M. Mándity, L. Fülöp, E. Vass, G. K. Tóth, T. A. Martinek, F. Fülöp, *Org. Lett*. **2010**, *12*, 5584-5587.
189. R. J. Doerksen, B. Chen, J. Yuan, J. D. Winkler, M. L. Klein, *Chem. Commun*. **2003**, 2534-2535.
190. W. A. Bonner, *Origins Life Evol. Biospheres* **1991**, *21*, 59-111.
191. J. L. Bada, *Nature* **1995**, *374*, 594-595.
192. M. Klussmann, D. G. Blackmond, in *Chemical Evolution II: From the Origins of Life to Modern Society*, *Vol. 1025*, American Chemical Society, **2009**, pp. 133-145.
193. T. Li, K.-H. Budt, Y. Kishi, *Chem. Commun*. **1987**, 1817-1819
194. A. Saghatelian, Y. Yokobayashi, K. Soltani, M. R. Ghadiri, *Nature* **2001**, *409*, 797-801.
195. R. R. Hill, D. Birch, G. E. Jeffs, M. North, *Org. Biomol. Chem*. **2003**, *1*, 965-972.
196. E. Torres, J. Puigmarti-Luis, A. P. del Pino, R. M. Ortuno, D. B. Amabilino, *Org. Biomol. Chem*. **2010**, *8*, 1661-1665.

APPENDIX

I.

ChemPubSoc Europe

DOI: 10.1002/open.201700078

Open Access ChemistryOPEN Communications

Homochirality of β-Peptides: A Significant Biomimetic Property of Unnatural Systems

István M. Mándity,[a] Imane Nekkaa,[a] Gábor Paragi,[b] and Ferenc Fülöp*[a, c]

Homochirality, an interesting phenomenon of life, is mainly an unresolved problem and was thought to be a property of living matter. Herein, we show that artificial β-peptides have the tendency toward homochiral diastereoselective chain elongation. Chain-length-dependent stereochemical discrimination was investigated in the synthesis of foldamers with various side chains and secondary structures. It was found that there is a strong tendency toward the synthesis of homochiral oligomers. The size of the side chain drastically influenced the selectivity of the stereodiscriminative chain-elongation reaction. It is noteworthy that water as the co-solvent increases the selectivity. Such behavior is a novel fundamental biomimetic property of foldamers with a potential of future industrial application.

Homochirality is an inherent property of vital polymers, for example, peptides, proteins, RNA, DNA, as well as oligo- and polysaccharides.[1] It is still not clear whether homochirality is a result of an autocatalytic procedure[2] or if it originates from extraterrestrial optically active non-racemic mixtures.[3] Numerous investigations have been carried out by various research groups to investigate the origin and role of this phenomenon.[1c,4] In the case of peptides, mainly the stereochemical discrimination in their synthesis has been investigated. For example, a racemate of activated amino acids was reacted with a given enantiomerically pure amino acid or peptide chain. The results reveal a strong tendency for the formation of homochiral sequences.[5] This effect is even more dominant when water is utilized as a co-solvent.[5a] In the case of self-templated peptide fragment coupling, again, homochiral compounds are formed.[6] On the other hand, when dipeptides were created, heterochiral sequences appeared.[7] In the case of peptides containing strongly structure-promoting α,α-disubstituted amino acid, the formation of heterochiral sequences is favored when large and bulky side chains are utilized.[8] However, for smaller side chains, the synthesis of homochiral peptides is preferred.[9] For similar sequences, helicity alone can govern the direction of enantioselectivity. For example, *P*-helices favor the incorporation of L-amino acids, whereas *M*-helices prefer the coupling of the *d*-enantiomer.[10]

Foldamers are artificial self-organizing biomimetic polymers.[11] These systems have a strong tendency to form highly stable and versatile secondary structures, for example, helices, strands, turns, and so on.[11g,12] Foldamers have numerous biomedical activities.[13] They are antibacterial amphiphills,[14] cell and membrane penetrating peptides,[15] *anti*-Alzheimer compounds,[16] and effectively modulate protein–protein interactions.[17] Based on this fact, they are nowadays considered as proteomimetics.[13a] Some of the most thoroughly investigated foldamers are the β-peptides,[11d–f,18] which possess additional biomimetic properties akin to natural α-peptides including hierarchical self-organization,[19] conformational polymorphism, and real folding reactions.[20]

Herein, we show that stereochemical discrimination towards the homochiral oligomers manifests for β-peptides too, akin to the biological homochirality of natural polymers. The phenomenon can be observed for various β-peptides with different secondary structures, side-chain shape, and chain length.

β-Peptide foldamers containing various cyclic side chains and possessing different secondary structures were selected for the examination of diastereo-discriminative peptide coupling with chain lengths varying from trimer to hexamer. As a reference, α-L-leucine homooligopeptides were selected. The investigated structures are shown in Scheme 1.

Oligomers **1**–**4** are composed of [1*R*,2*R*]-*trans*-2-aminocyclopentanecarboxylic acid ([1*R*,2*R*]-*trans*-ACPC) building blocks and they are known to form H12 helices.[11b] As a next step, for compounds **5**–**8**, the five-membered cyclic side chains were changed for a six-membered cyclohexane ring, while retaining the same stereochemistry. These oligomers were constructed from [1*R*,2*R*]-*trans*-2-aminocyclohexanecarboxylic acid ([1*R*,2*R*]-ACHC) residues.[11a] The formed secondary structure is a H14 helix. To investigate the effect of a strand structure, oligomers created from [1*S*,2*R*]-*cis*-ACHC were also assembled (β-peptides **9**–**12**). Homochiral homooligomers made from *cis*-β-amino acids are known to form strand structures.[19,21] This fact is further supported by a stereochemical patterning approach, which declares that β-peptides possessing different stereochemistry on the two sides of an amide bond form a strand structure.[12b]

As control structures, homooligomeric α-peptides composed of L-Leu were synthesized too (**13**–**16**). The isobutyl side chain

[a] Dr. I. M. Mándity, I. Nekkaa, Prof. Dr. F. Fülöp
Institute of Pharmaceutical Chemistry
University of Szeged
Eötvös u. 6, 6720 Szeged (Hungary)
E-mail: fulop@pharm.u-szeged.hu

[b] Dr. G. Paragi
MTA-SZTE Supramolecular and Nanostructured Materials Research Group
Dóm tér 8, 6720 Szeged (Hungary)

[c] Prof. Dr. F. Fülöp
Research Group of Stereochemistry of the Hungarian Academy of Sciences
Dóm tér 8, 6720 Szeged (Hungary)

Supporting Information for this article can be found under: https://doi.org/10.1002/open.201700078.

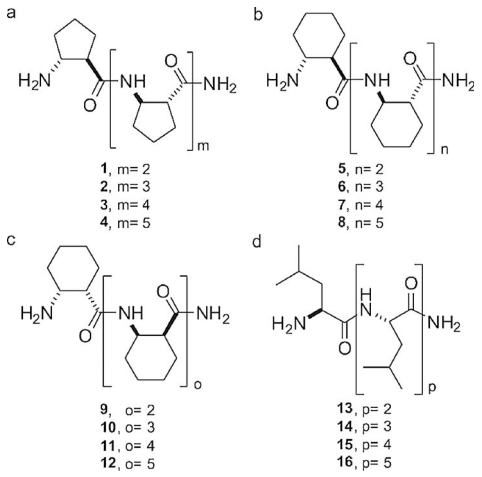

Scheme 1. The investigated structures possessing five- and six-membered side chains and *cis* or *trans* relative configuration.

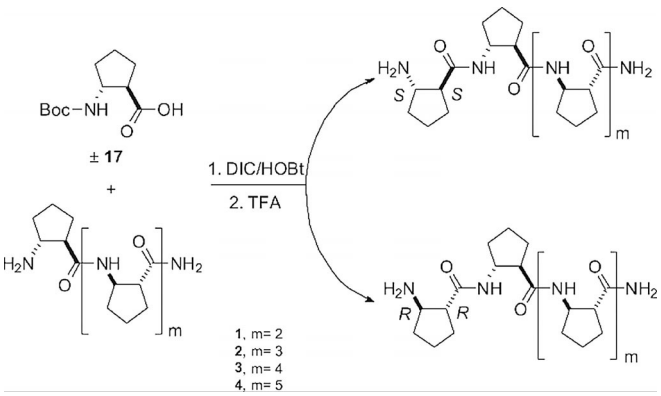

Scheme 2. The chain elongation of a β-peptide with a Boc-protected racemic amino acid yielding two diastereomers shown by the example of the *trans*-ACPC residue.

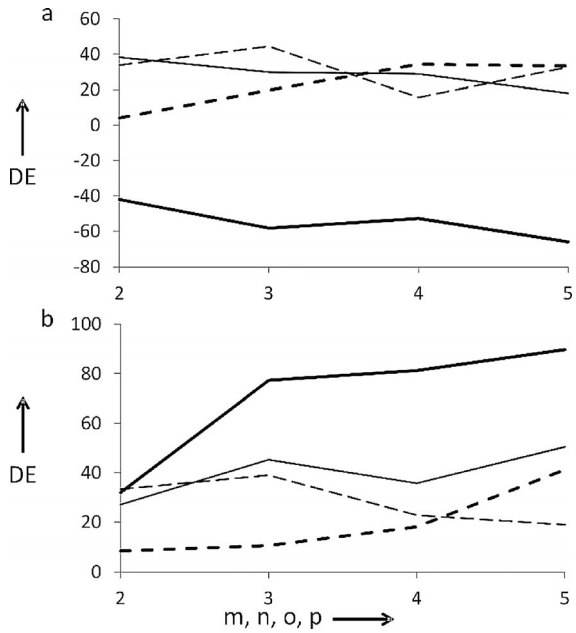

Figure 1. *DE* values obtained for **1**–**4** (thin solid line), **5**–**8** (thick solid line), **9**–**12** (thin dashed line), and **13**–**16** (thick dashed line) in the absence (a) and in the presence of water (b) as a function of chain length.

was selected in accordance with the β-amino acids described above, as only β-peptides comprising aliphatic side chains were tested.

The peptides were assembled by utilizing highly efficient continuous-flow solid-phase peptide synthesis technology developed in our laboratory.[22] The technology allows the construction of various peptides by using very low, generally 1.5-fold, amino-acid equivalents. The peptides were elongated in the instrument, and the products were cleaved and purified through regular reversed-phase HPLC methodology.

The stereochemical discrimination properties of the β-peptides were tested by means of a solution-phase peptide-coupling technique. The purified peptides were dissolved in a 2:1 mixture of dichloromethane (DCM) and *N*,*N*-dimethylformamide (DMF). Subsequently, 10 equivalents of the *tert*-butyloxycarbonyl (Boc)-protected racemic amino acid was coupled by using *N*,*N*′-diisopropylcarbodiimide (DIC) and hydroxybenzotriazole (HOBt) coupling agents. The reaction time was 48 h. Importantly, the effect of water on the stereochemical discrimination was also investigated, as it is known to be a crucial factor.[5a,6] Thus, the reactions described above were performed in the solvent system DCM/DMF/H_2O 2:1:1 with a reaction time of 48 h. The solvents were removed in vacuo and Boc deprotection was carried out by TFA treatment. Finally, the product was lyophilized and the raw material was analyzed by using HPLC–MS. The complete procedure is shown in Scheme 2 with the example of oligomers built from *trans*-ACPC. The homochiral chain-elongated reference compounds were always synthetized independently and the heterochiral diastereomers were deduced from the HPLC–MS chromatogram.

Based on the area integrals of the homochiral and heterochiral peptides, the diastereomeric excess (*DE*) of the reaction was calculated for all peptides in both the presence and the absence of water. The *DE* values are shown in Figure 1 in a chain-length-dependent manner.

In the absence of water, a strong tendency towards the homochiral structures was observable for peptides containing the [1*R*,2*R*]-*trans*-ACPC unit (**1**–**4**). A slight decrease in selectivity was found as a function of chain length. The situation is completely different for the oligomers composed of [1*R*,2*R*]-*trans*-ACHC (**5**–**8**), which contain a more bulky side chain. The selectivity changed, the formation of the heterochiral product became favored, and a nice chain-length-dependent correlation was found. A change in selectivity towards the heterochiral sequences in a stereo-discriminative chain elongation was observed for peptides composed of α,α-disubstituted amino acids with large bulky side chains.[9] A simple change in the side chain caused a drastic difference in the stereochemical discrimination properties of β-peptides. To investigate the effect of *cis* relative configuration, compounds containing [1*S*,2*R*]-*cis*-ACHC (**9**–**12**) were also studied. Again, a definite tendency was observed towards the homochiral oligomers. The chain length did not significantly alter the *DE* value. As

a reference, α-peptides composed of L-Leu were investigated. The diastereoselectivity showed a clear chain-length-dependent manner and the homochiral product was favored. Importantly, the chain elongation of the trimer L-Leu showed only very minor diastereo-differentiation.

In general, the presence of water enhanced the selectivity toward the formation of homochiral homooligomers. In the case of peptides built of [1*R*,2*R*]-*trans*-ACPC, *DE* values increased compared to those formed in non-aqueous experiments and a clear chain-length-dependent increase could also be observed. The most dramatic difference compared to the experiment performed without water can be observed for oligomers comprising [1*R*,2*R*]-*trans*-ACHC. The selectivity changed to the opposite direction and homochiral compounds were profoundly formed during the coupling of the Boc-protected racemic *trans*-ACHC. In this case, a more dominant chain-length-dependent fashion can be observed and, importantly, the diastereoselective chain elongation of the hexamer reached a *DE* of almost 90%. The effect of *cis* relative configuration was also investigated in the presence of water. The results indicate again the profound formation of the homochiral oligomer. Interestingly, *DE* values decreased to some extent as a function of chain length. The reference L-Leu oligomers preferred the incorporation of the homochiral amino acids in a chain-length-dependent manner. Nonetheless, water, in general, increased the *DE* values compared to the results of the water-free experiments.

To understand the effect of water in the diastereoselective chain-elongation reaction, the effect of water on the foldameric systems itself should be considered. Foldameric systems are known to show secondary structure-dependent self-association with water as the solvent.[19,20] Helical structures self-associate into vesicles, whereas strand structures form nano-sized fibrils. It has been reported that the self-association of peptides is a crucial factor behind biological homochirality.[5a,6] Consequently, we turned to investigate the effect of self-association of β-peptides on the stereochemical discrimination by means of theoretical calculations. Oligomer **7**, containing *trans*-ACHC, has been selected as an example, as it showed the most dramatic water-dependent diastereo-discrimination.

Having a draft picture about the reaction barriers or possible steric hindrances, DFT calculations were carried out at the OLYP/tz2p level of theory.[23] This method can provide acceptable geometries or reaction barriers for organic compounds.[24] Transition states were calculated for the systems composed of Boc-protected [1*R*,2*R*]- and [1*S*,2*S*]-*trans*-ACHC hydroxybenzotriazole ester and oligomer **6**. The structure of the latter was previously optimized in the form of a H14 helix. The reason for selecting β-peptide **6** is that it forms a helical structure with the shortest chain length,[11a] which is the optimum structure for quantum chemical calculations with acceptable calculation times. Solvent effects were taken into account by means of the COSMO solvent model, utilizing the permittivity of chloroform and water.[25] The calculated relative barrier energies are shown in Table 1.

The reaction barrier of the heterochiral construct was found to be lower than those for the homochiral one in both solvents. Consequently, the simplified model system cannot reproduce the changes in the trends caused by the absence or presence of water.

Table 1. Relative barrier energies (in kcal mol^{-1}) for the transition state of the chain elongation **6** in water and chloroform.

Solvent	Homochiral chain elongation	Heterochiral chain elongation
chloroform	2.4	1.0
water	4.8	0.0

However, investigating the 3D structure of the homo- and heterochirally elongated compounds, self-association might increase geometrical strain. To examine the effect of self-association on the stereochemical discrimination in the chain elongation of β-peptides, further theoretical calculations were carried out and first a membrane segment was constructed and optimized by utilizing the MMFF94[26] force field. The assembly is shown in Figure 2a. For this purpose, oligomer **7** was selected, as it has been reported to form solely a H14 helix.[20]

Our effort to perform similar density functional investigations and calculate the height of the barrier was not successful, because of the size of the systems. However, hetero- and ho-

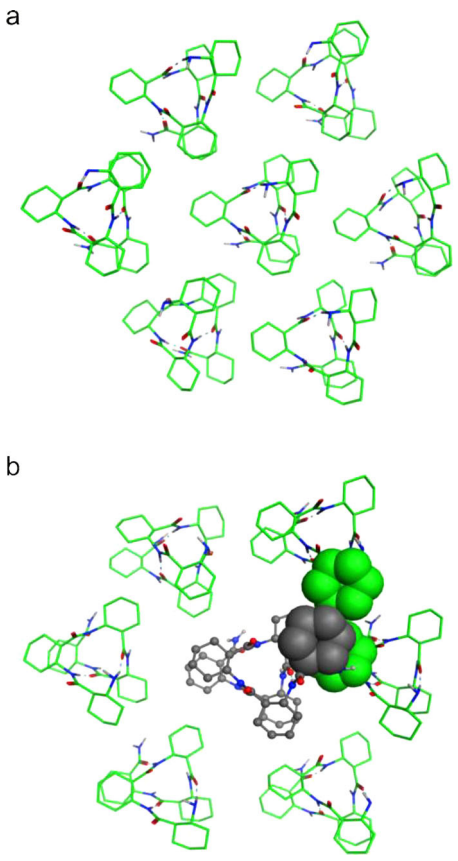

Figure 2. a) Molecular model for the vesicular membrane segment formed of **7** (top view). b) The incorporation of the heterochirally chain-elongated construct to the membrane (grey-colored ball-and-stick representation). The clashes of the side chains are depicted by the overlapping of the space filling model of the involved residues.

mochirally elongated oligomers were merged into the membrane. For the heterochiral constructs, a clear collision was found between the helices of oligomer **7** building the membrane segment and the investigated compound shown in Figure 2b. This interaction hinders and blocks the heterochiral chain elongation, and, consequently, the formation of homochiral oligomers is favored.

We can conclude that the biological homochirality as a property is also occurring with unnatural compounds, like β-peptide foldamers. The phenomenon was investigated by means of diastereoselective amino-acid coupling. β-Peptide oligomers composed of either *cis* or *trans* alicyclic β-amino acids showed a tendency towards the homochiral constructs. The oligomers composed of [1*R*,2*R*]-*trans*-ACHC residues showed an interesting property. In non-aqueous solvent systems, these compounds favored the formation of the heterochiral construct; whereas, in the presence of water, the opposite homochiral oligomers were preferred. Theoretical calculations indicated that water plays a crucial role in this phenomenon through the induction of self-association. In all cases, water enhanced the diasetereoselectivity towards the homochiral oligomers. This property was observed for the L-Leu-containing reference α-peptides, further underlining the key role of water in the induction of biological homochirality. It should be noted that a relationship between the chain length and diastereoselectivity of the chain-elongation reaction might be established in the presence of water. In the case of oligomers composed of *trans*-ACPC, *trans*-ACHC, or L-Leu residues, the longer chain length provided higher *DE* values in the presence of water. For the strand-forming compounds containing *cis*-ACHC residues, in contrast, the chain length did not drastically influence diastereoselectivity. The results gained in this fundamental study might provide the basis for industrial synthesis of β-peptides.

Experimental Section

Peptide Synthesis

Homooligomer foldamers **1**–**16** were synthesized by using a standard solid-phase technique utilizing fluorenylmethyloxycarbonyl (Fmoc) chemistry. The peptide chains were elongated on TentaGel R RAM resin (0.19 mmol g^{-1}) and the syntheses were carried out manually on a 0.1 mmol scale. Couplings were performed with HATU/DIPEA without difficulties. The formed peptide sequences were cleaved from the resin with 95% trifluoroacetic acid (TFA) and 5% H_2O at room temperature for 3 h. TFA was then removed and the resulting free peptides were solubilized in aqueous acetic acid (10%), filtered, and lyophilized. The crude peptides were investigated by using HPLC–MS.

Diastereodiscriminative Coupling Reactions

In an illustrative procedure, solutions of peptides **1**–**16** (0.01 mmol) were prepared separately with HOBt (0.12 mmol) and DIC (0.12 mmol) in CH_2Cl_2/DMF (2:1) in the absence or in the presence of water (2:1:1). Then Boc-protected racemic amino acids (0.1 mmol) were added. The mixtures were stirred for 48 h, CH_2Cl_2 was removed by evaporation, and water was subsequently added to the residue by liophilization. The product was treated with 95% TFA and 5% water to remove Boc protecting groups. The solutions were then stirred for 30 min, TFA was removed in vacuo, the residue was diluted with water, and then lyophilized. Samples were analyzed by using HPLC–MS.

Acknowledgements

We are grateful to the Hungarian Research Foundation (OTKA No. K 115731). The financial support of the GINOP-2.3.2–15–2016-00014 project is acknowledged, as well as support by the ÚNKP-16-4-III New National Excellence Program of the Ministry of Human Capacities. G.P. would like to thank the Marie Curie Intra European Fellowship and the GINOP-2.3.2–15–2016-00034 grant for the financial support.

Conflict of Interest

The authors declare no conflict of interest.

Keywords: chirality · diastereoselectivity · foldamer · homochiralty · β-peptide

[1] a) W. A. Bonner, *Origins Life Evol. Biospheres* **1991**, *21*, 59–111; b) J. L. Bada, *Nature* **1995**, *374*, 594–595; c) M. Klussmann, D. G. Blackmond, in *Chemical Evolution II,: From the Origins of Life to Modern Society, Vol. 1025*, American Chemical Society, **2009**, pp. 133–145.

[2] a) K. Soai, T. Shibata, I. Sato, *Acc. Chem. Res.* **2000**, *33*, 382–390; b) K. Soai, T. Shibata, H. Morioka, K. Choji, *Nature* **1995**, *378*, 767–768.

[3] a) M. H. Engel, S. A. Macko, *Nature* **1997**, *389*, 265–268; b) B. A. McGuire, P. B. Carroll, R. A. Loomis, I. A. Finneran, P. R. Jewell, A. J. Remijan, G. A. Blake, *Science* **2016**, *352*, 1449–1452.

[4] a) A. Brewer, A. P. Davis, *Nat. Chem.* **2014**, *6*, 569–574; b) M. Wu, S. I. Walker, P. G. Higgs, *Astrobiology* **2012**, *12*, 818–829; c) J. S. Siegel, *Chirality* **1998**, *10*, 24–27.

[5] a) T. Li, K.-H. Budt, Y. Kishi, *Chem. Commun.* **1987**, 1817–1819; b) S. I. Goldberg, J. M. Crosby, N. D. Iusem, U. E. Younes, *J. Am. Chem. Soc.* **1987**, *109*, 823–830; c) T. Hitz, M. Blocher, P. Walde, P. L. Luisi, *Macromolecules* **2001**, *34*, 2443–2449; d) K. Wen, L. E. Orgel, *Origins Life Evol. Biospheres* **2001**, *31*, 241–248.

[6] a) M. R. Ghadiri, D. H. Lee, K. Severin, Y. Yokobayashi, *Nature* **1997**, *390*, 591–594; b) D. H. Lee, J. R. Granja, J. A. Martinez, K. Severin, M. R. Ghadiri, *Nature* **1996**, *382*, 525–528; c) A. Saghatelian, Y. Yokobayashi, K. Soltani, M. R. Ghadiri, *Nature* **2001**, *409*, 797–801.

[7] R. R. Hill, D. Birch, G. E. Jeffs, M. North, *Org. Biomol. Chem.* **2003**, *1*, 965–972.

[8] a) C. Toniolo, M. Crisma, F. Formaggio, C. Peggion, *Biopolymers* **2001**, *60*, 396–419; b) C. Toniolo, E. Benedetti, *Macromolecules* **1991**, *24*, 4004–4009; c) C. Toniolo, E. Benedetti, *Trends Biochem. Sci.* **1991**, *16*, 350–353; d) M. De Poli, W. Zawodny, O. Quinonero, M. Lorch, S. J. Webb, J. Clayden, *Science* **2016**, *352*, 575–580; e) B. A. F. Le Bailly, J. Clayden, *Chem. Commun.* **2016**, *52*, 4852–4863; f) B. A. F. Le Bailly, L. Byrne, J. Clayden, *Angew. Chem. Int. Ed.* **2016**, *55*, 2132–2136; *Angew. Chem.* **2016**, *128*, 2172–2176; g) J. E. Jones, V. Diemer, C. Adam, J. Raftery, R. E. Ruscoe, J. T. Sengel, M. I. Wallace, A. Bader, S. L. Cockroft, J. Clayden, S. J. Webb, *J. Am. Chem. Soc.* **2016**, *138*, 688–695.

[9] M. Crisma, A. Moretto, F. Formaggio, B. Kaptein, Q. B. Broxterman, C. Toniolo, *Angew. Chem. Int. Ed.* **2004**, *43*, 6695–6699; *Angew. Chem.* **2004**, *116*, 6863–6867.

[10] L. Byrne, J. Sola, J. Clayden, *Chem. Commun.* **2015**, *51*, 10965–10968.

[11] a) D. H. Appella, L. A. Christianson, I. L. Karle, D. R. Powell, S. H. Gellman, *J. Am. Chem. Soc.* **1996**, *118*, 13071–13072; b) D. H. Appella, L. A. Christianson, D. A. Klein, D. R. Powell, X. L. Huang, J. J. Barchi, S. H. Gellman, *Nature* **1997**, *387*, 381–384; c) S. H. Gellman, *Acc. Chem. Res.* **1998**, *31*, 173–180; d) D. Seebach, M. Overhand, F. N. M. Kuhnle, B. Martinoni, L.

Oberer, U. Hommel, H. Widmer, *Helv. Chim. Acta* **1996**, *79*, 913 – 941; e) P. I. Arvidsson, M. Rueping, D. Seebach, *Chem. Commun.* **2001**, 649 – 650; f) F. Fülöp, T. A. Martinek, G. K. Toth, *Chem. Soc. Rev.* **2006**, *35*, 323 – 334; g) T. A. Martinek, F. Fulop, *Chem. Soc. Rev.* **2012**, *41*, 687 – 702; h) A. Altmayer-Henzien, V. Declerck, J. Farjon, D. Merlet, R. Guillot, D. J. Aitken, *Angew. Chem. Int. Ed.* **2015**, *54*, 10807 – 10810; *Angew. Chem.* **2015**, *127*, 10957 – 10960; i) M. Alauddin, E. Gloaguen, V. Brenner, B. Tardivel, M. Mons, A. Zehnacker-Rentien, V. Declerck, D. J. Aitken, *Chem. Eur. J.* **2015**, *21*, 16479 – 16493.

[12] a) T. A. Martinek, I. M. Mandity, L. Fulop, G. K. Toth, E. Vass, M. Hollosi, E. Forro, F. Fulop, *J. Am. Chem. Soc.* **2006**, *128*, 13539 – 13544; b) I. M. Mándity, E. Weber, T. A. Martinek, G. Olajos, G. K. Toth, E. Vass, F. Fulop, *Angew. Chem. Int. Ed.* **2009**, *48*, 2171 – 2175; *Angew. Chem.* **2009**, *121*, 2205 – 2209; c) A. Altmayer-Henzien, V. Declerck, D. Merlet, J.-P. Baltaze, J. Farjon, R. Guillot, D. J. Aitken, *J. Org. Chem.* **2013**, *78*, 6031 – 6039.

[13] a) I. M. Mándity, F. Fülöp, *Expert Opin. Drug Discovery* **2015**, *10*, 1163 – 1177; b) C. M. Goodman, S. Choi, S. Shandler, W. F. DeGrado, *Nat. Chem. Biol.* **2007**, *3*, 252 – 262; c) D. Seebach, J. Gardiner, *Acc. Chem. Res.* **2008**, *41*, 1366 – 1375; d) W. S. Horne, *Expert Opin. Drug Discovery* **2011**, *6*, 1247 – 1262; e) M. Jost, J.-C. Greie, N. Stemmer, S. D. Wilking, K. Altendorf, N. Sewald, *Angew. Chem. Int. Ed.* **2002**, *41*, 4267 – 4269; *Angew. Chem.* **2002**, *114*, 4438 – 4440; f) N. Koglin, C. Zorn, R. Beumer, C. Cabrele, C. Bubert, N. Sewald, O. Reiser, A. G. Beck-Sickinger, *Angew. Chem. Int. Ed.* **2003**, *42*, 202 – 205; *Angew. Chem.* **2003**, *115*, 212 – 215; g) N. Sewald, *Angew. Chem. Int. Ed.* **2003**, *42*, 5794 – 5795; *Angew. Chem.* **2003**, *115*, 5972 – 5973; h) S. Urman, K. Gaus, Y. Yang, U. Strijowski, N. Sewald, S. De Pol, O. Reiser, *Angew. Chem. Int. Ed.* **2007**, *46*, 3976 – 3978; *Angew. Chem.* **2007**, *119*, 4050 – 4053; i) L. Nagel, C. Plattner, C. Budke, Z. Majer, A. L. DeVries, T. Berkemeier, T. Koop, N. Sewald, *Amino Acids* **2011**, *41*, 719 – 732.

[14] a) C. Ghosh, G. B. Manjunath, P. Akkapeddi, V. Yarlagadda, J. Hoque, D. S. S. M. Uppu, M. M. Konai, J. Haldar, *J. Med. Chem.* **2014**, *57*, 1428 – 1436; b) D. Liu, W. F. DeGrado, *J. Am. Chem. Soc.* **2001**, *123*, 7553 – 7559.

[15] a) M. Rueping, Y. Mahajan, M. Sauer, D. Seebach, *ChemBioChem* **2002**, *3*, 257 – 259; b) T. B. Potocky, J. Silvius, A. K. Menon, S. H. Gellman, *ChemBioChem* **2007**, *8*, 917 – 926.

[16] a) Y. Imamura, N. Watanabe, N. Umezawa, T. Iwatsubo, N. Kato, T. Tomita, T. Higuchi, *J. Am. Chem. Soc.* **2009**, *131*, 7353 – 7359; b) L. Fülöp, I. M. Mandity, G. Juhasz, V. Szegedi, A. Hetenyi, E. Weber, Z. Bozso, D. Simon, R. Benko, Z. Kiraly, T. A. Martinek, *Plos One* **2012**, *7*, e39485.

[17] a) V. Azzarito, K. Long, N. S. Murphy, A. J. Wilson, *Nat. Chem.* **2013**, *5*, 161 – 173; b) V. Azzarito, J. A. Miles, J. Fisher, T. A. Edwards, S. L. Warriner, A. J. Wilson, *Chem. Sci.* **2015**, *6*, 2434 – 2443; c) L. M. Johnson, W. S. Horne, S. H. Gellman, *J. Am. Chem. Soc.* **2011**, *133*, 10038 – 10041; d) E. F. Lee, J. D. Sadowsky, B. J. Smith, P. E. Czabotar, K. J. Peterson-Kaufman, P. M. Colman, S. H. Gellman, W. D. Fairlie, *Angew. Chem. Int. Ed.* **2009**, *48*, 4318 – 4322; *Angew. Chem.* **2009**, *121*, 4382 – 4386.

[18] R. P. Cheng, S. H. Gellman, W. F. DeGrado, *Chem. Rev.* **2001**, *101*, 3219 – 3232.

[19] T. A. Martinek, A. Hetenyi, L. Fulop, I. M. Mandity, G. K. Toth, I. Dekany, F. Fulop, *Angew. Chem. Int. Ed.* **2006**, *45*, 2396 – 2400; *Angew. Chem.* **2006**, *118*, 2456 – 2460.

[20] A. Hetényi, I. M. Mandity, T. A. Martinek, G. K. Toth, F. Fulop, *J. Am. Chem. Soc.* **2005**, *127*, 547 – 553.

[21] a) F. Rúa, S. Boussert, T. Parella, I. Diez-Perez, V. Branchadell, E. Giralt, R. M. Ortuno, *Org. Lett.* **2007**, *9*, 3643 – 3645; b) E. TorRes, J. Puigmarti-Luis, A. P. del Pino, R. M. Ortuno, D. B. Amabilino, *Org. Biomol. Chem.* **2010**, *8*, 1661 – 1665; c) E. TorRes, E. Gorrea, K. K. Burusco, E. Da Silva, P. Nolis, F. Rua, S. Boussert, I. Diez-Perez, S. Dannenberg, S. Izquierdo, E. Giralt, C. Jaime, V. Branchadell, R. M. Ortuno, *Org. Biomol. Chem.* **2010**, *8*, 564 – 575.

[22] I. M. Mándity, B. Olasz, S. B. Ötvös, F. Fülöp, *ChemSusChem* **2014**, *7*, 3172 – 3176.

[23] a) N. C. Handy, A. J. Cohen, *Mol. Phys.* **2001**, *99*, 403 – 412; b) P. V. J. G. Snijders, E. J. Baerends, *At. Nucl. Data Tab.* **1981**, *26*, 483 – 509; c) B. G. Johnson, P. M. W. Gill, J. A. Pople, *J. Chem. Phys.* **1993**, *98*, 5612 – 5626; d) C. Lee, W. Yang, R. G. Parr, *Phys. Rev. B* **1988**, *37*, 785 – 789.

[24] a) V. A. Guner, K. S. Khuong, K. N. Houk, A. Chuma, P. Pulay, *J. Phys. Chem. A* **2004**, *108*, 2959 – 2965; b) A. P. Bento, M. Sola, F. M. Bickelhaupt, *J. Chem. Theory Comput.* **2008**, *4*, 929 – 940.

[25] A. Klamt, G. Schuurmann, *J. Chem. Soc. Perkin Trans. 2* **1993**, 799 – 805.

[26] T. A. Halgren, *J. Comput. Chem.* **1999**, *20*, 720 – 729.

Received: April 19, 2017
Version of record online ■■ ▮▮, 2017

I. M. Mándity, I. Nekkaa, G. Paragi, F. Fülöp*

■■ – ■■

Homochirality of β-Peptides: A Significant Biomimetic Property of Unnatural Systems

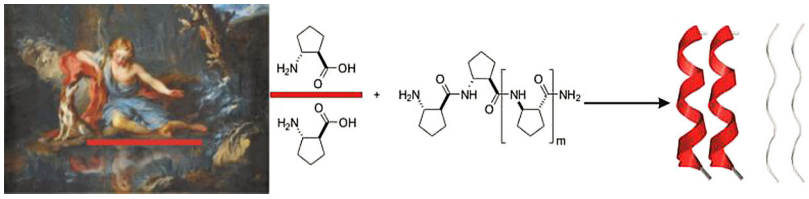

Homochirality of artificial systems: A characteristic property of biotic systems is found to be a profound asset of unnatural β-peptides. Diastereodiscriminative chain elongation of β-peptides with various secondary structures and side chains reveals a strong tendency toward the construction of homochiral oligomers. Water, as the cradle of life, further enhances this property. These results might be useful in future industrial synthesis development.

II.

BEILSTEIN JOURNAL OF ORGANIC CHEMISTRY

Continuous-flow retro-Diels–Alder reaction: an efficient method for the preparation of pyrimidinone derivatives

Imane Nekkaa[1], Márta Palkó[1], István M. Mándity[1] and Ferenc Fülöp[*1,2]

Full Research Paper

Open Access

Address:
[1]Institute of Pharmaceutical Chemistry, University of Szeged, Eötvös u. 6, H-6720 Szeged, Hungary, and [2]MTA-SZTE Stereochemistry Research Group, Hungarian Academy of Sciences, Eötvös u. 6, H-6720 Szeged, Hungary

Email:
Ferenc Fülöp[*] - fulop@pharm.u-szeged.hu

* Corresponding author

Keywords:
continuous-flow; desulfurisation; norbornene-fused heterocycles; pyrimidinones; retro-Diels–Alder reaction

Beilstein J. Org. Chem. **2018,** *14,* 318–324.
doi:10.3762/bjoc.14.20

Received: 13 November 2017
Accepted: 22 January 2018
Published: 01 February 2018

Associate Editor: A. Kirschning

Abstract

The syntheses of various pyrimidinones as potentially bioactive products by means of the highly controlled continuous-flow retro-Diels–Alder reaction of condensed pyrimidinone derivatives are presented. Noteworthy, the use of this approach allowed us to rapidly screen a selection of conditions and quickly confirm the viability of preparing the desired pyrimidinones in short reaction times. Yields typically higher than those published earlier using conventional batch or microwave processes were achieved.

Introduction

The continuous-flow (CF) technology has gained significant importance in modern synthetic chemistry [1-3] and becomes a core technology in the pharmaceutical, agrochemical, and fine chemical industries [4,5]. The use of this technology opens a new door to a quick optimization, acceleration [6], and easy scale-up with a wide and growing range of chemical transformations in combination with an inherently safe and green nature [7-12]. Advantageously, safety issues are complied with excellent mixing and heat transfer [7-14]. These allow the access to elevated temperatures and pressures accredited to superheating of organic solvents in a controlled and safe fashion [6,14-17]. The accurate tuning of residence time can further broaden the versatility of CF processes by governing the outcome of chemical reactions, determining the reaction rate and the conversion and by influencing product selectivities [17-19]. Thus, flow chemistry has long been selected to provide a simple means to use more rigorous reaction conditions and revisit difficult reactions that have been neglected in the past [21].

The retro-Diels–Alder (rDA) reaction has become an important tool for synthetic chemists in their search towards the synthesis and design of novel heterocyclic scaffolds. This pyrolytic disso-

ciation arises when one or both fragments are notably stable [22]. The unsaturation present in the original starting material is produced in the DA addition, and the same atoms are involved in both the bond formation and cleavage steps [23-25]. The rDA process is an efficient technique for the introduction of a double bond into a heterocyclic skeleton [26] as well as for the enantiodivergent [27] and the enantiocontrolled [28] syntheses of heterocyclic compounds. The rDA products can be gained, due to a thermal [4 + 2]-cycloreversion, by distillation under reduced pressure [29], boiling in solvent [30,31], and applying microwave irradiation [32-35] or flash vacuum pyrolysis [35,36]. rDA reactions under mild conditions have been widely examined and discussed for the laboratory preparation of heteromonocycles or condensed-ring heterocycles [37-40]. However, the CF rDA method was introduced when Meyers' group performed the preparation of a precursor intermediate for the construction of diverse tetracycline antibiotics [41]. Our aim in the present study was to synthesize functionalized pyrimidinone systems through rDA reactions. Many of these products are of high importance in drug design due to their diverse biological properties including antimicrobial, antiviral, antioxidant and antitumor activities. In addition, they are present in several natural frameworks [42-44].

We wanted to exploit the benefits of flow processing for reaction optimization and synthesis and develop novel sustainable synthetic methodologies with possible useful applications for the pharmaceutical industry. Our results show that the developed CF technology is superior to existing conventional batch technologies.

Results and Discussion

The starting materials, i.e., fused tricyclic or tetracyclic pyrimidinones **1**–**8** have been previously prepared by literature methods [26,45-50]. Cyclization of the corresponding di-*exo*- or di-*endo*-amino acids or esters with ethyl *p*-chlorobenzimidate resulted in tricyclic pyrimidinones **1**, **2a** and **2b** [26,45-49]. Methanopyrrolo-, methanopyrido- and methanoazepino[2,1-*b*]quinazolinones **3**–**6** were prepared by ring enlargement of di-*exo*-norbornene-fused azetidinones with lactim ethers [50]. For the preparation of 2-thioxopyrimidinones **7**, **8a** and **8b**, the most common method is the reaction of the appropriate amino esters with phenyl isothiocyanate, followed by cyclization of the resulting thiourea with hydrogen chloride under reflux [45,49]. The starting materials were selected to comprise molecules where good (>80%), medium (70–80%) and no conversion was observed under batch rDA conditions. Batch reactions were carried out by the following ways: heating under neat conditions, refluxing in solvents having a high boiling point [chlorobenzene (CB) or 1,2-dichlorobenzene (DCB)], and under microwave (MW) conditions in DCB.

In order to provide a rapid and efficient access to the desired pyrimidinones **9**–**14** (Scheme 1), we reinvestigated these rDA reactions by using another method involving flow chemistry. Therefore, a modular flow system was designed, equipped with a heated 304 stainless steel coil and an adjustable back-pressure regulator (0–300 bar) controlling the use of solvents under superheated conditions. The coil was heated in an oven to the desired temperature and solutions of the starting materials **1**–**8** were loaded into the reactor via a HPLC pump. Solvents were selected on the basis of the solubility of the starting materials. A schematic representation of the flow reactor setup is illustrated in Figure 1. Products **9**–**14** thus prepared were identified by means of HPLC–MS and NMR spectroscopic analysis. All physical and spectroscopic data of pyrimidinones **9**–**14** were identical with their literature data (Supporting Information File 1).

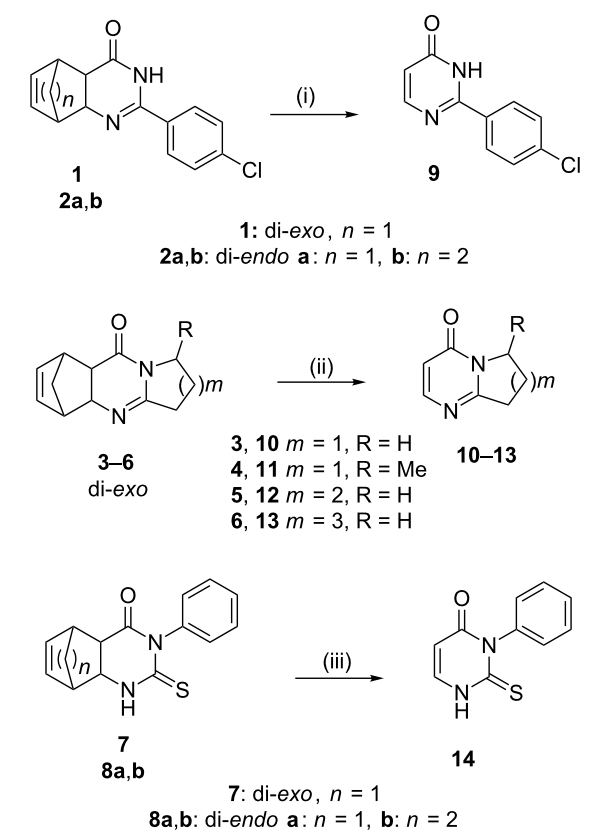

Scheme 1: Flow synthesis for the preparation of fused pyrimidinones **9**–**14** by rDA reaction. Solvent and conditions (F_R is the flow rate): (i) MeCN, toluene, F_R = 0.5 mL min^{-1}, 230–250 °C; (ii) MeOH, F_R = 0.5 mL min^{-1}, 120–150 °C; (iii) MeCN, F_R = 0.5 mL min^{-1}, 220–250 °C.

The rDA reaction is basically a thermally-driven process. Consequently, by careful reaction parameter optimization, a balance should be found between the desired rDA cycloreversion reaction and the unwanted thermal degradation of the rDA

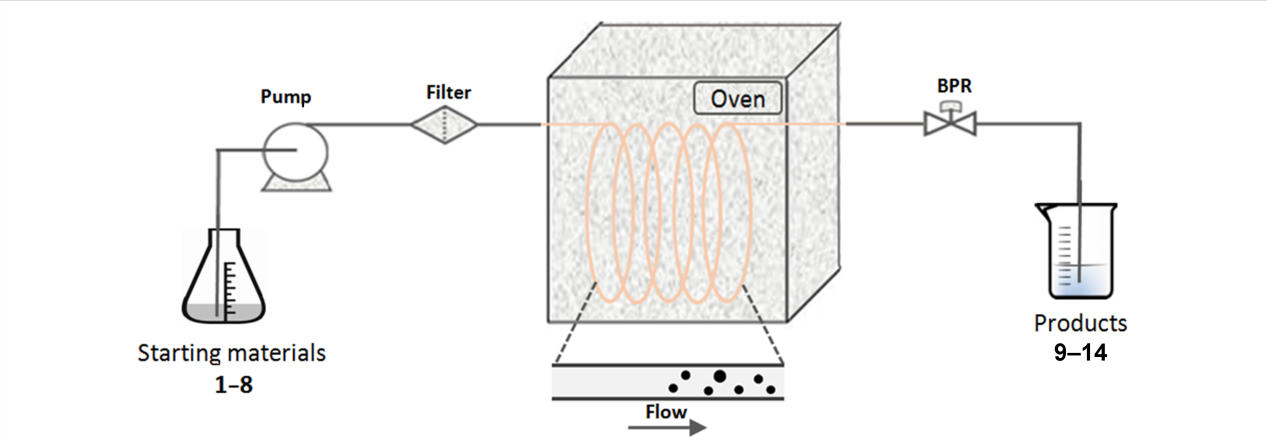

Figure 1: Schematic outline of the continuous-flow reactor.

product. The conversion and yield of a reaction under CF conditions is influenced directly by the residence time and reaction temperature, which are crucial determining factors in flow chemistry [18-20]. Thus, these two parameters were fine-tuned for all of the starting materials. The residence time was set by the use of coils with different lengths. The pressure and flow rate of the reactions were kept at constant values of 10 bars and 0.5 mL min^{-1}, respectively. The full reaction parameter optimization is shown only for compound **1** in Table 1.

The tricyclic di-*exo*-2-(4-chlorophenyl)tetrahydro-5,8-methano-4(*3H*)-quinazoline (**1**) was dissolved in acetonitrile (MeCN) and first the effect of the temperature was investigated. The results show that with 10 min residence time the best conversion value (86%) was obtained at 230 °C (Table 1, entry 4). It should be noted that at higher temperature, a significant amount of degradation product was observed and a brown oil was isolated (Table 1, entries 5 and 6). To further improve the conversion, the residence time was increased by utilizing longer coils (Table 1, entries 7 and 8). It was found that complete conversion can be obtained at 15 min residence time and the desired rDA product was isolated with 92% yield (Table 1, entry 7, Table 2, entry 1). With longer residence times, again, degradation of the product was observed. Importantly, the complete reaction parameter optimization was carried out only in 105 min. The parameters of the optimized reaction conditions and related results are summarized in Table 2.

In the case of di-*endo*-isomer **2a**, higher temperature (250 °C) but a shorter residence time was satisfactory to isolate **9** in a yield of 95%. Furthermore, we proceeded to investigate the elimination of cyclohexadiene from compound **2b**. Because of solubility reasons, the solvent was changed to toluene, which is known to be compatible with high-temperature conditions [51-53]. Retrodiene product **9** was afforded with full conversion and in an excellent yield of 93%, which is higher than the maximum yield (85%) reached in our previous batch work [54]. Importantly, this result was achieved with a residence time of 30 min.

Subsequently, tetracyclic methanopyrrolo-, methanopyrido- and methanoazepino[2,1-*b*]quinazolinones **3–6** were examined. Because of their excellent solubility, reactions were carried out in methanol (MeOH). Importantly, much milder reaction conditions gave satisfactory results. With the utilization of

Table 1: Reaction parameter optimization for the CF rDA reaction of **1**.

entry	temperature [°C]	residence time [min]	conversion [%]	degradation product [%]
1	200	10	64	–
2	210	10	82	–
3	220	10	83	–
4	230	10	86	0
5	240	10	100	7
6	250	10	100	18
7	230	15	100	0
8	230	30	100	13

Table 2: Comparison between batch reactions[a] and the CF process for the synthesis of pyrimidinones **9**–**14**.

starting material	product	batch reaction (lit.)	CF in the present work			
		method: yield[c] [%]	solvent[b]	temp [°C]	residence time [min]	yield[c] [%]
1	**9**	A: 85 [47] B: 56 [46]	MeCN	230	15	92
2a	**9**	B: 54 [46] C: 85 [54]		250	10	95
2b	**9**	A: 63 [49] B: 58 [49] C: 72 [49]	toluene	230	30	93
3	**10**	B: 70–80 [50]	MeOH	130	10	95
4	**11**			150	10	97
5	**12**			120	10	95
6	**13**			130	10	94
7	**14**	B: 80 [45] C: 89 [54]		210	15	96
8a	**14**	B: 80 [45]	MeCN	220	10	96
8b	**14**	A: B: C: 0 [49] (no rDA occurred)		250	30	30[d]
8b	**15b**	–	EtOH/H_2O = 2:1	250	30	90

Batch reaction[a]: Method A: reflux, CB, 12 h; Method B: performed at their melting points; Method C: MW, solvent: DCB (**2a**), EtOH (**7**), solvent-free (**8b**). [b]Solvents were selected on the basis of solubilities. [c]Isolated yield. [d]After column chromatography.

120–150 °C and only 10 min residence time, full conversions and high yields (94–97%) were obtained. Lower yields were previously found (70–80%) using a batch process, even upon melting compounds **3**–**6** for 20 min [50].

The effect of the thioxo group on the rDA reaction was investigated too with compounds **7**, **8a** and **8b**. In the case of **7**, a yield of 96% was reached at full conversion at 210 °C in 15 min residence time. In the reaction of **8a**, the di-*endo* isomer of **7**, a slightly higher temperature was necessary, while an appropriate residence time of only 10 min was satisfactory to have **14** with 96% isolated yield.

On the basis of these encouraging results, we decided to further examine the scope and limitation of the rDA reaction with the use of our CF reactor. Di-*endo*-3-phenyl-2-thioxohexahydro-5,8-ethanoquinazolin-4(*1H*)-one (**8b**) was selected, since this compound did not lose cyclohexadiene to form monocyclic **14** under batch and microwave conditions [49]. A solution of **8b** in MeCN was treated in the heated coil reactor at 250 °C, with a residence time of 30 min. Importantly, according to the HPLC–MS analysis, compound **8b** underwent thermal decomposition but only a moderate conversion (36%) was detected and **14** was isolated by means of column chromatography with a yield of 30%. This result is due to the lack of the quasi-aromatic character of the leaving cyclohexadiene, and possibly also due to the temperature limitation of our system. Surprisingly, however, we could detect traces of di-*endo*-3-phenyl-4a,5,8,8a-tetrahydro-5,8-ethanoquinazolin-4(*3H*)-one (**15b**), resulting from desulfurisation of **8b** (Scheme 2). This observation prompted us to investigate whether desulfurisation can occur under the flow reactor conditions. In the literature, a similar desulfurisation batch reaction was performed with nickel catalysis, in ethanol (EtOH)/water (2:1) solution [55-57]. Thus, thioxo derivative **8b** was dissolved in this mixture, and the CF method was repeated. Desulfurisation of **8b**, at 250 °C without adding any catalytic metal, provided tricyclic **15b** in good yield (90%). Most probably, the reaction was catalyzed by nickel, a component of the 304 stainless steel reactor coil [58,59]. These results also underline the importance to select appropriate solvents and tubing [60,61] for thermally driven reactions. In support of our results, tricyclic **15b** was also prepared alternately: the mixture of 3-aminobicyclo[2.2.2]oct-5-ene-carboxylic acid, triethylorthoformate, aniline and acetic acid was subjected to microwave irradiation at 120 W at 80 °C for 20 min. After completion of the reaction, as monitored by TLC, 20% methanolic solution in water was added to get precipitation. The solid was filtered off and washed with water to get di-*endo*-3-phenyl-4a,5,8,8a-tetrahydro-5,8-ethanoquinazolin-4(*3H*)-one (**15b**). All spectroscopic data of the alternately synthesized compound were the same as those obtained by the flow chemical method. The protocol for the synthesis of **15b** and the ^{1}H and ^{13}C NMR spectra of **15b** are shown in Supporting Information File 1 of this study.

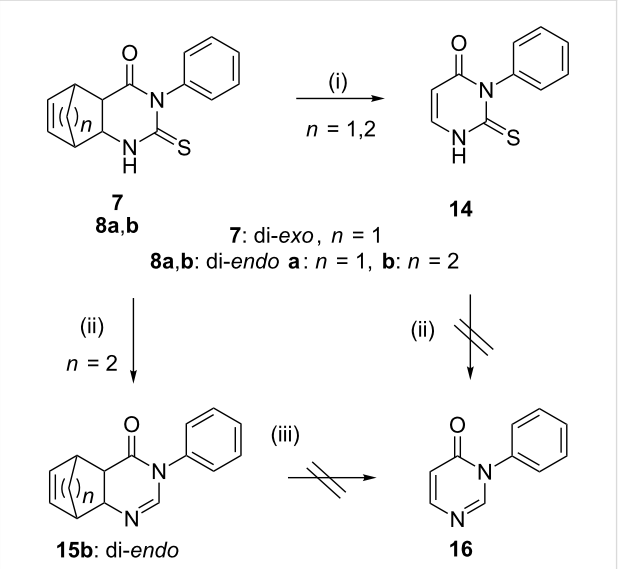

Scheme 2: Synthesis of tricyclic ethanoquinazolin-4(*3H*)-one **15b**; (i) MeCN, F_R = 0.5 mL min^{-1}, 220–250 °C; (ii) EtOH/H_2O = 2:1, F_R = 0.5 mL min^{-1}, 250 °C; (iii) MeCN, F_R = 0.5 mL min^{-1}, 250 °C.

A further attempt was made to perform the rDA reaction with **15b** at 250 °C with a residence time of 15 min in MeCN. However, the formation of **16** was not observed, that is the starting tetrahydroquinazolinone derivative **15b** did not undergo a thermally driven rDA reaction (Scheme 2). Furthermore, by applying the same conditions on **14**, no desulfurisation occurred and the formation of **16** was not detected either.

Conclusion

In the case of compounds **1**–**8**, HPLC–MS measurements revealed full conversions to the desired pyrimidinones **9**–**14**, whereas only a moderate conversion of **8b** to **14** was observed. Mainly the retrodiene decomposition of compounds **1**–**8** occurred, since these latter possess the quasi-aromatic character, through the splitting-off of cyclopentadiene or cyclohexadiene. The stereochemistry (di-*endo* versus di-*exo* condensation) of the starting pyrimidinones **1**, **2**, **7** and **8** has no significant effect on the reaction yields. By using this safe, stable and scalable flow process, pyrimidinones **9**–**14** were afforded in high purity without the need for further purification steps. In addition, excellent yields and shorter reaction times are significant further advantages when compared to the corresponding batch processes. Moreover, the flow technology allowed the replacement of high-boiling and toxic solvents, which are commonly employed in batch process, e.g., CB or DCB, by less harmful, environmentally benign solvents such as toluene, MeCN, methanol, and ethanol.

In summary, we have developed a simple flow-based method for the preparation of pyrimidinone derivatives, precursors of a series of pharmacologically active materials, through the rDA reaction. The design of the reactor enabled accurate control of both residence time and reaction temperature. CF syntheses were performed under high-temperature conditions with varied solvents. The CF reactor set-up ensured enhanced safety and afforded yields higher than those for the batch and microwave processes. These could be achieved through careful reaction parameter optimization. It is particularly true for **8b**, which was unreactive under batch conditions, in contrast to a yield of 30% in CF. We envisage that this method can be readily extended to the preparation of other synthetically important building blocks requiring harsh conditions in batch methods. A simple, efficient and scalable production was implemented with a short processing time, which might open up new horizons for a potential CF industrial synthesis of heterocycles.

Supporting Information

Supporting Information File 1

Experimental procedures and analytical data.
[https://www.beilstein-journals.org/bjoc/content/supplementary/1860-5397-14-20-S1.pdf]

Acknowledgements

We are grateful to the Hungarian Research Foundation (OTKA No. K 115731). The financial support of the GINOP-2.3.2-15-2016-00014 project is acknowledged.

References

1. Lapkin, A. A.; Plucinski, P. K. Engineering Factors for Efficient Flow rocesses in Chemical Industries. *Chemical Reactions; Processes under Flow Conditions;* Chapter 1, Vol. 5; The Royal Society of. Chemistry, 2010; pp 1–43.
2. Jähnisch, K.; Hessel, V.; Löwe, H.; Baerns, M. *Angew. Chem., Int. Ed.* **2004,** *43,* 406–446. doi:10.1002/anie.200300577
3. Wegner, J.; Ceylan, S.; Kirschning, A. *Adv. Synth. Catal.* **2012,** *354,* 17–57. doi:10.1002/adsc.201100584
4. Rehm, T. H.; Hofmann, C.; Reinhard, D.; Kost, H.-J.; Löb, P.; Besold, M.; Welzel, K.; Barten, J.; Didenko, A.; Sevenard, D. V.; Lix, B.; Hillson, A. R.; Riegel, S. D. *React. Chem. Eng.* **2017,** *2,* 315–323. doi:10.1039/c7re00023e
5. Roberge, D. M.; Zimmermann, B.; Rainone, F.; Gottsponer, M.; Eyholzer, M.; Kockmann, N. *Org. Process Res. Dev.* **2008,** *12,* 905–910. doi:10.1021/op8001273
6. Hessel, V.; Kralisch, D.; Kockmann, N.; Noël, T.; Wang, Q. *ChemSusChem* **2013,** *6,* 746–789. doi:10.1002/cssc.201200766
7. Wegner, J.; Ceylan, S.; Kirschning, A. *Chem. Commun.* **2011,** *47,* 4583–4592. doi:10.1039/C0CC05060A
8. Wiles, C.; Watts, P. *Green Chem.* **2012,** *14,* 38–54. doi:10.1039/C1GC16022B
9. Newman, S. G.; Jensen, K. F. *Green Chem.* **2013,** *15,* 1456–1472. doi:10.1039/C3GC40374B

10. Wiles, C.; Watts, P. *Green Chem.* **2014,** *16,* 55–62. doi:10.1039/c3gc41797b
11. Müller, S. T. R.; Wirth, T. *ChemSusChem* **2015,** *8,* 245–250. doi:10.1002/cssc.201402874
12. Kockmann, N.; Thenée, P.; Fleischer-Trebes, C.; Laudadio, G.; Noël, T. *React. Chem. Eng.* **2017,** *2,* 258–280. doi:10.1039/c7re00021a
13. DeMello, A. J. *Nature* **2006,** *442,* 394–402. doi:10.1038/nature05062
14. Noël, T.; Su, Y.; Hessel, V. *Top. Organomet. Chem.* **2016,** *57,* 1–41. doi:10.1007/3418_2015_152
15. Baxendale, I. R. *J. Chem. Technol. Biotechnol.* **2013,** *88,* 519–552. doi:10.1002/jctb.4012
16. Hessel, V. *Chem. Eng. Technol.* **2009,** *32,* 1655–1681. doi:10.1002/ceat.200900474
17. Illg, T.; Löb, P.; Hessel, V. *Bioorg. Med. Chem.* **2010,** *18,* 3707–3719. doi:10.1016/j.bmc.2010.03.073
18. Mándity, I. M.; Ötvös, S. B.; Szöllösi, G.; Fülöp, F. *Chem. Rec.* **2016,** *16,* 1018–1033. doi:10.1002/tcr.201500286
19. Hsieh, C.-T.; Ötvös, S. B.; Wu, Y.-C.; Mándity, I. M.; Chang, F.-R.; Fülöp, F. *ChemPlusChem* **2015,** *80,* 859–864. doi:10.1002/cplu.201402426
20. Mándity, I. M.; Ötvös, S. B.; Fülöp, F. *ChemistryOpen* **2015,** *4,* 212–223. doi:10.1002/open.201500018
21. Movsisyan, M.; Delbeke, E. I. P.; Berton, J. K. E. T.; Battilocchio, C.; Ley, S. V.; Stevens, C. V. *Chem. Soc. Rev.* **2016,** *45,* 4892–4928. doi:10.1039/C5CS00902B
22. Wollweber, H. *Diels–Alder-Reaction;* Georg Thieme Verlag: Stuttgart, 1972; pp 152–270.
23. Ichihara, A. *Synthesis* **1987,** 207–222. doi:10.1055/s-1987-27894
24. Rickborn, B. The Retro–Diels–Alder Reaction Part I. C-C Dienophiles. *Organic Reactions;* John Wiley & Sons, Inc., 2004. doi:10.1002/0471264180.or052.01
25. Klunder, A. J. H.; Zhu, J.; Zwanenburg, B. *Chem. Rev.* **1999,** *99,* 1163–1190. doi:10.1021/cr9803840
26. Stájer, G.; Csende, F.; Fülöp, F. *Curr. Org. Chem.* **2003,** *7,* 1423–1432. doi:10.2174/1385272033486369
27. González-Temprano, I.; Osante, I.; Lete, E.; Sotomayor, N. *J. Org. Chem.* **2004,** *69,* 3875–3885. doi:10.1021/jo049672o
28. Suzuki, K.; Inomata, K.; Endo, Y. *Org. Lett.* **2004,** *6,* 409. doi:10.1021/ol036253p
29. Nising, C. F.; Ohnemuller, U. K.; Bräse, S. *Synthesis* **2006,** 2643–2645. doi:10.1055/s-2006-942484
30. Citron, C. A.; Wickel, S. M.; Schulz, B.; Draeger, S.; Dickschat, J. S. *Eur. J. Org. Chem.* **2012,** 6636–6646. doi:10.1002/ejoc.201200991
31. Clay, D. R.; Rosenberg, A. G.; McIntosh, M. C. *Tetrahedron: Asymmetry* **2011,** *22,* 713–716. doi:10.1016/j.tetasy.2011.04.022
32. Gallagher, T.; Sanchez, S.; Bateson, J. H.; O'Hanlon, P. J. *Pure Appl. Chem.* **2009,** *77,* 2033–2040. doi:10.1351/pac200577122033
33. Eddolls, J. P.; Iqbal, M.; Robert, S. M.; Santoro, M. G. *Tetrahedron* **2004,** *60,* 2539–2550. doi:10.1016/j.tet.2004.01.047
34. Iqbal, M.; Li, Y.; Evans, P. *Tetrahedron* **2004,** *60,* 2531–2538. doi:10.1016/j.tet.2004.01.048
35. Arai, Y.; Kontani, T.; Koizumi, T. *Chem. Lett.* **1991,** 2135–2138. doi:10.1246/cl.1991.2135
36. Hasbullah, S. A.; Jones, S. *Tetrahedron: Asymmetry* **2010,** *21,* 2719–2725. doi:10.1016/j.tetasy.2010.10.021
37. Csende, F.; Stájer, G.; Fülöp, F. *Comprehensive Organic Synthesis,* 2nd ed.; Elsevier: Amsterdam, 2014; Vol. 5, pp 518–594.
38. Stájer, G.; Miklós, F.; Kanizsai, I.; Csende, F.; Sillanpää, R.; Sohár, P. *Eur. J. Org. Chem.* **2004,** 3701–3706. doi:10.1002/ejoc.200400247
39. Fülöp, F.; Miklós, F.; Forró, E. *Synlett* **2008,** 1687–1689. doi:10.1055/s-2008-1077793
40. Miklós, F.; Stájer, G.; Fülöp, F. *Lett. Org. Chem.* **2006,** *3,* 915–916. doi:10.2174/157017806779468086
41. Kummer, D. A.; Li, D.; Dion, A.; Myers, A. G. *Chem. Sci.* **2011,** *2,* 1710–1718. doi:10.1039/C1SC00303H
42. Januszczyk, P.; Fogt, J.; Boryski, J.; Izawa, K.; Onishi, T.; Neyts, J.; De Clercq, E. *Nucleosides, Nucleotides Nucleic Acids* **2009,** *28,* 713–723. doi:10.1080/15257770903128870
43. Bakavoli, M.; Bagherzadeh, G.; Vaseghifar, M.; Shiri, A.; Pordel, M.; Mashreghi, M.; Pordeli, P.; Araghi, M. *Eur. J. Med. Chem.* **2010,** *45,* 647–650. doi:10.1016/j.ejmech.2009.10.051
44. Guo, C.; Linton, A.; Jalaie, M.; Kephart, S.; Ornelas, M.; Pairish, M.; Greasley, S.; Richardson, P.; Maegley, K.; Hickey, M.; Li, J.; Wu, X.; Ji, X.; Xie, Z. *Bioorg. Med. Chem. Lett.* **2013,** *23,* 3358–3363. doi:10.1016/j.bmcl.2013.03.090
45. Stájer, G.; Szabó, A. E.; Pintye, J.; Bernáth, G.; Sohár, P. *J. Chem. Soc., Perkin Trans. 1* **1985,** 2483–2487. doi:10.1039/p19850002483
46. Stájer, G.; Szabó, A. E.; Fülöp, F.; Bernáth, G.; Sohár, P. *Chem. Ber.* **1987,** *120,* 259–264. doi:10.1002/cber.19871200302
47. Stájer, G.; Szabó, A. E.; Bernáth, G.; Sohár, P. *Synthesis* **1987,** 290–292. doi:10.1055/s-1987-27922
48. Csende, F.; Fülöp, F.; Stájer, G. *Curr. Org. Synth.* **2008,** *5,* 173–185. doi:10.2174/157017908784221576
49. Palkó, M.; Sohár, P.; Fülöp, F. *Molecules* **2011,** *16,* 7691–7705. doi:10.3390/molecules16097691
50. Fülöp, F.; Palkó, M.; Bernáth, G.; Sohár, P. *Synth. Commun.* **1997,** *27,* 195–203. doi:10.1080/00397919708005019
51. Lamborelle, N.; Simon, J. F.; Luxen, A.; Monbaliu, J.-C. M. *Org. Biomol. Chem.* **2015,** *13,* 11602–11606. doi:10.1039/c5ob02036k
52. Martin, R. E.; Lenz, M.; Alzieu, T.; Aebi, J. D.; Forzy, L. *Tetrahedron Lett.* **2013,** *54,* 6703–6707. doi:10.1016/j.tetlet.2013.09.069
53. Patel, S. K.; Long, T. E. *Tetrahedron Lett.* **2009,** *50,* 5067–5070. doi:10.1016/j.tetlet.2009.06.082
54. Miklós, F.; Stájer, G.; Fülöp, F. *Lett. Org. Chem.* **2006,** *3,* 915–916. doi:10.2174/157017806779468086
55. Chakrabarty, M.; Sarkar, S.; Harigaya, Y. *Synthesis* **2003,** 2292–2294. doi:10.1055/s-2003-42409
56. Goff, D.; Zhang, J.; Singh, R.; Holland, S.; Heckrodt, T.; Ding, P.; Yu, J.; Litvak,, J. Bicyclic aryl and bicyclic heteroaryl substituted triazoles useful as Axl inhibitors. WO Patent WO2008083353A1, July 10, 2008. *Chem. Abstr.* **2008,** *149,* 153089.
57. Shao, D. Method for synthesizing 5,6-dihydropyrido[2,3-d]pyrimidine-4,7(3*H*,8*H*)-dione. CN Patent CN104098562A, Oct 15, 2014. *Chem. Abstr.* **2014,** *161,* 647237.
58. Kawano, A.; Masuda, S.; Saito, M.; Tsuchiya, H.; Fujimoto, S. *J. Electrochem. Soc.* **2016,** *163,* C506–C513. doi:10.1149/2.0081609jes
59. Oldfield, J. W.; Todd, B. *Desalination* **1999,** *124,* 75–84. doi:10.1016/S0011-9164(99)00090-9
60. Bogdan, A. R.; Sach, N. W. *Adv. Synth. Catal.* **2009,** *351,* 849–854. doi:10.1002/adsc.200800758
61. Bogdan, A. R.; James, J. *Chem. – Eur. J.* **2010,** *16,* 14506–14512. doi:10.1002/chem.201002215

License and Terms

The definitive version of this article is the electronic one which can be found at:
doi:10.3762/bjoc.14.20

III.

ChemPubSoc Europe

DOI: 10.1002/ejoc.201800682

EurJOC European Journal of Organic Chemistry

Full Paper

Continuous-Flow Chemistry

Continuous-Flow retro-Diels–Alder Reaction: A Process Window for Designing Heterocyclic Scaffolds

Imane Nekkaa,[a] Márta Palkó,[a] István M. Mándity,[a,b,c] Ferenc Miklós,[a] and Ferenc Fülöp*[a,d]

Abstract: The synthesis of racemic and enantiopure tricyclic and tetracyclic pyrrolopyrimidinones, pyrimidoisoindoles, and spiropyrimidinones, as valuable new chemical entities (NCE), based on a highly controlled continuous-flow (CF) retro-Diels–Alder protocol is presented. This approach ensures enhanced safety, and gave the target pyrimidinone derivatives **17**–**25** in yields higher than those obtained in batch and microwave processes. These results were achieved through careful optimization of the reaction parameters. We also developed an alternative time-efficient route for the synthesis of intermediate quinazolinones **2**–**16** involving a three-step domino ring-closure reaction followed by spirocyclization under continuous-flow conditions, starting from β-aminonorbornene carboxamides **1a**–**1d** and γ-keto acids or cycloalkanones.

Introduction

Heterocyclic skeletal transformations are some of the most powerful synthetic methods for the construction of complex molecular frameworks from simple feedstocks.[1] In this context, Diels–Alder (DA) and retro-Diels–Alder (rDA) reactions are the prevailing approaches, since they lead to valuable N-heterocycles with high biological activities, such as isoindoloquinazolinones, pyrroloquinazolinones, and 2-spiroquinazolinones. The reactivity and skeletal transformations of these compounds under mild conditions have been widely examined and discussed by our group.[2] The DA/rDA approach makes use of the rigidity and chirality of the DA adducts that are formed by reactions between cyclic dienes and cyclic dienophiles.[3,4] The rDA enantiomers are obtained when enantiomerically pure DA products are modified diastereoselectively and then undergo thermal [4+2] cycloreversion through distillation under reduced pressure[5] or boiling in a solvent,[6] or through the use of microwave (MW) irradiation[7] or flash vacuum pyrolysis.[8]

We recently revealed the potential of the use of continuous-flow (CF) technology for the synthesis of various functionalized pyrimidinone systems through rDA reactions.[9] Our interest in CF processes can be explained, at least in part, by the number of potential advantages that CF processes have over traditional batch chemistry. These include the ease of scale-up, high reproducibility, excellent heat transfer and mixing, as well as the inherently greater safety resulting from the small reactor volumes.[10–19] Moreover, the accurate tuning of residence times can further broaden the versatility of CF processes.[20] Thus, flow chemistry has for a long time been chosen as an efficient method for the synthesis of more complex chemical structures that are otherwise inaccessible.

Focussing on the biological potential of fused pyrimidinones, and continuing our work on the synthesis of new N-heterocycles, we intended to further capitalize on the CF rDA protocol by synthesizing more complex pyrimidinone-fused moieties in both racemic and enantiopure forms. Pyrrolopyrimidines have a wide range of applications in medicinal chemistry; they show antimicrobial,[21] antitumor,[22] antiasthmatic,[23] antihypertensive,[24] and anti-inflammatory[25] activities. Pyrimidoisoindoles show high vasorelaxtant,[26a] antiplasmodial,[26b] and antifungal[27] actions. The spiroquinazolinone, spiropiperidine, and spiroadamantane skeletons, in turn, are known to have a wide range of pharmacological properties, including antimalarial[28] and anti-influenza activities.[29] Moreover, they also function as inhibitors of several key enzymes, such as nitric oxide synthase[30] and nosine-5′-monophosphate dehydrogenase.[31] In addition, they are present in several natural frameworks, e.g., prostanoids, alkaloids, and nucleosides.

In this paper, we describe an extension of our previously reported CF rDA process for the synthesis of racemic and enantiopure tricyclic and tetracyclic pyrrolopyrimidinones, pyrimidoisoindoles, and spiropyrimidinone derivatives. We have also developed an alternative preparation for quinazolinone intermediates by: (i) a three-step domino ring-closure reaction, and (ii) spirocyclization under CF conditions with *diexo*- and *diendo*-β-aminonorbornene carboxamides and γ-keto acids or

[a] *Institute of Pharmaceutical Chemistry, University of Szeged, Eötvös u. 6, 6720 Szeged, Hungary*
E-mail: fulop@pharm.u-szeged.hu
http://www2.pharm.u-szeged.hu/gyki/index.php/en/
[b] *Institute of Organic Chemistry, Semmelweis University, Hogyes Endre u. 7, 1092 Budapest, Hungary*
[c] *MTA TTK Lendület Artificial Transporter Research Group, Institute of Materials and Environmental Chemistry, Research Center for Natural Sciences, Hungarian Academy of Sciences, Magyar Tudosok krt. 2, 1117 Budapest, Hungary*
[d] *MTA-SZTE Stereochemistry Research Group, Hungarian Academy of Sciences, Eötvös u. 6, 6720 Szeged, Hungary*

Supporting information and ORCID(s) from the author(s) for this article are available on the WWW under https://doi.org/10.1002/ejoc.201800682.

cycloalkanones as starting materials. The developed flow-based method gave the desired pyrimidinones in high yields, and ensures enhanced safety.

Results and Discussion

Our previous investigations on the CF rDA reactions of condensed pyrimidinone derivatives revealed that the CF approach is superior to existing conventional batch methods.[9] In this work, starting materials were selected with the aim of testing the viability of the proposed CF rDA protocol with more complex fused pyrimidinone moieties, and also of investigating molecules that have never been subjected to rDA reactions under batch conditions. We started our study with readily available aminocarboxamides **1a**–**1d**, which were prepared by known literature approaches. Both *diendo*- and *diexo*-3-aminobicyclo[2.2.l]hept-5-ene-2-carboxylic acids, as well as *diexo*-3-amino-7-oxabicyclo[2.2.1]hept-5-enecarboxylic acid, were esterified with ethanol, and the resulting ester bases were liberated from the hydrochlorides. These aminoesters were kept for three weeks in a large excess of methanol saturated with ammonia to give amides **1a**, **1c**, and **1d**.[2d,2f,2l] For the preparation of 3-*exo*-amino-*N*-methylbicyclo[2.2.l]hept-5-ene-2-*exo*-carboxamide (**1b**), a mixture of the appropriate ester and a methylaminesolution (25 % in methanol) was kept for 6 d at room temperature.[2e] Our synthetic efforts began with the preparation of the required intermediates **2**–**16** using an optimized procedure based on previously reported methods,[2l–2r] as illustrated in Schemes 1 and 2.

The cyclization reactions of racemic *diexo*-3-aminobicyclo-[2.2.1]hept-5-ene-2-carboxamide (**1a**) or *diexo*-3-*N*-methylbicyclo[2.2.1]hept-5-ene-2-carboxamide (**1b**) with γ-oxocarboxylic acids in toluene under reflux in the presence of *para*-toluenesulfonic acid (*p*TsA), through three-step domino reactions, resulted in single diasteroisomers of pyrrolo[1,2-*a*]quinazolines **2**–**4** or isoindolo[2,1-*a*]quinazolines **5**–**7** (Scheme 1). Upon heating with cyclohexanone in refluxing ethanol (EtOH), β-aminonorbornene carboxamides **1a**, **1c**, and **1d** were cyclized to give methylene- and epoxy-bridged 2-spiroquinazolinones **8**–**10**. These compounds could alternatively be prepared under dry (solvent-free) conditions by stirring for 2 d; spiropiperidine derivatives **11**–**13** were formed by the condensation of carboxamides **1a**, **1c**, and **1d** with 1-benzylpiperidin-4-one in water at room temperature (Scheme 2).

For the preparation of spiro[quinazoline-2,2′-adamantane] derivatives **14**–**16**, we developed an alternative synthetic pathway involving the use of MW irradiation on **1a**, **1c**, **1d** with adamantanone in EtOH (Scheme 2). This reaction has previously also been carried out in a vibrational ball mill with iodine (I_2) as a catalyst.[2r] In addition, we wanted to further develop this cyclization method by searching for a time-efficient method for the synthesis of functionalized intermediates **2**–**16**. To this end, a CF-based strategy seemed highly appropriate , since this approach has emerged as an intense area of current research, being used for the synthesis of many different heterocyclic scaffolds.[32] β-Amino amides **1a**–**1d** were mixed with γ-keto acids or cyclic ketones and loaded into the CF reactor constructed previously (Figure 1), using the same operating conditions and

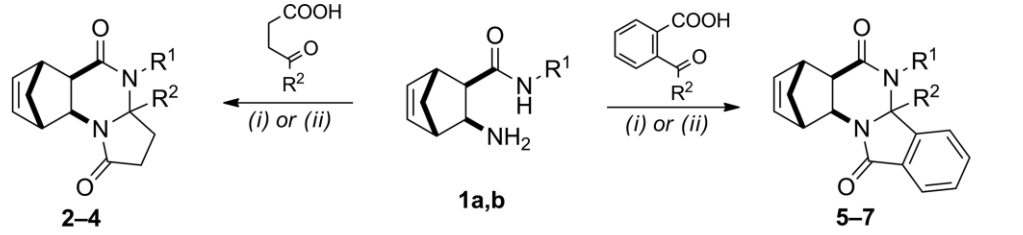

Scheme 1. Solvent and conditions: (i) toluene, reflux, *p*TsA, 16 h;[2l–2n] (ii) CF: toluene, flow rate = 0.2 mL min^{-1}, 110 °C, *p*TsA, 6 h.

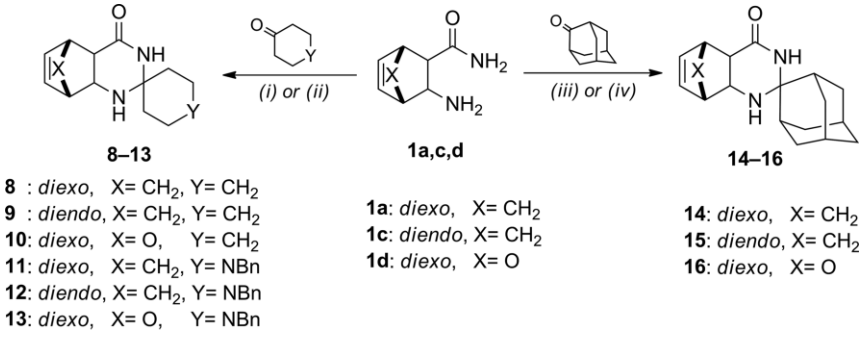

Scheme 2. Solvent and conditions: (i) **8**, **9**: solventless, room temp., 2 d.[2q] **10**: EtOH, reflux, 2 h.[2o] **11**–**13**: H_2O, room temp., 24 h;[2q] (ii) CF: EtOH, flow rate = 0.2 mL min^{-1}, 100 °C, 6 h; (iii) MW: EtOH, 100 °C, 1 h; (iv) CF: EtOH, flow rate = 0.2 mL min^{-1}, 100 °C, 6 h.

solvents used before in batch syntheses. Mixtures of **1a** or **1b** and γ-keto acids were dissolved in toluene, and introduced into the flow reactor at 110 °C, with 6 h as the reaction time: Tetra- and pentacyclic derivatives **2**–**7** were obtained in slightly higher yields (79–93 %) than the previous batch method.Heating solutions of **1a**, **1c**, or **1d** with cycloalkanones in EtOH at 100 °C gave spiroquinazolinones **8**–**16** with reaction times of 6 h in similar yields (79–95 %). Note, however, that shorter reaction times were needed for cyclization in the CF reactions (see Table S1 in the Supporting Information).

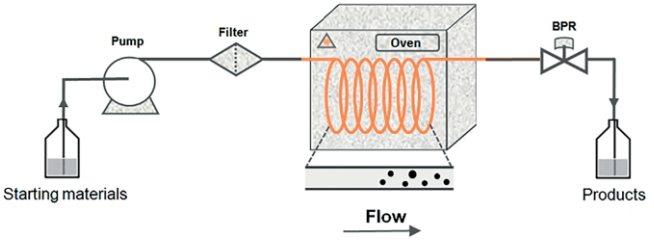

Figure 1. Set-up of the continuous-flow reactor.

The residence time and reaction temperature are crucial determining factors in flow chemistry;[20] they control the course of a reaction by affecting both the conversion and the yield. Thus, these two parameters were well-tuned for all starting materials. The residence time was set by the use of coils with different lengths. The pressure and flow rate were kept at constant values of 10 bar and 0.2 mL min^{-1}, respectively. The reaction process was monitored by means of HPLC–MS and ^1H NMR spectroscopic analysis.

Our next step was to investigate the transformation of quinazolinone derivatives **2**–**16** into retrodiene products **17**–**25** through a thermal [4+2] cycloreversion involving the elimination of cyclopentadiene or furan from DA adducts (Scheme 3).

We began by investigating the CF rDA reactions of tetra- and pentacyclic derivatives **2**–**7**, since these compounds include more complex fused pyrimidinone moieties, which might be a challenge for our proposed CF rDA protocol.

We screened different solvents, and found that polar aprotic solvents such as acetonitrile (MeCN) or methanol (MeOH) were preferred over nonpolar solvents (dichloromethane, toluene), especially when high concentrations were used. We thus opted for MeCN as a suitable and benign solvent, and used it subsequently to study the effect of different temperatures. We quickly established that temperatures of 220–250 °C gave full conversions with a residence time of 15 min, without the unwanted thermal degradation of the rDA products; lower temperatures slowed down the reactions significantly. Having established these reaction conditions, tetracyclic pyrrolo[1,2-*a*]-quinazolinones **2**–**4** and pentacyclic isoindolo[1,2-*a*]quinazolinones **5**–**7** were dissolved in MeCN, and after 5 min of stirring at ambient temperature, the homogeneous mixtures were introduced into the reactor by an HPLC pump (Figure 1). Heating the mixtures at 220 or 250 °C led to the expected pyrrolopyrimidinones **17**–**19** and pyrimidoisoindoles **20**–**22**, with residence times of 15 min (Table 1, entries 1–8) in isolated yields over 90 % after purification by column chromatography. These results match the parent batch experiments in terms of isolated yields.[2l,2m]

To establish the range of applicability of our CF rDA process, the syntheses of enantiomerically pure pyrrolo[1,2-*a*]pyrimidine **19** and pyrimido[2,1-*a*]isoindole **20** through rDA reaction under CF conditions were undertaken (Scheme 4). The source of chirality, (1*R*,2*R*,3*S*,4*S*)-3-amino-*N*-methylbicyclo[2.2.1]hept-5-ene-2-carboxamide [(–)-**1b**] was prepared by known literature protocols.[2e] In a stereocontrolled ring-closing reaction, (–)-**1b** was treated with 3-oxo-3-(*p*-tolyl)propanoic acid to give (+)-**4** as a single diastereoisomer in good yield. The ready loss of cyclopentadiene through the CF rDA protocol at 220 °C resulted in (*S*)-1-methyl-8a-(*p*-tolyl)-1,7,8,8a-tetrahydropyrrolo[1,2-*a*]pyrimidine-2,6-dione enantiomer (+)-**19** in high yield (Table 1, entry 4) with an *ee* value of 97 %. When carboxamide (–)-**1b** was

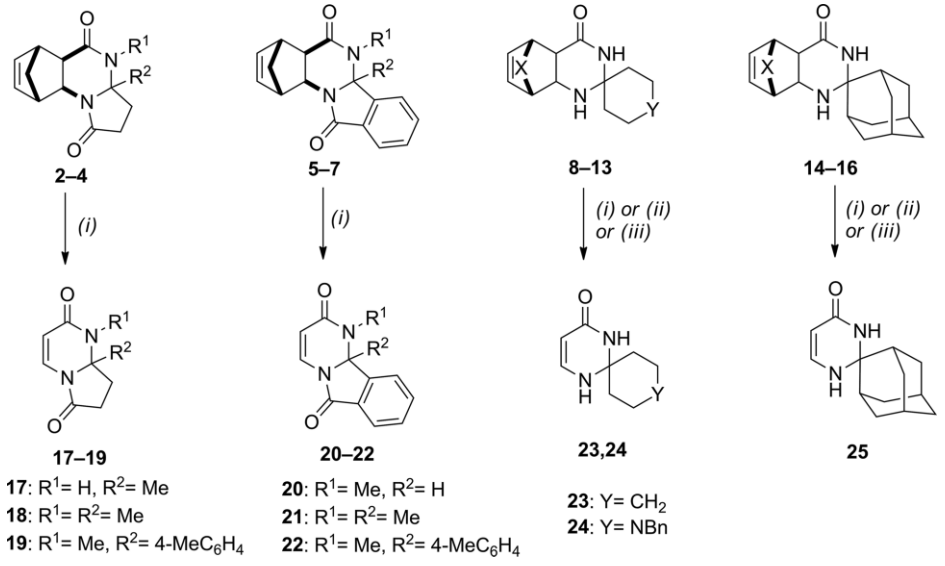

Scheme 3. (i) CF: MeCN, toluene, flow rate = 0.2 mL min^{-1}, 150–250 °C; (ii) heating at melting points; (iii) MW: 1,2-DCB (1,2-dichlorobenzene), 150–240 °C, 1 h.

Table 1. CF process for the synthesis of pyrimidinones **17**–**25** under the optimized reaction conditions.

Entry	Starting material	Product	CF Optimized reaction conditions Solvent[a]	*T* [°C]	Residence time [min]	Yield[b] [%]
1	**2**	**17**	MeCN	250	15	98
2	**3**	**18**		220	15	97
3	**4**	**19**		220	15	95
4	(+)-**4**	(+)-**19**		220	15	97
5	**5**	**20**		220	15	98
6	(+)-**5**	(–)-**20**		250	15	93
7	**6**	**21**		220	15	96
8	**7**	**22**		250	15	97
9	**8**			240	60	73
10	**9**	**23**		240	60	75
11	**10**			150	60	95
12	**11**		toluene/	240	60	53
13	**12**	**24**	MeOH,	240	60	70
14	**13**		4:1	150	60	92
15	**14**			240	60	51
16	**15**	**25**		240	60	57
17	**16**			150	60	86

[a] Solvents were selected on the basis of solubilities. [b] Isolated yield.

treated with 2-formylbenzoic acid, pentacyclic isoindolo-[1,2-*a*]quinazolinone (+)-**5** was formed. CF-induced thermolysis of (+)-**5** at 250 °C gave the expected (*S*)-1-methyl-1,10b-dihydropyrimido[2,1-*a*]isoindole-2,6-dione [(–)-**20**] within a residence time of 15 min, with full conversion, in high yield, and with an *ee* value of 98 % (Table 1, entry 6).

Our next CF rDA investigation was carried out with spiroquinazolinones **8**–**16**, which have not been subjected to rDA reactions previously through conventional batch approaches. Spiroquinazolinone derivatives **8**–**16** were first subjected to CF using the previously optimized parameters. They were dissolved in MeCN and loaded into the CF reactor (Figure 1) at different temperatures based on their melting points. An initial assessment of the results revealed that compounds **8**–**16** underwent thermal decomposition, but only moderate conversions were observed with significant amounts of rDA degradation products. Following these disappointing results, we decided to optimize our operating parameters further. We screened different solvents, and found that a mixture of toluene and MeOH (4:1 v/v) worked best to give new 2-spiropyrimidin-4-ones **23**–**25**. It is important to note that toluene is known to be an effective solvent under superheated CF rDA conditions.[9,33] This effect is even more pronounced when MeOH is used as a cosolvent. The transformation of *diexo*-methylene-bridged 2-spiroquinazolinone **8** is illustrative. The substrate was dissolved in toluene/MeOH (4:1), and the solution was introduced into the heated 304 stainless steel coil reactor at 240 °C with a residence time of 60 min (Table 1, entry 9). The residence time was increased by using a longer coil in order to further improve the conversion. Under these conditions, 1,5-diazaspiro[5.5]undec-3-en-2-one (**23**) was isolated in a moderate yield of 73 %.

We also wanted to investigate the CF rDA reaction of *diendo* isomer **9** in the hope that we could increase the yield of **23**. Since *diendo* stereoisomers are thermally unstable compared to their *diexo* analogues, they undergo rDA reactions more easily. Thus, **9** was subjected to the same conditions as described above (Table 1, entry 10). With a residence time of 60 min, rDA product **23** was obtained in almost the same yield (75 %) as with *diexo* isomer **8**. This result shows that a change in stereochemistry does not have any significant effect on the reaction yield. Subsequently, we turned to epoxy-bridged 2-spiroquinazolinone **10** with the expectation that it would be much easier to remove furan as the diene than cyclopentadiene, and that this would be achieved at lower temperatures. This may improve the yield by increasing the conversion and minimizing the amount of degradation products because of the lower temperatures used. Therefore, we used a temperature of 150 °C. Complete conversion was obtained with a residence time of 60 min, and the desired spiro compound **23** was isolated in a yield of 95 % (Table 1, entry 11). Encouraged by these promising results, a series of experiments was undertaken to gain a better understanding of the effect of the thermally-driven CF rDA on the transformation of other spiroquinazolinone scaffolds. Accordingly, we treated compounds **11**–**16** under the CF reaction conditions described above. Benzylpiperidine derivative **24** and adamantane **25** were obtained in good yields of 92

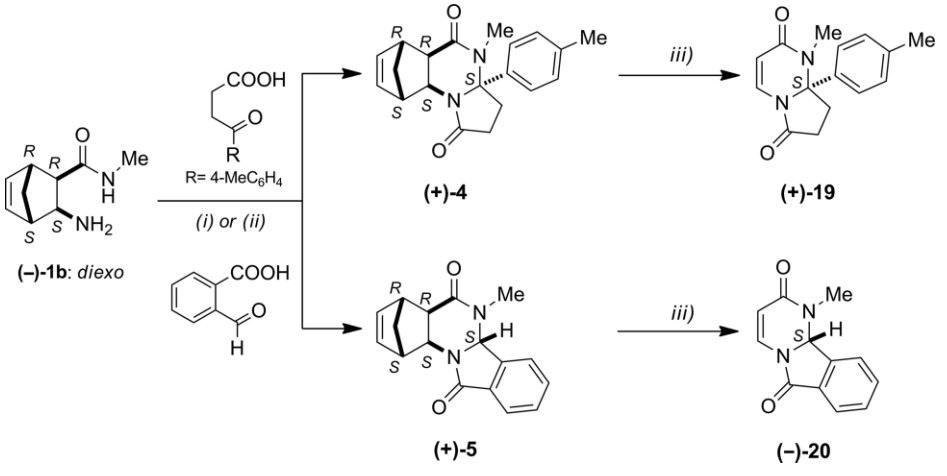

Scheme 4. Solvent and conditions: (i) toluene, reflux, *p*TsA, 16 h; (ii) CF: toluene, *p*TsA, flow rate = 0.2 mL min^{-1}; (iii) CF: MeCN, toluene, flow rate = 0.2 mL min^{-1}, 220 °C.

and 86 %, respectively (Table 1, entries 14 and 17). Importantly, the yields obtained from the oxa-bridged spiro compunds were always higher than those for the methylene-bridged analogues.

Based on our previous findings, we wanted to explore whether spiro compounds **8**–**16** undergo thermal decomposition under conventional batch conditions. For this purpose, we planned to test two different batch methods (Scheme 3). The first method involved simple heating of compounds **8**–**16** at their melting points; in the second method, the rDA reactions were carried out under MW conditions. Thus, in solvent-free experiments, compounds **8**–**16** were heated at around 10 °C above their melting points. Although HPLC–MS analysis showed full degradation of starting materials **8**–**16**, rDA products **23**–**25** were not detected in any case. In contrast, when MW irradiation was used with spiroquinazolinone derivatives **8**–**16**, we observed slightly higher than medium or no conversion to the retrodiene products **23**–**25**.

The best MW-promoted cycloreversion for the synthesis of compounds **23**–**25** was achieved when epoxy-spiroquinazolinones **10**, **13**, and **16** were irradiated in 1,2-dichlorobenzene at 180 °C for 30 min. These conditions gave isolated yields of 78, 89, and 78 %, respectively (Figure 2). These yields are lower than those obtained in the CF rDA process (Table 1, entries 11, 14, and 17). A throughput comparison for spiropyrimidinones **23**–**25** prepared by the batch and CF processes is shown in Figure 2. These data clearly demonstrate the superiority of CF technology compared to conventional batch methods.

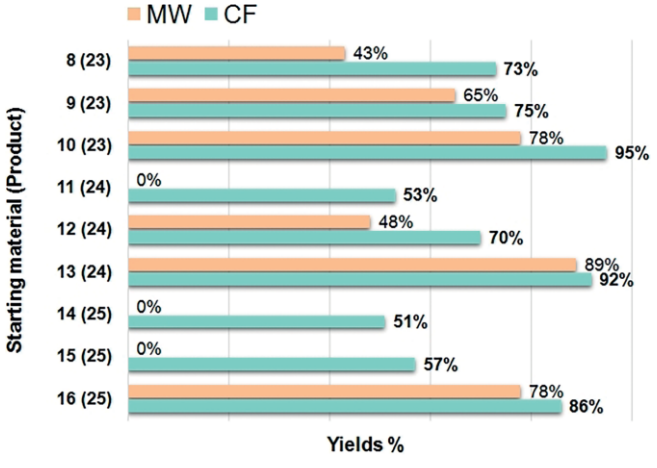

Figure 2. Comparison in terms of isolated yields between the CF rDA and MW processes for the synthesis of functionalized spiropyrimidinones **23**–**25**. MW-induced rDA (orange); CF rDA (blue).

Conclusions

A detailed investigation of the CF rDA reaction, a new and efficient approach to the synthesis of pyrrolopyrimidinone (**17**–**19**), pyrimidoisoindole (**20**–**22**), and spiropyrimidinone (**23**–**25**) derivatives has been carried out. The preparation of intermediates **2**–**16** through domino ring closure or spirocyclization under CF conditions was achieved in high yields; this protocol represents an alternative time-efficient route. We proved that the CF rDA process is able to yield more complex structures that are otherwise inaccessible. In the case of pyrrolo[1,2-*a*]-quinazoline and isoindolo[2,1-*a*]quinazoline derivatives **2**–**7**, HPLC–MS measurements revealed full conversions to the desired pyrrolopyrimidinones and isoindolopyrimidinones **17**–**22**. In contrast, only moderate conversions to new spiropyrimodinones **23**–**25** were observed for the methylene-bridged spiroquinazolinones **8**, **9**, **11**, **14**, and **15**. It is interesting that epoxy-bridged spiroquinazolinones **10**, **13**, and **16**, in which an oxygen atom has been introduced at the 7-position of the β-aminonorbornene carboxamide skeleton, gave retrodiene products **23**–**25** in almost quantitative yields. Importantly, the stereochemistry (*diendo* vs. *diexo* condensation) of the starting quinazolinones **8**–**16** was found to have no significant effect on reaction yields. The CF reactor set-up ensured enhanced safety, and gave yields higher than those obtained in batch and microwave processes. This is particularly true for compounds **11**, **14**, and **15**, which were unreactive (0 % yield) under microwave conditions; yields of 53, 51, and 57 %, respectively, were observed under CF conditions. We envisage that this approach could be readily extended to the preparation of other synthetically important building blocks that require harsh conditions in batch methods.

Experimental Section

General Remarks: ^{1}H NMR spectra were recorded at 400.13 MHz or 500.20 MHz, and ^{13}C NMR spectra were recorded at 100.62 MHz or 125.77 MHz in $CHCl_3$ or [D_6]DMSO at ambient temperature, with a Bruker AM 400 or a Bruker Ascend™ 500 spectrometer. Chemical shifts (δ) are given in parts per million (ppm) relative to tetramethylsilane (δ = 0 ppm), which was used as an internal standard. ^{1}H NMR spectra were calibrated using the residual solvent signals of $CDCl_3$ (δ = 7.26 ppm) or [D_6]DMSO (δ = 2.50 ppm). ^{13}C NMR spectra were calibrated using the signal of $CDCl_3$ (δ = 77.16 ppm) or [D_6]DMSO (δ = 39.52 ppm). Signal multiplicities are reported as follows: s = singlet, d = doublet, t = triplet, q = quartet, m = multiplet; ArH = aromatic. Data for ^{13}C NMR are reported in terms of chemical shift (δ [ppm]) and multiplicity (C, CH, CH_2, CH_3 or NH). Coupling constants (*J*) are reported to the nearest 0.1 Hz. Copies of the ^{1}H and ^{13}C spectra can be found in the Supporting Information. HPLC–MS measurements were carried out with a Phenomenex 5 µm C18(2) 100 Å column (250 × 4.60 mm). The solvent systems used consisted of AcOH (0.1 %) in water (A) and AcOH (0.1 %) in MeCN (B); gradient: 5–100 % B over 35 min, at a flow rate of 1 mL min^{-1}. Chromatograms and spectra were recorded in positive-ion mode with electrospray ionization with a Thermo LCQ Fleet mass spectrometer. FTIR spectra were obtained using KBr pastilles with an AVATAR 330 FTIR Thermo Nicolet spectrometer. Flow reactions were carried out with a modular flow system equipped with heated 304 stainless steel tubing coils [Supelco premium grade 304 empty stainless steel tubing; dimensions: length (*L*) × outer diameter (*OD*) × inner diameter (*ID*) = 100 ft × 1/16 in × 0.03 in] and an adjustable back-pressure regulator (ThalesNano, BPR, 0–300 bar). The tube reactor was heated in a Heraeus oven to the desired temperatures. The pressure was set at 10 bar, and the flow rate was kept at a constant value of 0.2 mL min^{-1}. Microwave-promoted reactions were carried out in sealed reaction vials (10 mL) in a microwave (CEM, Discover) cavity. Melting points were measured with a Hinotex X4 micro melting-point apparatus with a heating rate of 4 °C/min. Optical rotations for the rDA products were recorded with a Perkin-Elmer 341 polarimeter. The corresponding *ee* values were 97 % for (+)-**19** and

98 % for (–)-**20**. Analysis of these compounds was carried out using an HPLC instrument equipped with a Phenomenex IA column. For (+)-**19**: *n*-hexane/*i*PrOH, 70:30, 0.1 % Et_2NH, flow rate 0.5 mL min^{-1}, detection at 254 nm, t_R = 63.50 min (antipode: 56.95 min); for (–)-**20**: *n*-hexane/*i*PrOH , 70:30, flow rate 1.0 mL min^{-1}, detection at 254 nm, t_R = 28.50 min (antipode: 22.51 min). All physical and spectroscopic data of fused pyrimidinones **2**–**22** were identical with the corresponding literature data.[2l,2m,2o,2q,2r]

General Procedures for Flow Reactions

Synthesis of Ring-Closure Products 2–16

Synthesis of Pyrrolo[1,2-*a*]quinazolines 2, 3, 4 and Isoindolo-[1,2-*a*]quinazolines 5, 6, and 7: A mixture of *diexo*-3-aminobicyclo[2.2.1]hept-5-ene-2-carboxamide (**1a**) or *diexo*-3-amino-*N*-methylbicyclo[2.2.1]hept-5-ene-2-carboxamide (**1b**) (1 mmol) and either levulinic acid, 3-oxo-3-(*p*-tolyl)propanoic acid, 2-formylbenzoic acid, 2-acetylbenzoic acid, or 2-(4-methylbenzoyl)benzoic acid (1.2 mmol) along with a catalytic amount of *p*TsA was dissolved in toluene (50 mL). The system temperature was set to 110 °C, the pressure to 10 bar, and the flow rate to 0.2 mL min^{-1}. When the pressure and the temperature of the flow system were stable, the solution loaded into the reactor was passed through the heated reactor coil with a reaction time of 6 h. The flow output was collected. The solvent was removed by evaporation, and the solid residue was dissolved in EtOAc/MeOH, 9:1 (v/v). The solution was transferred to a neutral SiO_2 column, which was eluted with the same solvent mixture. The analytical and spectroscopic data of **2**–**7** were identical to those found in the literature.[2l,2m]

(3a*R,5a*R**,6*R**,9*S**,9a*S**)-3a-Methyl-2,3,3a,4,5a,6,9,9a-octahydro-6,9-methanopyrrolo[1,2-*a*]quinazoline-1,5-dione (2):** Colourless crystals (93 %). M.p. 239–242 °C. HPLC–MS (ESI): t_R = 12.00 min, *m*/*z* = 233 $[M + H]^+$, 167 $[M_{rDA} + H]^+$. The analytical and spectroscopic data of **2** were identical to those reported in the literature.[2l]

(3a*R,5a*R**,6*R**,9*S**,9a*S**)-6,9-Methano-3a,4-dimethyl-2,3,3a,4,5a,6,9,9aoctahydropyrrolo[1,2-*a*]quinazoline-1,5-dione (3):** Colourless crystals (85 %). M.p. 207–209 °C. HPLC–MS (ESI): t_R = 13.89 min, *m*/*z* = 247 $[M + H]^+$, 181 $[M_{rDA} + H]^+$. The analytical and spectroscopic data of **3** were identical to those reported in the literature.[2m]

(3a*S,5a*R**,6*R**,9*S**,9a*S**)-6,9-Methano-4-Methyl-3a-(*p*-tolyl)-2,3,3a,4,5a,6,9,9a-octahydropyrrolo[1,2-*a*]quinazoline-1,5-dione (4):** Colourless crystals (79 %). M.p. 214–216 °C. HPLC–MS (ESI): t_R = 24.49 min, *m*/*z* = 323 $[M + H]^+$, 229 $[M_{rDA} + H]^+$. The analytical and spectroscopic data of **4** were identical to those reported in the literature.[2m]

(1*S,4*R**,4a*R**,6a*S**,12a*S**)-1,4-Methano-6-methyl-1,4,4a,6,6a,12a-hexahydroisoindolo[2,1-*a*]quinazoline-5,11-dione (5):** Colourless crystals (90 %). M.p. 197–198 °C. HPLC–MS (ESI): t_R = 18.70 min, *m*/*z* = 281 $[M + H]^+$, 215 $[M_{rDA} + H]^+$. The analytical and spectroscopic data of **5** were identical to those reported in the literature.[2m]

(1*S,4*R**,4a*R**,6a*R**,12a*S**)-1,4-Methano-6,6a-dimethyl-1,4,4a,6,6a,12a-hexahydroisoindolo[2,1-*a*]quinazoline-5,11-dione (6):** Colourless crystals (83 %). M.p. 196–197 °C. HPLC–MS (ESI): t_R = 21.84 min, *m*/*z* = 295 $[M + H]^+$, 229 $[M_{rDA} + H]^+$. The analytical and spectroscopic data of **6** were identical to those reported in the literature.[2m]

(1*S,4*R**,4a*R**,6a*R**,12a*S**)-1,4-Methano-6-methyl-6a-(*p*-tolyl)-1,4,4a,6,6a,12a-hexahydroisoindolo[2,1-*a*]quinazoline-5,11-dione (7):** Colourless crystals (85 %). M.p. 230–232 °C. HPLC–MS (ESI): t_R = 31.72 min, *m*/*z* = 371 $[M + H]^+$, 305 $[M_{rDA} + H]^+$. The analytical and spectroscopic data of **7** were identical to those reported in the literature.[2m]

Synthesis of Enantiomeric Pyrrolo[1,2-*a*]quinazoline (+)-4 and Isoindolo[1,2-*a*]quinazoline (+)-5: A mixture of (–)-(1*R*,2*R*,3*S*,4*S*)-3-amino-*N*-methylbicyclo[2.2.1]hept-5-ene-2-carboxamide [(–)-**1b**, 1 mmol] and either 3-oxo-3-(*p*-tolyl)propanoic acid or 2-formylbenzoic acid (1.2 mmol) along with *p*TsA (5 mg) in toluene (50 mL) was introduced into the flow reactor at a temperature of 110 °C, using the same flow rate (0.2 mL min^{-1}). The product mixture (brownish-yellow colour) leaving the flow system was evaporated. The residue was dissolved in EtOAc/MeOH (9:1) eluent, and this material was directly transferred onto a short SiO_2 column. The ^1H and ^{13}C NMR spectroscopic data for the optically active compounds were consistent with those reported for the racemates.

(+)-(3a*R*,5a*R*,6*R*,9*S*,9a*S*)-6,9-Methano-4-methyl-3a-(*p*-tolyl)-2,3,3a,4,5a,6,9,9a-octahydropyrrolo[1,2-*a*]quinazoline-1,5-dione [(+)-4]: Colourless crystals (82 %). M.p. 206–208 °C. $[\alpha]_D^{25}$ = +10.8 (*c* = 0.33, MeOH).

(+)-(1*S*,4*R*,4a*R*,6a*S*,12a*S*)-1,4-Methano-6-methyl-1,4,4a,6,6a,12a-hexahydroisoindolo[2,1-*a*]quinazoline-5,11-dione [(+)-5]: Colourless crystals (83 %). M.p. 250–252 °C. $[\alpha]_D^{25}$ = +62 (*c* = 0.48, MeOH).

Preparation of Spiroquinazolinones 8–16: A solution of aminocarboxamide **1a**, **1c**, or **1d** (1 mmol) and either cyclohexanone, 1-benzylpiperidine, or adamantanone (1.2 mmol) in EtOH (50 mL), was fed into the reactor, and passed through the heated reactor coil at 100 °C with a reaction time of 6 h. The flow output was collected. The solvent was removed by evaporation, and the remaining residue was dissolved in Et_2O (5 mL). The resulting crystals were collected by filtration and washed with Et_2O. The analytical and spectroscopic data on **8**–**16** were identical to those reported in the literature.[2o–2r]

(4a*R,5*R**,8*S**,8a*S**)-4a,5,8,8a-Tetrahydro-1*H*-spiro[5,8-methanoquinazoline-2,1′-cyclohexan]-4(3*H*)-one (8):** Colourless powder (95 %). M.p. 232–235 °C. HPLC–MS (ESI): t_R = 6.52 min, *m*/*z* = 233 $[M + H]^+$, 167 $[M_{rDA} + H]^+$. The analytical and spectroscopic data of **8** were identical to those reported in the literature.[2q]

(4a*S,5*R**,8*S**,8a*R**)-4a,5,8,8a-Tetrahydro-1*H*-spiro[5,8-methanoquinazoline-2,1′-cyclohexan]-4(3*H*)-one (9):** Colourless powder (98 %). M.p. 243–244 °C. HPLC–MS (ESI): t_R = 6.23 min, *m*/*z* = 233 $[M + H]^+$, 167 $[M_{rDA} + H]^+$. The analytical and spectroscopic data of **9** were identical to those reported in the literature.[2o]

(4a*S,5*R**,8*S**,8a*R**)-4a,5,8,8a-Tetrahydro-1*H*-spiro[5,8-epoxyquinazoline-2,1′-cyclohexan]-4(3*H*)-one (10):** Colourless crystals (89 %). M.p. 158–160 °C. HPLC–MS (ESI): t_R = 6.49 min, *m*/*z* = 235 $[M + H]^+$, 167 $[M_{rDA} + H]^+$. The analytical and spectroscopic data of **10** were identical to those reported in the literature.[2o]

(4a*R,5*R**,8*S**,8a*S**)-1′-Benzyl-4a,5,8,8a-tetrahydro-1*H*-spiro[5,8-methanoquinazoline-2,4′-piperidin]-4(3*H*)-one (11):** Colourless powder (95 %). M.p. 217–220 °C. HPLC–MS (ESI): t_R = 9.7 min, *m*/*z* = 324 $[M + H]^+$, 258 $[M_{rDA} + H]^+$. The analytical and spectroscopic data of **11** were identical to those reported in the literature.[2q]

(4a*S,5*R**,8*S**,8a*R**)-1′-Benzyl-4a,5,8,8a-tetrahydro-1*H*-spiro[5,8-methanoquinazoline-2,4′-piperidin]-4(3*H*)-one (12):** White powder (92 %). M.p. 248–250 °C. ^1H NMR (500 MHz, $[D_6]$DMSO): δ = 0.63 (d, *J* = 10.96 Hz, 1 H, 9-H), 1.35–1.41 (m, 3 H, 9-H, CH_2), 1.47–1.69 (m, 2 H, CH_2), 1.87 (m, *J* = 12.8 Hz, 1 H, 1-NH), 2.24–2.4 (m, 4 H, CH_2), 2.96 (s, 1 H, 8-H), 3.14 (s, 1 H, 5-H), 3.44 (s, 2

H, NCH_2Ar), 3.72 (t, J = 8.6 Hz, 1 H, 8a-H), 6.14–6.21 (m, 2 H, 6-H, 7-H), 7.20–7.32 (m, 5 H, ArH), 7.79 (s, 1 H, 3-NH) ppm. ^{13}C NMR (125.77 MHz, $CDCl_3$): δ = 36.53, 37.50, 42.80, 45.86, 46.37, 47.02, 49.03, 49.72, 54.39, 62.40, 67.87, 127.27, 127.29, 128.59. 128.61, 129.21, 129.24, 133.87, 133.89, 139.34, 139.36, 171.47. HPLC–MS (ESI): t_R = 9.42 min, m/z = 324 $[M + H]^+$, 258 $[M_{rDA} + H]^+$.

(4a*S,5*R**,8*S**,8a*R**)-1′-Benzyl-4a,5,8,8a-tetrahydro-1*H*-spiro[5,8-epoxyquinazoline-2,4′-piperidin]-4(3*H*)-one (13):** Colourless powder (90 %). M.p. 196–197 °C. ^{1}H NMR (500 MHz, $CDCl_3$): δ = 1.6–1.9 (m, 4 H, CH_2), 1.85–1.95 (m, 1 H, 1-NH), 2.14 (d, J = 6.5 Hz, 1 H, 4a-H), 2.48–2.64 (m, 4 H, CH_2), 3.36 (s, 1 H, 8a-H), 3.54 (s, 2 H, NCH_2Ar), 4.84 (s, 1 H, 8-H), 5.42 (s, 1 H, 5-H), 6.31 (s, 1 H, 3-NH), 6.36 (dd, J = 5.8, J = 1.5 Hz, 1 H, 7-H), 6.57 (dd, J = 5.86, J = 1.45 Hz, 1 H, 6-H), 7.27–7.33 (m, 1 H, ArH) ppm. ^{13}C NMR (125.77 MHz, $CDCl_3$): δ = 35.8, 42.8, 48.8, 49.4, 52.4, 62.7, 67.9, 81.8, 83.2, 128.3, 129.0, 133.5, 138.5, 170.3. HPLC–MS (ESI): t_R = 6.86 min, m/z = 326 $[M + H]^+$, 258 $[M_{rDA} + H]^+$.

(4a*R,5*R**,8*S**,8a*S**)-4a,5,8,8a-Tetrahydro-1*H*-spiro[5,8-methanoquinazoline-2,2′-adamantan]-4(3*H*)-one (14):** Colourless powder (82 %). M.p. 218–220 °C. HPLC–MS (ESI): t_R = 12.45 min, m/z = 285 $[M + H]^+$, 219 $[M_{rDA} + H]^+$. The analytical and spectroscopic data of **14** were identical to those reported in the literature.[2r]

(4a*S,5*R**,8*S**,8a*R**)-4a,5,8,8a-Tetrahydro-1*H*-spiro[5,8-methanoquinazoline-2,2′-adamantan]-4(3*H*)-one (15):** Colourless crystals (83 %). M.p. 207–210 °C. HPLC–MS (ESI): t_R = 11.49 min, m/z = 285 $[M + H]^+$, 219 $[M_{rDA} + H]^+$. The analytical and spectroscopic data of **15** were identical to those reported in the literature.[2r]

(4a*S,5*R**,8*S**,8a*R**)-4a,5,8,8a-Tetrahydro-1*H*-spiro[5,8-epoxyquinazoline-2,2′-adamantan]-4(3*H*)-one (16):** Colourless crystals (79 %). M.p. 175–178 °C. HPLC–MS (ESI): t_R = 14.19 min, m/z = 287 $[M + H]^+$, 219 $[M_{rDA} + H]^+$. The analytical and spectroscopic data of **16** were identical to those reported in the literature.[2r]

Synthesis of Retrodiene Products 17–22

Preparation of Racemic Pyrrolo[1,2-*a*]pyrimidines 17–19 and Pyrimido[1,2-*a*]isoindoles 20–22: Compounds **2**–**7** (100 mg) were each introduced into the flow reactor in a solution of MeCN (25 mL). The solution was inserted into the reactor, and passed through the heated reactor coil at 220 °C or 250 °C (for **2** and **7**), with a residence time of 15 min, and the flow output was collected. The solvent was removed by evaporation, and the residue was dissolved in Et_2O (5 mL). The resulting crystals were collected by filtration and washed with Et_2O.

8a-Methyl-1,7,8,8a-tetrahydropyrrolo[1,2-*a*]pyrimidine-2,6-dione (17): Colourless crystals (98 %). M.p. 165–166 °C. ^{1}H NMR (500 MHz, [D$_6$]DMSO): δ = 1.41 (s, 3 H, CH_3), 2.03–2.18 (m, 2 H, CH_2), 2.41–2.47 (m, 1 H, CH_2), 2.67–2.58 (m, 1 H, CH_2), 5.24 (dd, J = 7.70, J = 1.90 Hz, 1-H, 3-H), 7.30–7.32 (d, J = 7.72 Hz, 1 H, 4-H), 8.22 (s, 1 H, NH) ppm. ^{13}C NMR (125.77 MHz, [D$_6$]DMSO): δ = 24.5, 29.5, 33.9, 73.6, 105.5, 131.2, 163.58, 170.8 ppm. HPLC–MS (ESI): t_R = 7.11 min, m/z = 167 $[M + H]^+$.

1,8a-Dimethyl-8,8a-dihydropyrrolo[1,2-*a*]pyrimidine-2,6(1*H*,7*H*)-dione (18): Colourless crystals (98 %). M.p. 130–131 °C. ^{1}H NMR (500 MHz, $CDCl_3$): δ = 1.46 (s, 3 H, 8a-CH_3), 2.25–2.36 (m, 2 H, CH_2), 2.52–2.66 (m, 2 H, CH_2), 2.9 (s, 3 H, 1-CH_3), 5.47 (d, J = 7.6 Hz, 1 H, 3-H), 7.27 (d, J = 6.49 Hz, 1 H, 4-H) ppm. ^{13}C NMR (125.77 MHz, $CDCl_3$): δ = 19.4, 26.9, 29.6, 32.8, 106.0 129.6, 163.3, 169.7 ppm. HPLC–MS (ESI): t_R = 9.12 min, m/z = 181 $[M + H]^+$.

1-Methyl-8a-(*p*-tolyl)-8,8a-dihydropyrrolo[1,2-*a*]pyrimidine-2,6(1*H*,7*H*)-dione (19): Colourless crystals (99 %). M.p. 121–123 °C. ^{1}H NMR (500 MHz, $CDCl_3$): δ = 2.34 (s, 3 H, ArCH_3), 2.61–2.74 (m, 4 H, CH_2), 3.16 (s, 3 H, 1-CH_3), 5.48 (d, J = 7.66 Hz, 1 H, 3-H), 7.08 (d, J = 8.35 Hz, 2 H, , Ar), 7.17 (d, J = 8.04 Hz, 2 H, Ar), 7.32 (d, J = 7.64 Hz, 1 H, , 4-H) ppm. ^{13}C NMR (125.77 MHz, $CDCl_3$): δ = 20.9, 29.6, 30.0, 33.7, 80.3, 107.6, 124.7, 129.6, 130.3, 137.1, 139.2, 163.6, 170.8 ppm. HPLC–MS (ESI): t_R = 19.56 min, m/z = 257 $[M + H]^+$.

1-Methyl-1,10b-dihydropyrimido[2,1-*a*]isoindole-2,6-dione (20): Colourless crystals (98 %). M.p. 165–167 °C. ^{1}H NMR (500 MHz, $CDCl_3$): δ = 3.20 (s, 3 H, CH_3), 5.64 (d, J = 7.51 Hz, 1 H, 4-H), 5.99 (s, 1 H, 10b-H), 7.63–7.76 (m, 4 H, Ar), 7.98 (d, J = 7.51 Hz, 1 H, 3-H) ppm. ^{13}C NMR (125.77 MHz, $CDCl_3$): δ = 29.2, 70.9, 107.2, 125.3, 125.4, 130.6, 131.9, 132.7, 133.1, 138.7, 164.2, 165.4 ppm. HPLC–MS (ESI): t_R = 15.44 min, m/z = 215 $[M + H]^+$.

1,10b-Dimethyl-1,10b-dihydropyrimido[2,1-*a*]isoindole-2,6-dione (21): Colourless crystals (98 %). M.p. 236–238 °C. ^{1}H NMR (500 MHz, $CDCl_3$): δ = 1.72 (s, 3 H, 10b-CH_3), 3.13 (s, 3 H, 1-CH_3), 5.72 (d, J = 7.48 Hz, 1 H, 4-H), 7.54 (d, J = 7.49 Hz, 1 H, Ar), 7.63–7.76 (m, 3 H, Ar), 7.97 (d, J = 8.04 Hz, 1 H, 3-H) ppm. ^{13}C NMR (125.77 MHz, $CDCl_3$): δ = 22.4, 28.4, 107.8, 124.5, 125.3, 130.3, 130.3, 130.8, 133.2, 144.4, 163.9, 164.4 ppm. HPLC–MS (ESI): t_R = 16.80 min, m/z = 229 $[M + H]^+$.

1-Methyl-10b-(*p*-tolyl)-1,10b-dihydropyrimido[2,1-*a*]isoindole-2,6-dione (22): Colourless crystals (95 %). M.p. 183–184 °C. ^{1}H NMR (500 MHz, $CDCl_3$): δ = 2.31 (s, 3 H, ArCH_3), 3.31 (s, 3 H, 1-CH_3), 5.64 (d, J = 7.44 Hz, 1-H, 4-H), 6.85 (d, J = 8.34 Hz, 2 H, ArH), 7.09 (d, J = 7.93 Hz, 1 H, ArH), 7.36 (d, J = 7.42 Hz, 2 H, ArH), 7.62–7.66 (m, 2 H, ArH), 8.03–8.04 (m, 1 H, 3-H) ppm. ^{13}C NMR (125.77 MHz, $CDCl_3$): δ = 21.0, 30.8, 81.1, 108.8, 125.0 126.0, 126.1, 129.5, 130.4, 130.6, 130.7, 133.5, 134.8, 139.2, 145.1, 165.1, 165.3 ppm. HPLC–MS (ESI): t_R = 25.70 min, m/z = 305 $[M + H]^+$.

Preparation of Enantiomeric Pyrrolo[1,2-*a*]pyrimidine (+)-19 and Pyrimido[1,2-*a*]isoindole (–)-20: A solution of pyrrolo-[1,2-*a*]quinazoline derivative (–)-**4** (100 mg) or isoindolo[2,1-*a*]quinazoline derivative (+)-**5** (100 mg) in MeCN (25 mL) was introduced into the flow reactor at a temperature of 220 °C, using the same flow rate (0.2 mL min^{-1}), with a residence time of 15 min. The flow output was collected, and the solvent was removed by evaporation. The residue was dissolved in Et_2O (1 mL). The resulting crystals were collected by filtration and washed with Et_2O. The ^{1}H and ^{13}C NMR spectroscopic data for the optically active compounds were consistent with those reported for the racemates.

(+)-(*S*)-1-Methyl-8a-(*p*-tolyl)-8,8a-dihydropyrrolo[1,2-*a*]pyrimidine-2,6(1*H*,7*H*)-dione [(+)-19]: Colourless crystals (97 %). M.p. 167–169 °C. $[\alpha]_D^{25}$ = +195 (c = 0.3, MeOH); 97 % *ee*.

(–)-(*S*)-1-Methyl-1,10b-dihydropyrimido[2,1-*a*]isoindole-2,6-dione [(–)-20]: Colourless crystals (98 %). M.p. 203–205 °C $[\alpha]_D^{25}$ = –310 (c = 0.3, MeOH); 98 % *ee*.

Synthesis of Spiropyrimidinones 23–25: Spiroquinazoline derivatives **8**–**16** (100 mg) were each introduced into the flow reactor in solution in toluene/MeOH (4:1; 25 mL). The solution was inserted into the reactor and passed through the heated reactor coil, at 150 °C for the epoxy-bridged **10**, **13**, and **16**, or 240 °C for the methylene-bridged **8**, **9**, **11**, **12**, **14**, and **15**, with a residence time of 60 min. The flow output was collected, and the solvent was removed by evaporation. The residue was dissolved in EtOAc/MeOH (9:1); this material was transferred to a SiO_2 column, which was eluted with EtOAc/MeOH (9:1.

1,5-Diazaspiro[5.5]undec-3-en-2-one (23): Brownish crystals (95 %). M.p. 160–164 °C. IR (KBr): $\tilde{\nu}$ = 3263, 3025, 2939, 2863, 1627, 1516, 1434, 1337, 1213, 1122, 793, 730, 654 cm^{-1}. ^{1}H NMR (500 MHz,

[D_6]DMSO): δ = 1.18–1.79 (m, 10 H, CH_2), 4.31 (d, J = 7.2 Hz, 1 H, 3-H), 6.74–6.77 (m, 2 H, 4-H, NH), 6.96 (s, 1 H, NH) ppm. ^{13}C NMR (125.77 MHz, $CDCl_3$): δ = 21.7, 24.6, 36.9, 68.8, 92.2, 142.6, 166.2 ppm. HPLC–MS (ESI): t_R = 10.72 min, m/z = 167 $[M + H]^+$.

9-Benzyl-1,5,9-triazaspiro[5.5]undec-3-en-2-one (24): White crystals (92 %). M.p. 192–195 °C. IR (KBr): $\tilde{\nu}$ = 3243, 3026, 2947, 2808, 1614, 1527, 1424, 1219, 1104, 792, 739 cm^{-1}. ^{1}H NMR (500 MHz, [D_6]DMSO): δ = 1.96 (m, 4 H, CH_2), 2.48 (m, 4 H, CH_2), 3.53 (s, 2 H, NCH_2Ar), 4.49 (s, 1 H, NH), 4.80 (d, J = 7.39 Hz, 3-H, CH), 5.39 (s, 1 H, NH), 6.77–6.80 (t, J = 6.64 Hz, 1 H, 4-H), 7.28–7.34 (m, 5 H, ArH) ppm. ^{13}C NMR (125.77 MHz, [D_6]DMSO): δ = 34.0, 36.6, 48.9, 49.4, 62.7, 67.3, 92.7, 127.3, 128.4, 129.1, 142.7, 166.0 ppm. HPLC–MS (ESI): t_R = 257.15 min, m/z = 258 $[M + H]^+$.

1′*H*-Spiro[adamantane-2,2′-pyrimidin]-4′(3′*H*)-one (25): Brownish crystals (86 %). M.p. 220–212 °C. IR (KBr): $\tilde{\nu}$ = 3308, 2910, 1633, 1391, 1244, 1101, 783, 668, 618 cm^{-1}. ^{1}H NMR (500 MHz, $CDCl_3$): δ = 1.74–1.95 (m, 16 H, adamantane), 2.28 (m, *2* H, adamantane), 4.79 (m, 1 H, 5-H), 5.76 (m), 6.74–6.77 (m, 2 H, 4-H, NH), 6.85 (s, 1 H, 6-H) ppm. ^{13}C NMR (125.77 MHz, $CDCl_3$): δ = 26.1, 26.4, 32.3, 33.2. 35.0, 37.5, 71.9, 92.1, 142.8, 166.2 ppm. HPLC–MS (ESI): t_R = 18.10 min, m/z = 219 $[M + H]^+$.

General Procedure for Batch Reactions

Compounds **2**–**13** were prepared by the previously reported methods.[2l–2q]

Preparation of Spiroquinazolinone Derivatives 14–16: β-aminorbornene carboxamide **1a**, **1c**, or **1d** (1 mmol) was placed in a microwave test tube (10 mL) containing a magnetic stirrer bar and EtOH (2 mL). The reaction vial was then sealed with a Teflon cap, and placed into the CEM Discover microwave reactor. The solution was irradiated (150 W) for a period of 1 h at 100 °C. The resulting solution was transferred onto a SiO_2 column, which was eluted with toluene/MeOH (4:1).

(4a*R,5*R**,8*S**,8a*S**)-4a,5,8,8a-Tetrahydro-1*H*-spiro[5,8-methanoquinazoline-2,2′-adamantan]-4(3*H*)-one (14):** Colourless powder (75 %). M.p. 215–220 °C.

(4a*S,5*R**,8*S**,8a*R**)-4a,5,8,8a-Tetrahydro-1*H*-spiro[5,8-methanoquinazoline-2,2′-adamantan]-4(3*H*)-one (15):** Colourless crystals (77 %). M.p. 210–211 °C.

(4a*S,5*R**,8*S**,8a*R**)-4a,5,8,8a-Tetrahydro-1*H*-spiro[5,8-epoxyquinazoline-2,2′-adamantan]-4(3*H*)-one (16):** Colourless crystals (76 %). M.p. 175–181 °C.

Microwave-Induced rDA Reactions of 8–16: Microwave-mediated reactions were carried out in sealed reaction vials. Heterocycle **8**–**16** (200 mg) was placed in a microwave test tube (10 mL) containing a magnetic stirrer bar and 1,2-DCB (2 mL). The reaction vial was then sealed with a Teflon cap, and placed into the CEM Discover microwave reactor. The solution was irradiated (250 W) for a period of 30 min at 200 °C for **8**, **9**, **11**, **12**, **15**, and **16**, and at 180 °C for **10**, **13**, and **16**. The solution was cooled, and the solvent was evaporated. The residue was dissolved in *n*-hexane/EtOAc (1:1) eluent, and the resulting solution was transferred to a SiO_2 column. The yields of the products **23**–**25** are given in Figure 2. For **11**, **14**, and **15**, decomposition took place, and the formation of rDA products was not observed.

Acknowledgments

We are grateful to the Hungarian Research Foundation (OTKA No. K 115731). The financial support from the GINOP-2.3.2-15-2016-00014 project is acknowledged.

Keywords: Flow chemistry · Microreactors · Nitrogen heterocycles · Spiro compounds · Cycloaddition · Synthetic methods

[1] a) C. A. Carson, M. A. Kerr, *Chem. Soc. Rev.* **2009**, *38*, 3051–3060; b) R. A. Yoder, J. N. Johnston, *Chem. Rev.* **2005**, *105*, 4730–4756; c) Y. Cheng, Z.-T. Huang, M.-X. Wang, *Curr. Org. Chem.* **2004**, *8*, 325–351.
[2] a) G. Stájer, A. E. Szabó, G. Bernáth, P. Sohár, *Synthesis* **1987**, 290–292; b) M. Palkó, P. Sohár, F. Fülöp, *Molecules* **2011**, *16*, 7691–7705; c) F. Fülöp, M. Palkó, G. Bernáth, P. Sohár, *Synth. Commun.* **1997**, *27*, 195–203; d) G. Stájer, A. E. Szabó, F. Fülöp, G. Bernáth, P. Sohár, *Chem. Ber.* **1987**, *120*, 259–264; e) G. Stájer, A. E. Szabó, G. Bernáth, P. Sohár, *J. Chem. Soc. Perkin Trans. 1* **1987**, 237–240; f) G. Stájer, E. A. Szabó, P. Sohár, A. Csámpai, R. J. Sillanpää, *J. Mol. Struct.* **2006**, *784*, 239–243; g) P. Sohár, A. Csámpai, A. E. Szabó, G. Stájer, *J. Mol. Struct.* **2004**, *694*, 139–147; h) E. Forró, F. Fülöp, *Org. Lett.* **2003**, *5*, 1209–1212; i) E. Forró, F. Fülöp, *Tetrahedron: Asymmetry* **2004**, *15*, 573–575; j) B. Fekete, M. Palkó, M. Haukka, F. Fülöp, *Molecules* **2017**, *22*, 613–626; k) B. Fekete, M. Palkó, I. M. Mándity, M. Haukka, F. Fülöp, *Eur. J. Org. Chem.* **2016**, 3519–3527; l) F. Fülöp, F. Miklós, E. Forró, *Synlett* **2008**, 1687–1689; m) F. Miklós, Z. Tóth, M. M. Hänninen, R. Sillanpää, E. Forró, F. Fülöp, *Eur. J. Org. Chem.* **2013**, 4887–4894; n) F. Miklós, K. Bozó, Z. Galla, M. Haukka, F. Fülöp, *Tetrahedron: Asymmetry* **2017**, *28*, 1401–1406; o) F. Miklós, T. Á. Bagi, F. Fülöp, *ARKIVOC* **2009**, 5–12; p) F. Miklós, F. Fülöp, *Acta Chim. Slov.* **2009**, *56*, 674–679; q) F. Miklós, F. Fülöp, *Eur. J. Org. Chem.* **2010**, 959–965; r) F. Miklós, A. Petrisor, F. Fülöp, *ARKIVOC* **2015**, 158–171.
[3] a) A. Ichihara, *Synthesis* **1987**, 207–222; b) B. Rickborn, "The Retro–Diels–Alder Reaction Part I: C–C Dienophiles" in *Organic Reactions*, *John Wiley & Sons*, **2004**; c) A. J. H. Klunder, J. Zhu, B. Zwanenburg, *Chem. Rev.* **1999**, *99*, 1163–1190.
[4] a) F. Csende, G. Stájer, F. Fülöp in *Comprehensive Organic Synthesis, 2nd ed.* (Eds.: P. Knochel, G. A. Molander), Elsevier, Amsterdam, **2014**, vol. 5, pp. 518–594; b) G. Stájer, F. Miklós, I. Kanizsai, F. Csende, R. Sillanpää, P. Sohár, *Eur. J. Org. Chem.* **2004**, 3701–3706; c) F. Miklós, G. Stájer, F. Fülöp, *Lett. Org. Chem.* **2006**, *3*, 915–916; d) F. Csende, F. Fülöp, G. Stájer, *Curr. Org. Synth.* **2008**, *5*, 173–185.
[5] C. F. Nising, U. K. Ohnemüller, S. Bräse, *Synthesis* **2006**, 2643–2645.
[6] a) D. R. Clay, A. G. Rosenberg, M. C. McIntosh, *Tetrahedron: Asymmetry* **2011**, *22*, 713–716; b) C. A. Citron, S. M. Wickel, B. Schulz, S. Draeger, J. S. Dickschat, *Eur. J. Org. Chem.* **2012**, 6636–6646; c) D. A. Kummer, D. Li, A. Dion, A. G. Myers, *Chem. Sci.* **2011**, *2*, 1710–1718.
[7] a) M. Iqbal, Y. Li, P. Evans, *Tetrahedron* **2004**, *60*, 2531–2538; b) J. P. Eddolls, M. Iqbal, S. M. Roberts, M. G. Santoro, *Tetrahedron* **2004**, *60*, 2539–2550; c) T. Gallager, S. Sanchez, J. H. Bateson, P. J. O'Hanlon, *Pure Appl. Chem.* **2005**, *77*, 2033–2040.
[8] a) S. A. Hasbullah, S. Jones, *Tetrahedron: Asymmetry* **2010**, *21*, 2719–2725; b) S. Khota, S. Bhanerjee, *RSC Adv.* **2013**, *3*, 7642–7666.
[9] I. Nekkaa, M. Palkó, I. M. Mándity, F. Fülöp, *Beilstein J. Org. Chem.* **2018**, *14*, 318–324.
[10] J. Wegner, S. Ceylan, A. Kirschning, *Adv. Synth. Catal.* **2012**, *354*, 17–57.
[11] C. Wiles, P. Watts, *Green Chem.* **2014**, *16*, 55–62.
[12] N. Kockmann, P. Thenée, C. Fleischer-Trebes, G. Laudadio, T. Noël, *React. Chem. Eng.* **2017**, *2*, 258–280.
[13] A. J. DeMello, *Nature* **2006**, *442*, 394–402.
[14] T. Noël, Y. Su, V. Hessel, *Top. Organomet. Chem.* **2016**, *57*, 1–41.
[15] S. G. Newman, K. F. Jensen, *Green Chem.* **2013**, *15*, 1456–1472.
[16] I. R. Baxendale, *J. Chem. Technol. Biotechnol.* **2013**, *88*, 519–552.
[17] S. Kobayashi, *Chem. Asian J.* **2016**, *11*, 425–436.
[18] M. Movsisyan, E. I. P. Delbeke, J. K. E. T. Berton, C. Battilocchio, S. V. Ley, C. V. Stevens, *Chem. Soc. Rev.* **2016**, *45*, 4892–4928.
[19] J. Wegner, S. Ceylan, A. Kirschning, *Chem. Commun.* **2011**, *47*, 4583–4592.
[20] a) I. M. Mándity, S. B. Ötvös, G. Szöllösi, F. Fülöp, *Chem. Rec.* **2016**, *16*, 1018–1033; b) C. T. Hsieh, S. B. Ötvös, Y. C. Wu, I. M. Mándity, F. R. Chang, F. Fülöp, *ChemPlusChem* **2015**, *80*, 859–864; c) I. M. Mándity, S. B. Ötvös, F. Fülöp, *ChemistryOpen* **2015**, *4*, 212–223.
[21] a) B. Bradar, E. Reich, *Bioog. Med. Chem.* **2008**, *16*, 11481–1492; b) M. A. Ivanov, L. A. Aleksandrova, *Russ. J. Bioorg. Chem.* **2013**, *39*, 22–39; c) V. P. Kumar, J. A. Cisneros, K. M. Frey, A. Castellanos-Gonzalez, Y. Wang, A.

Gangjee, A. C. White Jr., W. L. Jorgensen, K. S. Anderson, *Bioorg. Med. Chem. Lett.* **2014**, *24*, 4158–4161.

[22] a) K. W. Temburnikar, C. R. Ross, G. M. Wilson, J. Balzarini, B. M. Cawrse, K. L. Seley-Radtke, *Bioorg. Med. Chem.* **2015**, *23*, 4354–4363; b) A. Lauria, C. Patella, I. Abbate, A. Martorana, A. M. Almerico, *Eur. J. Med. Chem.* **2012**, *55*, 375–383.

[23] S. Nagashima, T. Hondo, H. Nagata, T. Ogiyama, J. Maeda, H. Hoshii, T. Kontani, S. Kuromitsu, K. Ohga, M. Orita, K. Ohno, A. Moritomo, K. Shiozuka, M. Furutani, M. Takeuchi, M. Ohta, S. Tsukamoto, *Bioorg. Med. Chem.* **2009**, *17*, 6926–6936.

[24] V. Pittala, M. A. Siracusa, M. N. Modica, L. Salerno, A. Pedretti, G. Vistoli, A. Cagnotto, T. Mennini, G. Romeo, *Bioorg. Med. Chem.* **2011**, *19*, 5260–5276.

[25] P. G. Baraldi, R. Romagnoli, G. Saponaro, M. A. Tabrizi, S. Baraldi, P. Pedretti, C. Fusi, R. Nassini, S. Materazzi, P. Geppetti, D. Preti, *Bioorg. Med. Chem.* **2012**, *20*, 1690–1698*J*.

[26] a) E. del Olmo, B. Barboza, M. I. Ybarra, J. L. Lopez-Perez, R. Carron, M. A. Sevilla, C. Boselli, A. S. Feliciano, *Bioorg. Med. Chem. Lett.* **2006**, *16*, 2786–2790; b) E. del Olmo, M. G. Armas, M. I. Ybarra, J. L. Lopez, P. Oporto, A. Gimenez, E. Deharo, A. S. Feliciano, *Bioorg. Med. Chem. Lett.* **2003**, *13*, 2769–2772.

[27] K. Nesmerak, H. Pelouchova, V. Vsetecka, I. Nemec, J. Gabriel, *Folia Microbiol.* **1998**, *43*, 39–41.

[28] Q. Zhao, M. Vargas, Y. Dong, L. Zhou, X. Wang, K. Sriraghavan, J. Keiser, J. L. Vennestrom, *J. Med. Chem.* **2010**, *53*, 4223–4233.

[29] N. Kolocouris, G. Zoidis, G. B. Foscolos, G. Fytas, S. R. Prathalingham, J. M. Kelly, L. Naesens, E. De Clercq, *Bioorg. Med. Chem. Lett.* **2007**, *17*, 4358–4362.

[30] C. A. Tinker, G. H. Baeton, B. N. Smith, R. T. Cook, L. S. Cooper, L. Fraser-Rae, K. Hallam, P. Hamley, T. McInally, J. D. Nicholls, D. A. Pimm, V. A. Wallace, *J. Med. Chem.* **2003**, *46*, 913–916.

[31] L. H. Birch, M. G. Buckley, N. Davies, J. H. Dyke, J. E. Frost, J. P. Gilbert, R. D. Hannah, F. A. Haughan, J. M. Madigan, T. Morgan, R. W. Pitt, J. A. Ratcliffe, C. N. Ray, D. M. Richard, A. Sharpe, J. A. Taylor, M. J. Whitworth, C. S. Williams, *Bioorg. Med. Chem. Lett.* **2005**, *15*, 5335–5339.

[32] a) J. Tsoung, A. R. Bogdan, S. Kantor, Y. Wang, M. Charaschanya, S. W. Djuric, *J. Org. Chem.* **2017**, *82*, 1073–1084; b) J. Izquierdo, M. A. Pericàs, *ACS Catal.* **2016**, *6*, 348–356.

[33] a) R. E. Martin, M. Lenz, T. Alzieu, J. D. Aebi, L. Forzy, *Tetrahedron Lett.* **2013**, *54*, 6703–6707; b) N. Lamborelle, J. F. Simon, A. Luxen, J.-C. M. Monbaliu, *Org. Biomol. Chem.* **2015**, *13*, 11602–11606; c) S. K. Patel, T. E. Long, *Tetrahedron Lett.* **2009**, *50*, 5067–5070.

Received: May 8, 2018

IV.

(Submitted for publication)

Flow-chemistry enabled efficient patterning of β-peptides: backbone topology vs. helix formation

Imane Nekkaa,[a]† *Dóra Bogdán,*[b]† *Tamás Gáti,*[b,c] *Szabolcs Béni,*[d] *Tünde Juhász,*[e] *Márta Palkó,*[a] *Gábor Paragi,*[f,g] *Gábor K. Tóth,*[f,g] *Ferenc Fülöp,**[a] *István M. Mándity** [a,b,h]

[a] Institute of Pharmaceutical Chemistry, University of Szeged, H-6720 Szeged, Eötvös u. 6, Hungary,
[b] Department of Organic Chemistry, Faculty of Pharmacy, Semmelweis University H-1092 Budapest Hőgyes Endre u. 7, Hungary,
[c] Servier Research Institute of Medicinal Chemistry (SRIMC), Záhony utca 7, H-1031Budapest, Hungary
[d] Department of Pharmacognosy, Faculty of Pharmacy, Semmelweis University H-1085 Budapest, Üllői u. 26. Hungary,
[e] Institute of Materials and Environmental Chemistry, Research Center for Natural Sciences, Hungarian Academy of Sciences, H-1117, Budapest, Magyar Tudósok krt. 2, Hungary,
[f] Department of Medical Chemistry, University of Szeged, H-6720 Szeged, Dóm t. 8, Hungary
[g] MTA-SZTE Biomimetic Systems Research Group, H-6720 Szeged, Dóm t. 8, Hungary
[h] MTA TTK Lendület Artificial Transporter Research Group, Institute of Materials and Environmental Chemistry, Research Center for Natural Sciences, Hungarian Academy of Sciences, H-1117 Budapest, Magyar Tudósok krt. 2, Hungary
† The authors contributed equally, IN: amino acid and peptide synthesis, DB: NMR and ECD part

e-mail: fulop@pharm.u-szeged.hu, mandity.istvan@ttk.mta.hu.

ABSTRACT

The helical folding ability of homooligomer β-pentapeptides constructed by using [1*R*,2*R*]-2-aminocyclohexanecarboxylic acid ([1*R*,2*R*]-ACHC) monomers and comprising enantiomeric bicyclic β-amino acids {*diexo*-3-aminobicyclo[2.2.1]hept-5-ene-2-carboxylic acid (*diexo*-ABHEC) and *diexo*-3-amino-7-oxabicyclo[2.2.1]hept-5-ene-2-carboxylic acid (*diexo*-AOBHEC)} as well as *Z*-dehydro-β-alanine or β-alanine residues in the middle of the peptide chain has been studied. Both *ab initio* theory and spectroscopic techniques (NMR, ECD) proved unequivocally that oligomers incorporating [1*R*,2*R*,3*S*,4*S*]-ABHEC, [1*R*,2*S*,3*R*,4*S*]-AOBHEC and β-alanine as third residue tend to adopt a H14-helix motif. In contrast, if the middle unit is [1*S*,2*S*,3*R*,4*R*]-ABHEC or [1*S*,2*R*,3*S*,4*R*]-AOBHEC or *Z*-dehydro-β-alanine, stable self-organization could not be observed. The results show that the different behavior of the incorporated enatiomeric pairs rely on steric hindrances caused by

the synperiplanar orientation of the ψ angle of the bicyclic residue. However, for *Z*-dehydro-β-alanine, helix formation is excluded because of the conjugation of the carbon–carbon double bond and the residue flanking amide bonds, providing a planar orientation for these atoms yielding an elongated structure.

KEYWORDS: bicyclic bridged amino acids, continuous-flow, chirality, foldamers helical structure, β-peptides, self-organization.

INTRODUCTION

Foldamers are artificial self-organizing biomimetic polymers. They have high tendency to fold into a conformationally ordered state in solution.[1,2] The main motivation for designing peptidomimetic foldamers is the fact that these compounds are stable to proteolysis or metabolism and have better membrane permeability compared to α-peptide chains.[3,4] One of the most important representative of these peptidomimetic agents is β-peptides. The additional carbon atom in β-amino acids allows various alterations in substitution of the individual residues, which can result in remarkable changes of the complete folding behavior.[5-24] β-Peptides exhibit a wide range of bioactivities, e.g. antimicrobial,[25,26] tertiary structural elements with ion-binding ability,[9,27,28] and protein–protein interactions (PPIs) modifying activity.[29-32] In addition, they have high importance in the creation of novel materials for tissue engineering.[33]

Conformationally constrained β-peptide oligomers containing cyclic side-chains can fold into various helical conformations, such as H14,[34,35] H12,[36] H10/12[36] and H14/16[37] helices. Homooligomers composed of [1*R*,2*R*]-2-aminocyclohexanecarboxylic acid ([1*R*,2*R*]-ACHC) monomers form a highly stable H14 helix in various solvents.[34,38] This H14 helix conformation contains three β-amino acid residues per turn, stabilized by H-bonds between $C{=}O^{i}$ and NH^{i-2} pillars.[39] Furthermore, there are information for the bulky, strongly hydrophobic bicyclic side-chains. For instance, peptides containing *N*-Boc-protected *diexo*-3-aminobicyclo[2.2.1]hept-5-ene-2-carboxylic acid (*diexo*-ABHEC) enantiomer residues exhibit right- and left-handed consecutive 6-strands (6-membered intra-residue hydrogen bonding).[40] In contrast, with alternating backbone configuration of oligomers containing [2*S*,3*R*]/[2*R*,3*S*]-ABHEC enantiomer units, with protected or free at both ends, they are not capable of helix formation; their secondary structures are a robust bend-strand[41] or a circle-like fold.[42] Furthermore, β-peptides synthesized through the use of the bicyclic *diexo*-3-amino-7-

oxabicyclo[2.2.1]hept-5-ene-2-carboxylic acid (*diexo*-AOBHEC) units adopt an 8-membered hydrogen-bonded ring conformation.[43]

Herein, in order to study the effect of new structural elements on conformation, we examined the helix-forming property of oligomers containing enantiomeric bicyclic β-amino acid residues and their chemical derivatives. For this end, pentamers made of [1*R*,2*R*]-ACHC building blocks possessing an enantiomer of bicyclic residue in the middle of the peptide chain were assembled by revolutionary continuous-flow (CF) synthetic methods. As bridged residues, enantiomers of *diexo*-ABHEC and *diexo*-AOBHEC were used to compare the ability of folding regarding the configuration and study the effect of an oxygen-bridged residue on self-organization. From these structures, in a straightforward continuous-flow retro-Diels-Alder (CF rDA) reaction step, an analogous derivative containing the *Z*-dehydro-β-alanine residue was prepared. To attain the β-alanine-containing foldamer, the saturation of the dehydro compound was carried out in a CF hydrogenation reactor. The combined use of NMR and ECD measurements with molecular modelling results showed the differences of helix stability in the abovementioned structures.

RESULTS AND DISCUSSION

We planned to create new pentameric systems built from [1*R*,2*R*]-ACHC comprising a bicyclic amino acid enantiomer in the third residue position. Therefore, β-peptides **1-4**, illustrated in Scheme 1, were synthesized by a highly efficient continuous-flow solid-phase peptide synthesis (CF SPPS) technology developed in our laboratory.[44] The technology allows the construction of various peptides by using very low, generally 1.5-fold, amino-acid excess. The peptides were elongated in the instrument, and the products were cleaved and purified through regular reversed-phase HPLC methodology. The [1*R*,2*R*,3*S*,4*S*]-ABHEC and [1*S*,2*S*,3*R*,4*R*]-ABHEC enantiomers were incorporated into peptide **1** and **3**, respectively. However, peptides **2** and **4** were synthesized by the utilization of racemic *N*-protected *diexo*-AOBHEC amino acids and the resulting diastereomers were separated by means of RP-HPLC and their configuration was determined by NMR measurements and theoretical calculations. To investigate the effect of *Z*-dehydro-β-alanine on self-organization, compounds **1-4** containing *diexo*-ABHEC and *diexo*-AOBHEC were subjected to CF rDA protocol reported recently[45,46] (Scheme 1). As an illustration, solutions of β-peptide homooligomers **1-4** dissolved in MeOH were introduced into the reactor by an HPLC pump. Heating the mixtures of **2** and **4** at 150 °C or **1** and **3** at 230 °C led to the expected oligomer **5** within a residence time of 14 min, with total conversion. Our last step was to study the folding behavior of

saturated β-alanine-containing peptide **6**, by changing the third unit from *Z*-dehydro-β-alanine to β-alanine unit. Peptide **6** was prepared by saturating rDA product **5** in an H-Cube® CF hydrogenation reactor on a 10% Pd/charcoal catalyst at 50 °C and 50 bar affording oligomer **6** in a good yield of 95%. The foldamers were analyzed by HPLC-MS and characterized through the use of different NMR methods, including TOCSY and ROESY, in different solvents: 4 mM solutions in H_2O/D_2O (90:10), CD_3OH and DMSO-d_6. The NMR signal dispersions were good for most of the compounds in these solvents; no signal broadening was observed and signal assignment could be performed in a straightforward manner.

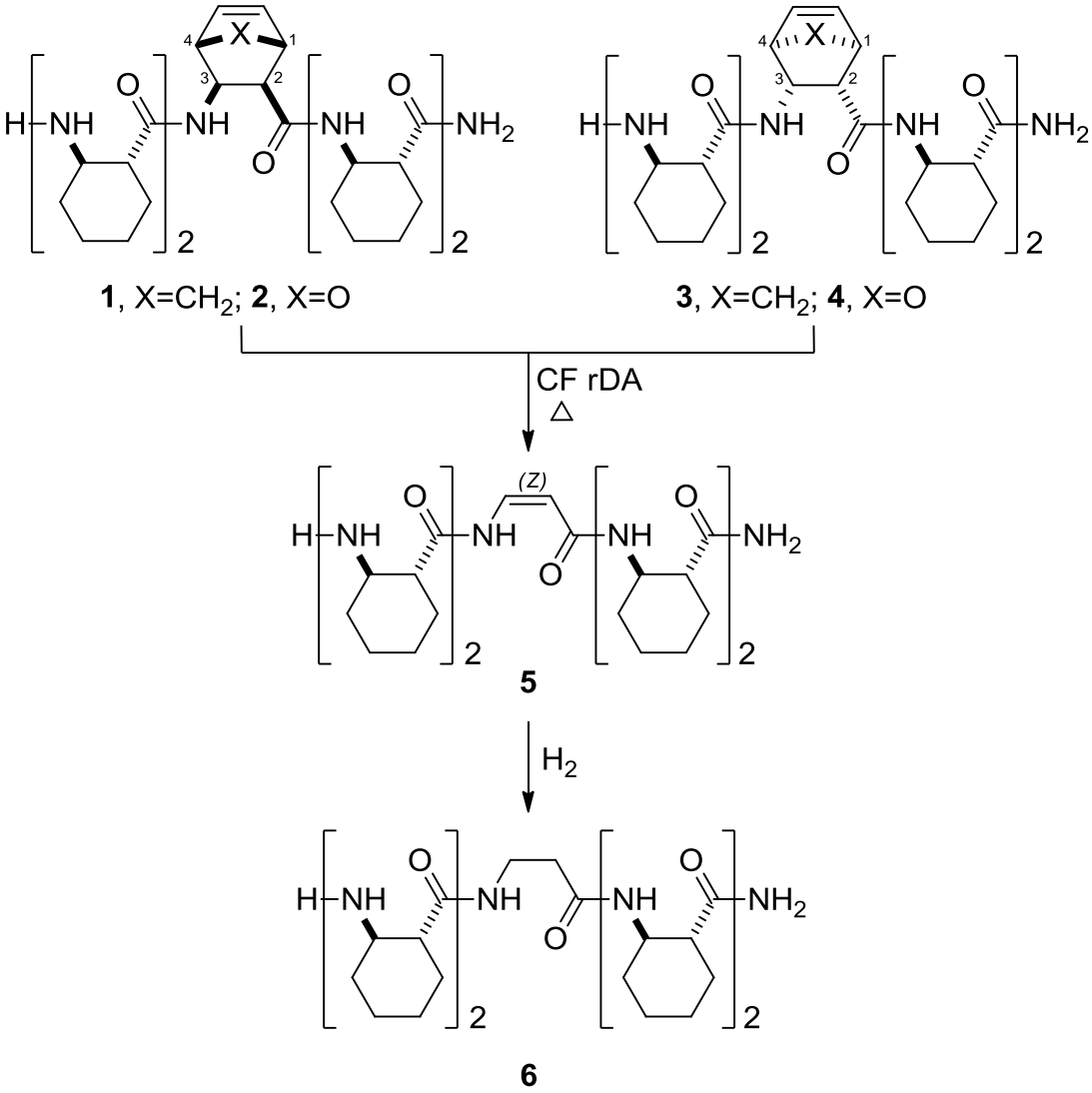

Scheme 1. Investigated foldamer structures composed of [1*R*,2*R*]-ACHC units incorporating [1*R*,2*R*,3*S*,4*S*]-ABHEC (**1**), [1*R*,2*S*,3*R*,4*S*]-AOBHEC* (**2**), [1*S*,2*S*,3*R*,4*R*]-ABHEC (**3**), [1*S*,2*R*,3*S*,4*R*]-AOBHEC* (**4**), *Z*-dehydro-β-alanine (**5**) and β-alanine (**6**) as third β-amino acid units. * The absolute configuration was determined by means of NMR investigations and theoretical calculations.

Furthermore, the analytical HPLC chromatograms of foldamers in diastereomeric relation, i.e. **1** vs. **3** and **2** vs. **4**, showed drastic differences. Foldamers **1** and **2** possess substantially higher retention times than **3** and **4**. This finding suggests that **1** and **2** are more hydrophobic than **3** and **4**. According to previous results,[37,47] the ordered helical structure is more hydrophobic since the amide bonds are in the center of the structure and only the hydrophobic side-chains interact with the chromatographic system. Consequently, helix formation might be anticipated for compounds **1** and **2**.

For a further assessment of the conformational stability, NH–ND amide proton exchange experiments were applied in CD_3OD. Relative residual signal intensities are plotted in Figure 1. In all cases, N-terminal NH_2 and C-terminal amide NH_2 disappeared immediately after dissolution. For **3**, an immediate proton exchange was observed indicating an unfolded structure. For **4** and **5**, proton exchange occurred in about 1 hour demonstrating weak structure stabilizing H-bonds and poorly shielded amide protons. Significantly longer proton exchange times (10 hours, over 1 day) were shown for structures **1**, **2** and **6**. These observations may suggest highly shielded NH protons from the solvent and stable H-bonds, which indicate a helical secondary structure. These exchange rates are in accordance with the results measured for H14 helical β-peptides.[48]

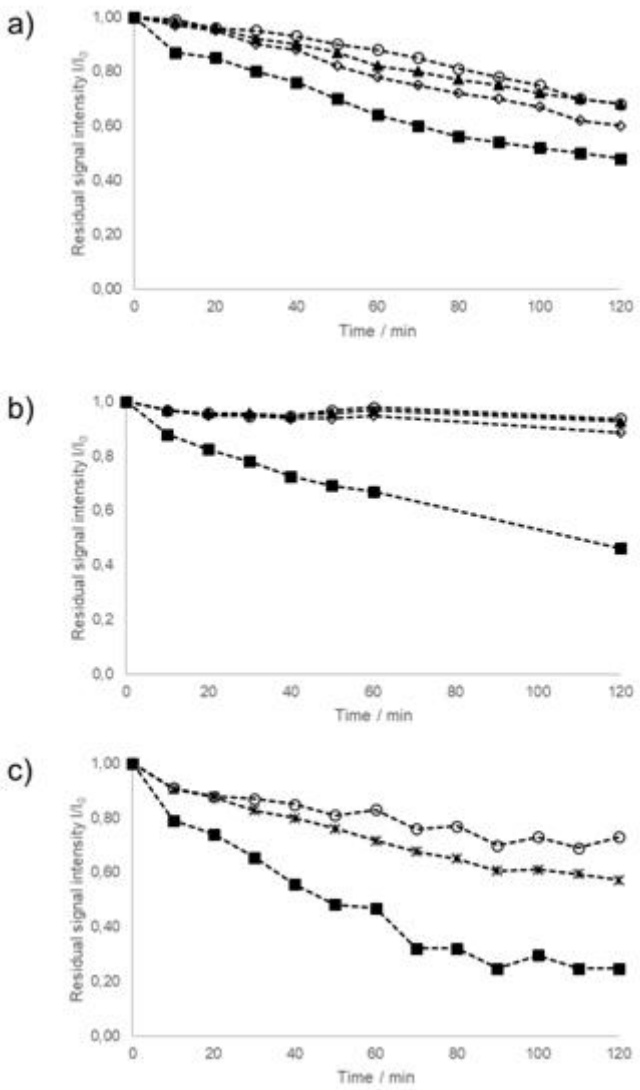

Figure 1. NH–ND exchange plots for **1** (a), **2** (b), **6** (c) in CD_3OD. ■: NH_2; ○:NH_3; ▲: NH_4; ◊: NH_5; *: NH_4+NH_5.

To characterize the high-resolution structure of the foldamers, ROESY NMR spectra were taken in H_2O/D_2O, CD_3OH and DMSO-d_6. For **1**, **2**, **6** long-range NOE interactions could be detected between C_β protons of residues i=1,2 and C_α protons of residues (i+3) in all three solvents. Such correlations are typical for 14-helices (Figure 2). Additionally, in the spectrum of **2** NOE cross peak of $NH_i/C_\beta H_{i+2}$ could be observed in CD_3OH and DMSO, too, which is a further sign for H14 helix formation. Weak correlations were shown from $C_\beta H_i$–$C_\alpha H_{i+3}$ in the case of **4** in CD_3OH and DMSO, as well as for **3** in CD_3OH. For **5** no long-range NOE cross peaks were seen regarding secondary structure interactions. These results suggest that a stable H14 helix formation was observed only for **1**, **2** and **6**. In contrast, for **3** and **4** only a considerably less stable helical organization was observed, while the introduction of the double bond to the back-bone ruled out the helix formation for **5**.

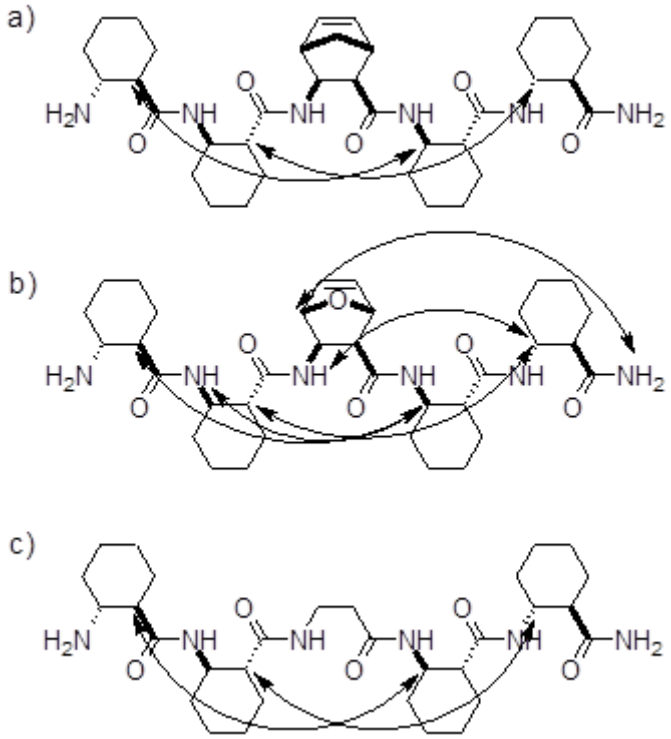

Figure 2. Long-range NOE interactions representing evidences for secondary structure of **1** (a), **2** (b) and **6** (c) in H_2O/D_2O (90:10), CD_3OH and DMSO-d_6. Spectra were taken at 298 K in 4 mM concentration.

To further support the results, electronic circular dichroism spectra were recorded in water and methanol at room temperature. This method allowed us to compare the stability of H14 helix in the investigated compounds and test the effect of built-in structural elements. The CD spectra of these β-peptides showed a broad maximum at 205–218 nm and a minimum at 183–198 nm in both solvents—these values are characteristic for a H14-helical structure.[38] The decreased intensities for **3**, **4** and **5** suggest the reduced stability of the secondary structure. In the case of **5** an additional absorption maximum at 262–266 nm could also be detected corresponding to the double bond inserted to the backbone. The practically identical absorption maxima and minima in water and methanol proved the absence of solvent-driven structural changes (Figure 3).

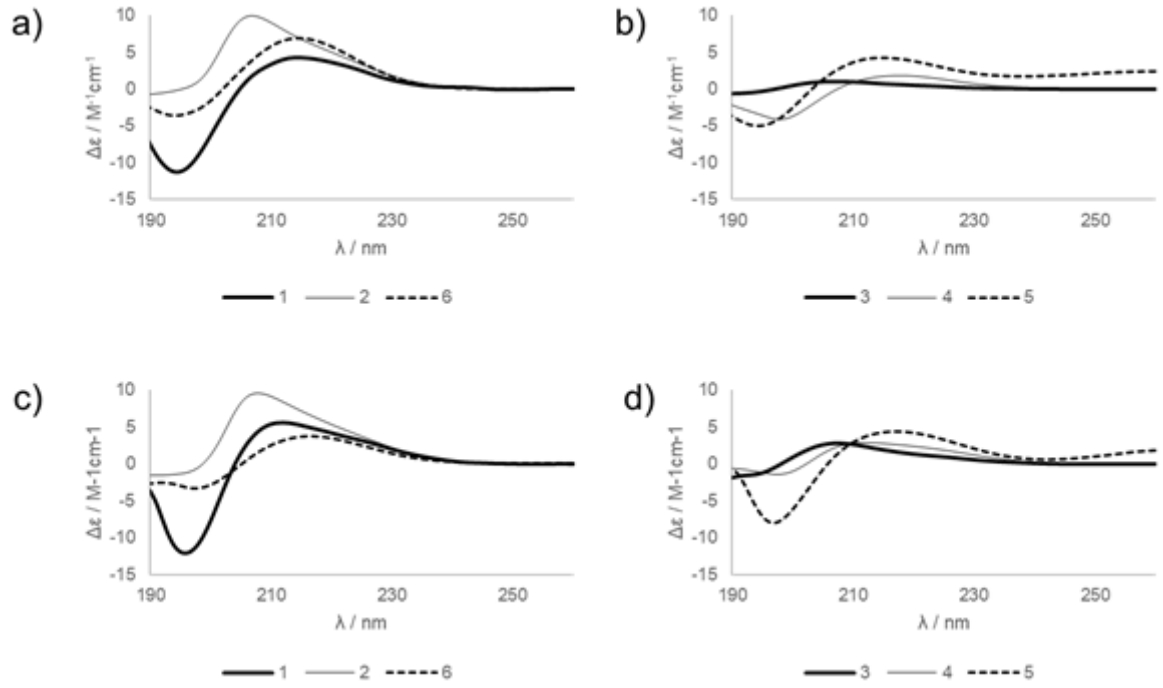

Figure 3. ECD spectra of 1 mM solutions of **1-6** in water (a,b) and methanol (c,d).

To acquire a theoretical support to understand the experimental outcomes regarding the preferred stereoisomer concerning compounds **1** and **3** or compounds **2** and **4**, high-level DFT calculations were performed. NMR and ECD measurements based on constrained molecular modelling structures were used as a preordered starting point for quantum level geometrical optimizations. For compounds **1-4** the geometries converged to the predicted H14 helix both in water and vacuum models. However, there are considerable differences in the stability of the helices. In Table 1 the total energies of the optimized structures in implicit solvent and vacuum are presented for each stereoisomer. The results show that quantumchemical investigations reinforce the experimental findings. Namely, compounds **1** and **2** have lower total energy in calculations than foldamers **3** and **4**. This result is independent from the application of the implicit solvent model. A deeper investigation of the calculated conformations revealed structural discrepancies for these oligomers when compared with regular H14 helical β-peptides. It was found that the *diexo*-substituted bicyclic residue enforces overlapping of the $H_{C\beta 3}$–$(NH)_3$ protons for peptides **1** and **2** and $(CO)_3$–$H_{C\alpha 3}$ atoms for compounds **3** and **4**. Such interaction is, in general, not favorable for helix formation. However, according to the observed results, the 1–2 hydrogen–hydrogen interaction is less problematic than the 1–2 oxygen–proton interaction. This phenomenon may rely on the larger size of the oxygen atom, since the electrostatic interaction of the partially negatively polarized oxygen atom and the hydrogen atom would be favorable. The effect of the size is underlined by interatomic distances. For $H_{C\beta 3}$–$(NH)_3$ it is 2.1 Å while for $(CO)_3$–$H_{C\alpha 3}$ it is 2.5 Å. The

enlarged distance indicates a more unfavorable interaction, which destabilizes the helical structure. This phenomenon can be examined by analyzing the φ angle for **1**, **2** and ψ angle for **3** and **4**. Both angles are enforced nearly to a synperiplanar conformation, because of the bridged bicyclic residue and hydrogen bond orientation of the H14 helix. This unfavorable interaction is partially compensated by the modification of the φ angle for **1**, **2** and the ψ angle for **3** and **4**. However, in the case of **1** and **2**, where H–H interaction is the source of the problem, only a minor modification (22°) is satisfying for helix stabilization and synperiplanar interaction modification. However, in the case of **3** and **4**, where H–O interaction causes the problem, the synperiplanar interaction might be minimized only by changing the ψ angle to 42° because of the larger size of the oxygen atom, which induces the destabilization of the H14 helix.

Table 1 Total energies (in Hartree) of compound **1-4** optimized at M062x/cc-tzv level of theory in implicit solvent and vacuum.

	1	**3**	**2**	**4**
	[1*R*,2*R*,3*S*,4*S*]-	[1*S*,2*S*,3*R*,4*R*]-	[1*R*,2*S*,3*R*,4*S*]-	[1*S*,2*R*,3*S*,4*R*]-
	ABHEC		AOBHEC	
implicit solvent	-2110.73898	-2110.72979	-2146.65102	-2146.64546
vacuum	-2110.66906	-2110.65979	-2146.58150	-2146.57485

According to the MM level conformational investigation, the same H14 helical conformation was found for **6**, while a totally different 3D organization was found for **5**. The *Z*-dehydro-β-alanine moiety in the backbone completely changed the preferred geometry and an elongated structure was observed. The MM level optimized structures for compounds **1** and **5** are shown in Figure 4.

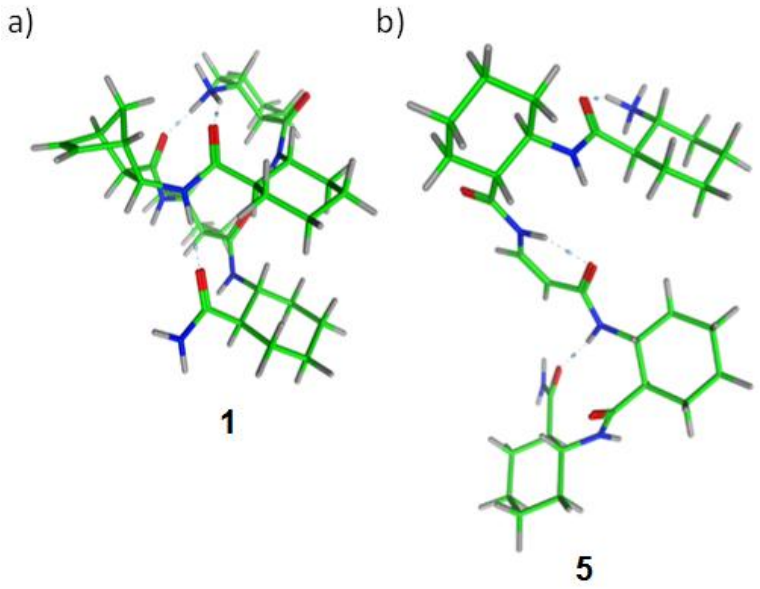

Figure 4. Optimized geometries for compounds **1** and **5** showing the H14 and the elongated geometries, respectively.

As MM methods fix the bond lengths, QM optimizations were applied for compounds **5** and **6** using the preordered MM optima to decipher the drastic structural differences. The results point to the conjugation in compound **5** between the double bond of the *Z*-dehydro-β-alanine residue and the flanking amides, since the bond length of $(CO)_2$–$(NH)_3$ and $(CO)_3$–$(NH)_4$ are longer, while the $(NH)_3$–$C_{\beta 3}$ and $C_{\alpha 3}$–$(CO)_3$ bonds are shorter than those for the unconjugated **6** molecule. Moreover, the atoms of the *Z*-dehydro-β-alanine central residue and the atoms of the flanking amide bonds are within the same plane. The optimum bond lengths of QM level calculations for compound **5** and **6** are shown in Table 2.

Table 2 Optimized bond lengths (in Å) of compound **5** and **6** at M062x/cc-tzv level implicit solvent calculations. The values in parenthesis are the results of the vacuum calculations.

Compound	Bond lengths			
	$(CO)_2 - (NH)_3$	$(CO)_3 - (NH)_4$	$(NH)_3 - C_{\beta 3}$	$C_{\alpha 3} - (CO)_3$
5	1.38 (1.39)	1.35 (1.34)	1.37 (1.37)	1.47 (1.48)
6	1.34 (1.35)	1.34 (1.34)	1.45 (1.45)	1.51 (1.51)

CONCLUSION

In summary, CF methods allowed the efficient construction of six new pentameric β-peptide systems, in which the ability of H14 helix formation was investigated. Our results on pentamers built from [1*R*,2*R*]-ACHC residues containing *diexo*-ABHEC or *diexo*-AOBHEC enantiomers as the third building block showed that the configuration of the middle element plays a crucial role on self-organization, and incorporation of an oxygen-bridged β-amino-acid also enables folding. In the case of the incorporation of [1*R*,2*R*,3*S*,4*S*]-ABHEC (peptide **1**), [1*R*,2*S*,3*R*,4*S*]-AOBHEC (peptide **2**) and β-alanine (peptide **6**) as third residue, NOE interactions proved the H14 helical structure, additionally the typical absorption maxima and minima could be detected in ECD too. Long NH–ND exchange times (10 hours, over 1 day) showed a folded structure with strong H-bonding interactions and strongly shielded protons. ROESY-NMR, NH–ND exchange measurements, ECD investigations and *ab initio* calculations indicated no or weak folding features when [1*S*,2*S*,3*R*,4*R*]-ABHEC (peptide **3**) or [1*S*,2*R*,3*S*,4*R*]-AOBHEC (peptide **4**) was the third amino acid in chain. *Z*-Dehydro-β-alanine (peptide **5**) as a rigid planar section of the system also resulted in an elongated self-organization because of the conjugation of the double bond and the flanking amide bonds. In the case of **3** and **4**, helix destabilization is caused by amide bond disorientation effect of the synperiplanar conformation overcoming the effect of H–O interaction of the ψ angle of the bicyclic residue. A similar interaction can be observed for **1** and **2** too, but because of the smaller size of the H atom the effect is less drastic, thus the H14 helix is not destabilized. These results serve as an important starting point for the design of helix assemblies involving the H14 helix.

EXPERIMENTAL SECTION

Peptide synthesis: Foldamers **1-4** were synthesized by means of continuous-flow solid-phase peptide synthesizer (CF-SPPS) involving 9H-fluoren-9-ylmethoxycarbonyl (Fmoc) technology. The peptide chains were elongated on Tentagel R RAM resin (0.20 mmol g^{-1}) and the syntheses were carried out manually on a 0.1 mmol scale. Couplings were performed with HATU/DIPEA in dimethylformamide (2 mL, DMF) at 60 bar pressure, 70 °C temperature and 0.15 mL min^{-1} flow rate. For the deprotection step; a solution mixture (2mL) contains 2% DBU and 2% piperidine dissolved in DMF was used. The formed peptide sequences were cleaved from the resin with 95% trifluoroacetic acid (TFA), and 5% H_2O at room temperature

for 3 h. TFA was then removed *in vacuo*, and the peptide was precipitated in dried diethylether. The resulting free peptide was filtered off, and dissolved in 10% aqueous acetic acid, and lyophilized. The crude peptides were purified by RP-HPLC.

Synthesis of oligomer 5 via continuous-flow retro-Diels-Alder (CF-rDA) reaction: Solutions of β-peptides **1-4** (50 mg) dissolved in MeOH (50 mL) were loaded, respectively, into the flow reactor (Figure 1a). The system temperature was set to 150 °C (for **2** and **4**) and 230 °C (for **1** and **3**), the pressure to 10 bar and the flow rate to 1 mL min^{-1}. The solvent was evaporated, and the residue was dissolved in 10% aqueous acetic acid (10mL) and subsequently lyophilized. The oligomer **5** was afforded in good yields (from **1**: 85 %; from **2**: 94 %; from **3**: 79 %; from **4**: 92 %). The peptide was analysed by HPLC-MS and purified by RP-HPLC techniques.

Synthesis of oligomer 6: hydrogenation reaction was performed in an H-Cube® (ThalesNano) flow reactor apparatus. Oligomer **5** (20 mg) was dissolved in MeOH (20 mL) and saturated on a 10% Pd/charcoal catalyst, the temperature was set to 50 °C, the pressure to 50 bar with a flow rate of 1 mL min^{-1}. The flow output was collected and after evaporation of the solvent the resulting peptide was dissolved in 10% aqueous acetic acid, and lyophilized. The oligomer **6** was obtained in a good yield (95%). The peptide **6** was analysed by HPLC-MS and the purity was determined by HPLC analysis.

NMR experiments and signal assignments: NMR spectra were recorded at 298 K on Bruker Avance DRX 600 MHz and Avance III 500 MHz spectrometers. Samples in 4 mM concentration were dissolved in 0.5 ml CD_3OH, DMSO-d_6, and water (H_2O/D_2O 90:10) and transferred to 5 mm NMR sample tubes. Chemical shifts are given on the δ-scale and referenced to the solvent signal. Pulse programs of all experiments (^1H, 2D-TOCSY, 2D-ROESY) were taken from Bruker software library.

CD measurements: CD spectra were measured on a Jasco J-1500 spectropolarimeter at room temperature in a 0.1 cm cylindrical quartz cell. Three spectra were accumulated for each sample. CD curves were corrected by the spectral contribution of the blank solvent. The concentration of the sample solutions was 1 mM in CH_3OH and H_2O. Molar circular dichroism is given in M^{-1} cm^{-1}. The data were normalized for the number of chromophores.

***Ab initio* calculations:** All calculations were performed with the Gaussian16 program package using the M06-2x functional in combination with cc-tvz basis set. For implicit water calculations the default PCM model was applied and the original convergence criteria were kept during geometrical optimization. Considering the protonation state of the pentamers the amino group at the *N*-terminal was always protonated during the calculations.

ACKNOWLEDGEMENTS

We are grateful to the Hungarian Research Foundation (OTKA No. K 115731). The financial support of the GINOP-2.3.2-15-2016-00014 and GINOP-2.3.2–15–2016-00034 projects are acknowledged.

REFERENCE

[1] S. H. Gellman, *Acc. Chem. Res*. **1998,** *31*, 173-180.
[2] D. J. Hill, M. J. Mio, R. B. Prince, T. S. Hughes, J. S. Moore, *Chem. Rev*. **2001,** *101*, 3893-4012.
[3] L. Otvos, J. D. Wade, *Front. Chem*. **2014,** *2*, 1-4.
[4] N. Qvit, S. J. S. Rubin, T. J. Urban, D. Mochly-Rosen, E. R. Gross, *Drug Discov. Today*. **2017,** *22*, 454-462.
[5] D. Seebach, A. K. Beck, D. J. Bierbaum, *Chem. Biodivers.* **2004,** *1*, 1111-1239.
[6] D. Seebach, D. F. Hook, A. Glättli, *Biopolymers* **2006,** *84*, 23-37.
[7] G. A. Eddinger, S. H. Gellman, *Angew. Chem. Int. Ed*. **2018,** *57*, 13829-13832.
[8] Y.-H. Shin, S. H. Gellman, *J. Am. Chem. Soc*. **2018,** *140*, 1394-1400.
[9] K. L. George, W. S. Horne, *J. Am. Chem. Soc*. **2017,** *139*, 7931-7938.
[10] W. S. Horne, *Nature Chem*. **2015,** *7*, 858-859.
[11] A. Altmayer-Henzien, V. Declerck, J. Farjon, D. Merlet, R. Guillot, D. J. Aitken, *Angew. Chem. Int. Ed*. **2015,** *54*, 10807-10810.
[12] C. M. Grison, S. Robin, D. J. Aitken, *Chem. Commun*. **2016,** *52*, 7802-7805.
[13] C. M. Grison, J. A. Miles, S. Robin, A. J. Wilson, D. J. Aitken, *Angew. Chem. Int. Ed*. **2016,** *55*, 11096-11100.
[14] S. S. Ragab, A. F. Kassir, R. Guillot, M.-C. Scherrmann, T. Boddaert, D. J. Aitken, *Chem. Commun*. **2018,** *54*, 1968-1971.
[15] K. Möhle, R. Günther, M. Thormann, N. Sewald, H.-J. Hofmann, *Biopolymers* **1999,** *50*, 167-184.
[16] F. Schumann, A. Müller, M. Koksch, G. Müller, N. Sewald, *J. Am. Chem. Soc.* **2000,** *122*, 12009-12010.
[17] M. Jost, J.-C. Greie, N. Stemmer, S. D. Wilking, K. Altendorf, N. Sewald, *Angew. Chem. Int. Ed*. **2002**, *41*, 4267-4269.
[18] N. Koglin, C. Zorn, R. Beumer, C. Cabrele, C. Bubert, N. Sewald, O. Reiser, *Angew. Chem. Int. Ed*. **2003,** *42*, 202-205.
[19] S. Urman, K. Gaus, Y. Yang, U. Strijowski, N. Sewald, S. De Pol, O. Reiser, *Angew. Chem. Int. Ed*. **2007,** *46*, 3976-3978.
[20] D. H. Appella, L. A. Christianson, I. L. Karle, D. R. Powell, S. H. Gellman, *J. Am. Chem. Soc.* **1996,** *118*, 13071-13072.
[21] D. H. Appella, L. A. Christianson, D. A. Klein, D. R. Powell, X. L. Huang, J. J. Barchi, S. H. Gellman, *Nature* **1997,** *387*, 381-384.
[22] R. P. Cheng, S. H. Gellman, W. F. DeGrado, *Chem. Rev.* **2001,** *101*, 3219-3232.
[23] F. Fülöp, T. A. Martinek, G. K. Tóth, *Chem. Soc. Rev*. **2006,** *35*, 323-334.
[24] T. A. Martinek, F. Fülöp, *Chem. Soc. Rev*. **2012,** *41*, 687-702.
[25] M. A. Schmitt, B. Weisblum, S. H. Gellman, *J. Am. Chem. Soc*. **2007,** *129*, 417-428.

[26] M.-R. Lee, N. Raman, S. H. Gellman, D. M. Lynn, S. P. Palecek, *ACS Chem. Biol.* **2017,** *12*, 2975-2980.
[27] T. D. Clark, L. K. Buehler, M. R. Ghadiri, *J. Am. Chem. Soc*. **1998,** *120*, 651-656.
[28] T. F. Cunningham, M. R. Putterman, A. Desai, W. S. Horne, S. Saxena, *Angew. Chem. Int. Ed*. **2015,** *54*, 6330-6334.
[29]. E. V. Denton, C. J. Craig, R. L. Pongratz, J. S. Appelbaum, A. E. Doerner, A. Narayanan, G. I. Shulman, G. W. Cline, A. Schepartz, *Org. Lett*. **2013,** *15*, 5318-5321.
[30]. É. Bartus, Z. Hegedüs, E. Wéber, B. Csipak, G. Szakonyi, T. A. Martinek, *ChemistryOpen*. **2017,** *6*, 236-241.
[31] J. W. Checco, S. H. Gellman, *ChemBioChem*. **2017,** *18*, 291-299.
[32] J. W. Checco, S. H. Gellman, *Curr. Opin. Struct. Biol.* **2016**, *39*, 96-105.
[33] S. Motamed, M. P. Del Borgo, K. Kulkarni, N. Habila, K. Zhou, P. Perlmutter, J. S. Forsythe, M. I. Aguilar, *Soft Matter.* **2016,** *12*, 2243-2246.
[34] D. H. Appella, L. A. Christianson, I. L. Karle, D. R. Powell, S. H. Gellman, *J. Am. Chem. Soc*. **1996,** *118*, 13071-13072.
[35] D. Seebach, M. Overhand, F. N. M. Kühnle, B. Martinoni, L. Oberer, U. Hommel, H. Widmer, *Helv. Chim. Acta.* **1996,** *79*, 913-941.
[36] D. Seebach, K. Gademann, J. V. Schreiber, J. L. Matthews, T. Hintermann, B. Jaun, L. Oberer, U. Hommel, H. Widmer, *Helv. Chim. Acta.* **2004,** *80*, 2033-2038.
[37] I. M. Mándity, E. Wéber, T. A. Martinek, G. Olajos, G. K. Tóth, E. Vass, F. Fülöp, *Angew. Chem. Int. Ed*. **2009,** *48*, 2171-2175.
[38] D. H. Appella, J. J. Barchi, S. R. Durell, S. H. Gellman, *J. Am. Chem. Soc.* **1999,** *121*, 2309-2310.
[39] E. Vaz, W. C. Pomerantz, M. Geyer, S. H. Gellman, L. Brunsveld, *ChemBioChem*. **2008,** *9*, 2254-2259.
[40] S. Chandrasekhar, B. N. Babu, A. Prabhakar, A. Sudhakar, M. S. Reddy, M. U. Kiran, B. Jagadeesh, *Chem. Commun*. **2006,** 1548-1550.
[41] S. Chandrasekhar, A. Sudhakar, M. U. Kiran, B. N. Babu, B. Jagadeesh, *Tetrahedron Lett.* **2008**, *49*, 7368.
[42] I. M. Mándity, L. Fülöp, E. Vass, G. K. Tóth, T. A. Martinek, F. Fülöp, *Org. Lett*. **2010,** *12*, 5584-5587.
[43] R. J. Doerksen, B. Chen, J. Yuan, J. D. Winkler, M. L. Klein. *Chem. Commun*. **2003,** 2534-2535.
[44] I. M. Mándity, B. Olasz, S. B. Ötvös, F. Fülöp, *ChemSusChem.* **2014,** *7*, 3172–3176.
[45] I. Nekkaa, M. Palkó, I. M. Mándity, F. Fülöp, *Beilstein J. Org. Chem.* **2018,** *14*, 318-324.
[46] I. Nekkaa, M. Palkó, I. M. Mándity, F. Miklós, F. Fülöp, *Eur. J. Org. Chem.* **2018,** *2018*, 4456-4464.
[47] L. Berlicki, L. Pilsl, E. Wéber, I. M. Mándity, C. Cabrele, T. A. Martinek, F. Fülöp, O. Reiser, *Angew. Chem. Int. Ed.* **2012,** *5*1, 2208-2212
[48] A. Hetényi, I. M. Mándity, T. A. Martinek, G. K. Tóth, F. Fülöp, *J. Am. Chem. Soc*. **2005,** *127*, 547-553.